

Philipp Müller, BSc

**Novel diaminopropyltin dicarboxylates as catalysts for  
polyurethane synthesis.**

**MASTER'S THESIS**

to achieve the university degree of

Master of Science

Master's degree programme: Chemistry

submitted to

**Graz University of Technology**

Supervisor

Univ.-Prof. Dipl.-Chem. Dr.rer.nat., Frank Uhlig

Institute for Inorganic Chemistry

Graz, July 2017

## AFFIDAVIT

I declare that I have authored this thesis independently, that I have not used other than the declared sources/resources, and that I have explicitly indicated all material which has been quoted either literally or by content from the sources used. The text document uploaded to TUGRAZonline is identical to the present master's thesis.

19.7.2017

Date

V. Müller

Signature

## Danksagung

Mein besonderer Dank gilt meinem Betreuer Prof. Frank Uhlig für die Möglichkeit an diesem Thema zu arbeiten, und mir die Freiheiten zu geben meine eigenen Ideen zu verwirklichen. Du hast mir stets mit deinem fachlichen Rat und deiner menschlichen Art geholfen.

Bei Dr. Ana Torvisco möchte ich mich für sämtliche Hilfestellung während meiner Masterarbeit bedanken. Auch, dass du dir die Zeit genommen hast mir die Kristallographie zu lehren.

Bei Roland Fischer bedanke ich mich für das Messen und Lösen von Röntgeneinkristallstrukturen.

Bei meinen Schreibraumkollegen Thomas Hafner und Lina Ma bedanke ich mich für die nette Zeit in und außerhalb des Labors.

Mein Dank gilt auch Dr. Johann Pichler für die Zeit, die du dir genommen hast mich diesem Thema näher zu bringen, während meiner ganzen Projektelabore sowie auch abseits des Labors.

Dr. Cathrin Zeppek danke ich für die nette Zeit auf dem Institut, sowie für die Hilfestellung während des Starts meiner Masterarbeit.

Beate Steller danke ich für die tolle gesamte Studienzeit. Auch deine Fähigkeiten als „persönliche Sekretärin“ sorgten dafür, dass ich keine Deadline verschlief.

Bei Dr. Schuh möchte ich mich besonders für die produktiven „Lernabende“ bedanken.

Auch der ganzen AG-Uhlig und dem Institut möchte ich für sämtliche Hilfestellung danken.

Letztlich möchte ich mich bei meinen Eltern bedanken, ohne die all das nicht möglich gewesen wäre.

## 1 Abstract

The success in isolating (3-aminopropyl)stannanes bearing free hydrogens at the nitrogen atom, with derivatives  $\text{Et}_2\text{SnX}(\text{CH}_2)_3\text{NH}_2$  ( $\text{X} = \text{F}, \text{Cl}, \text{Br}, \text{I}, \text{acetate}$ ) in this working group, has provided motivation for the preparation of the diamino analogues. A novel synthetic pathway involving the desilylation of a tin trimethyl silyl species ( $\text{Ph}_2\text{Sn}(\text{SiMe}_3)_2$ ) towards diamino propyltin dichloride is described.<sup>2</sup> Diamino propyltin dichloride is then converted to the respective tin carboxylate species  $(\text{RCOO})_2\text{Sn}((\text{CH}_2)_3\text{NH}_2)_2$  employing a range of carboxylic acids ( $\text{RCOOH}$ ,  $\text{R} = \text{alkyl}, \text{F}_3\text{C-F}_3\text{C-(CF}_2)_7\text{-}, \text{phenyl}, \text{cycloalkyls}$ ). Depending on the R group, the tin center can display a six or seven membered coordination sphere. In addition, also depending on the nature of R, discrete packing effects are observed in the solid state of diamino tin carboxylates. These compounds are a promising class of substances for technical applications.

## 2 Kurzfassung

Der Erfolg in der Synthese von (3-Aminopropyl)-Stannane, mit freien Wasserstoffen am Stickstoff, sowie die Herstellung der Derivate  $\text{Et}_2\text{SnX}(\text{CH}_2)_3\text{NH}_2$  ( $\text{X} = \text{F}, \text{Cl}, \text{Br}, \text{I}, \text{Acetat}$ ), in unserer Arbeitsgruppe, motivierte uns auch die Diamino Analoga zu synthetisieren. In dieser Arbeit wird ein Syntheseweg präsentiert, welcher die Synthese von Diaminopropylzinndichlorid, unter Verwendung einer Desilylierungsreaktion von  $(\text{Ph}_2\text{Sn}(\text{SiMe}_3)_2)$  beschreibt. Diaminopropylzinndichloride wird anschließend zum korrespondierenden Dicarboxylat  $(\text{RCOO})_2\text{Sn}((\text{CH}_2)_3\text{NH}_2)_2$  umgewandelt. Es werden eine Bandbreite an Carbonsäuren ( $\text{RCOOH}$ ,  $\text{R} = \text{Alkyl}, \text{F}_3\text{C-F}_3\text{C-(CF}_2)_7\text{-}, \text{Phenyl}, \text{Cycloalkyle}$ ) verwendet. In Abhängigkeit der R Gruppe, kann eine Koordinationszahl von sechs oder sieben am Zinnatom beobachtet werden. Diese neu synthetisierten Produkte sind eine vielversprechende Substanzklasse, hinsichtlich ihrer technischen Anwendungsmöglichkeiten.

**Für meine Eltern**

**Sic parvis magna**

*Großes aus kleinen Ursprüngen*

**Sir Francis Drake**

## CONTENTS

Danksagung .....	1
1 Abstract.....	2
2 Kurzfassung.....	3
3 Introduction .....	8
4 Literature .....	9
4.1 Toxicity of DBTDL.....	9
4.2 Catalysts for PU polymerisation .....	9
4.2.1 Tertiary amine catalysts and non-tin metal complexes .....	10
4.2.2 Organotin catalysts.....	12
4.2.3 Aim of Project.....	13
4.3 Synthesis of literature known aminoalkyl tin compounds.....	15
4.3.1 Monoamino trialkyl tin compounds.....	15
4.3.2 Diamino dialkyl tin compounds.....	20
5 Results and Discussion.....	22
5.1 Synthesis of precursor.....	22
5.2 Synthesis of tin dicarboxy compounds .....	30
5.3 Bonding situation in the solid state.....	34
5.3.1 Diaminopropyltin Dicarboxylates .....	36
5.3.2 Diaminopropyltin Monodentate Dicarboxylates – Coordination Number 6 .....	37
5.3.3 Mixed Diaminopropyltin Dicarboxylates –Coordination Number 7.....	45
5.3.4 Mixed Diaminopropyltin Dicarboxylate – Coordination Number 6.5 .....	49
5.3.5 Aminopropyltin Bidentate Dicarboxylate – Coordination Number 6.....	50
5.4 Extended structures .....	52
5.4.1 1D Chains.....	53
5.4.2 2D Sheets.....	54
5.4.3 3D Networks .....	58

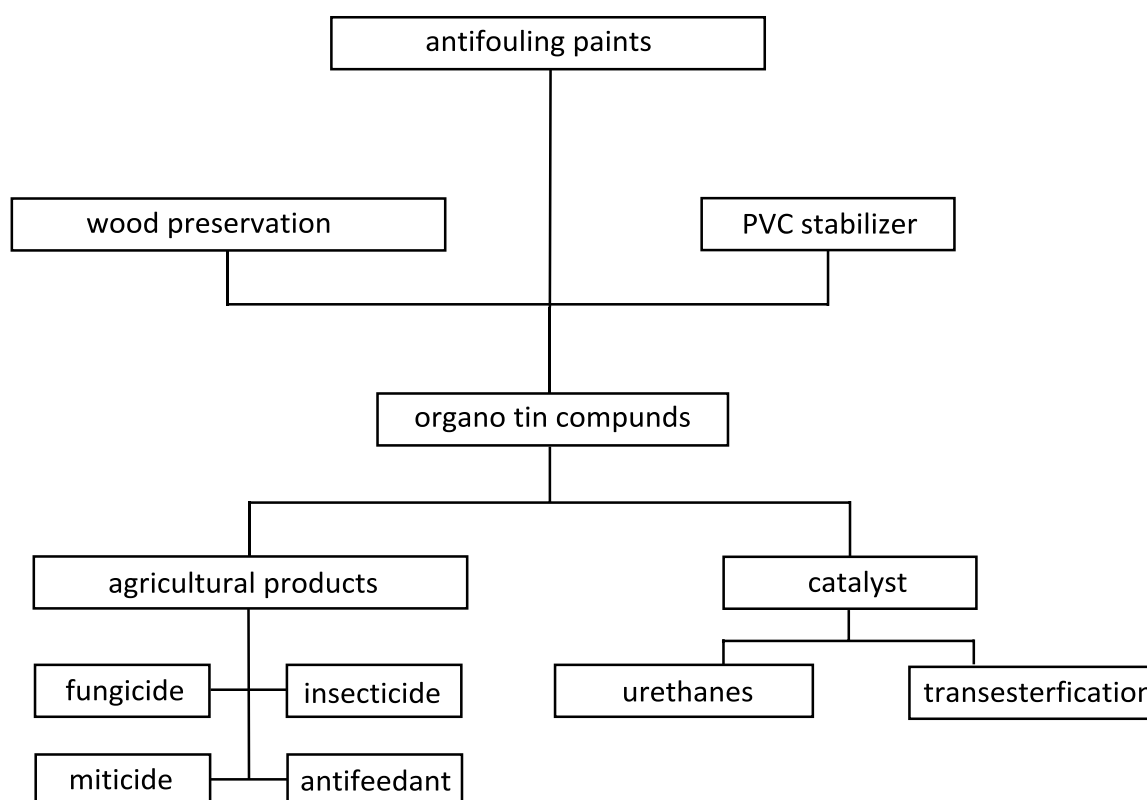


---

6	Conclusion and Outlook.....	62
7	Experimental Section.....	63
7.1	Materials and Methods.....	63
7.2	X-ray Crystallography.....	63
7.3	NMR-spectroscopy.....	65
7.4	Synthesis.....	66
7.4.1	Literature known compounds.....	66
7.4.2	New synthesized compounds.....	70
8	Appendix.....	78
8.1	Index of Figures.....	78
8.2	Index of Schemes.....	80
8.3	Index of Tables.....	82
9	References.....	83
9.1	Abbreviations.....	95
9.2	Crystallographic Data.....	98

### 3 Introduction

Tin is widely used in industry, not only in its metal form or as an alloy composite, but also as organometallic compounds such as fungicides,<sup>1-5</sup> insecticides,<sup>6-9</sup> or miticides.<sup>10-13</sup> An overview on the applications of organo tin derivatives is given in Scheme 1.<sup>1-9,14-21</sup> Most notable to mention is the use of tin compounds in the field of catalysis, such as transesterification reactions, for example the synthesis of fatty acid esters or polyesters.<sup>18-21</sup> Therefore, dibutyl tin dichloride is used as catalysts for reactions under moderate conditions. In addition to the above mentioned reaction, the synthesis of polyurethanes is the major use of tin catalysts. Discussions about their toxicity led to a partial ban of these compounds by EU law. Thus, alternative catalysts have to be explored or new strategies have to be investigated, for example using biphasic technology in combination with perfluorinated organotin compounds during the polymer synthesis.<sup>22,23</sup>



Scheme 1: Overview applications of organotin compounds

## 4 Literature

### 4.1 Toxicity of DBTDL

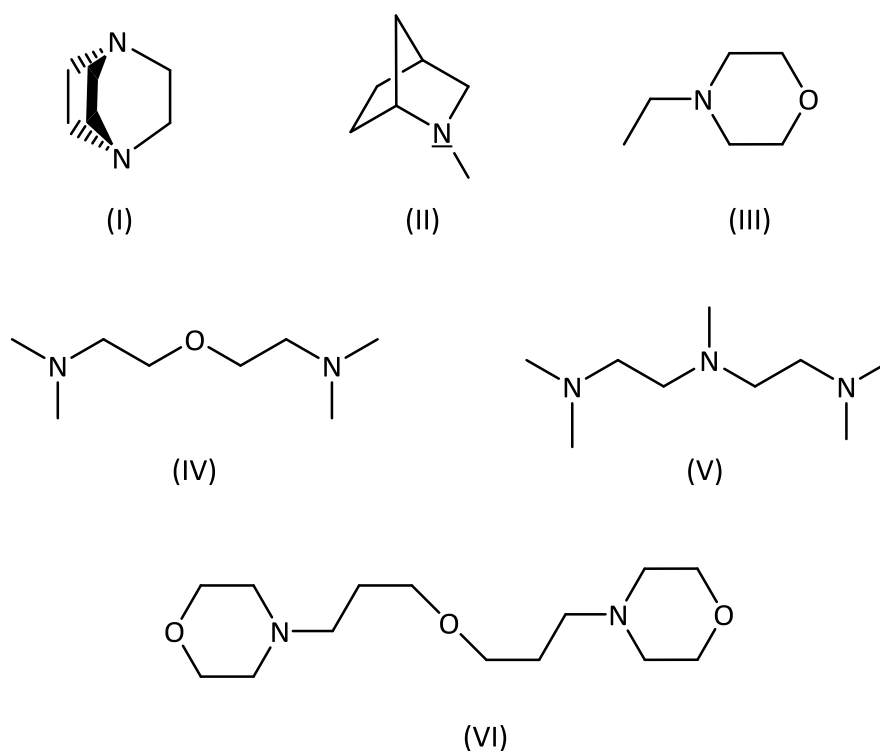
The toxicity of organotin compounds strongly depends on the substitution pattern on the metal center. In general, it could be said that the toxicity decreases as followed:  $R_3SnX > R_2SnX_2 > RSnX_3$ . Also, aryl substitutes are less toxic than alkyl chains. The shorter the carbon chain is, the more toxic the compound. The most toxic tin species for mammals is triethyltin acetate with an  $LD_{50}$  of 4 mg/kg in rats.<sup>24</sup> In comparison, the  $LD_{50}$  value of DBTDL (dibutyltin dilaurate) is 175 mg/kg.<sup>25</sup> Issues arise with the persistence and bioaccumulation in the environment and their lipophilicity.<sup>26</sup> In general, these derivatives show harmful effects on aquatic life. Based on the presence of DBTDL in many materials, such as PVC or PU, toxicological studies have been made. These studies indicate a high impact of these compounds on higher eukaryotic life. Rats exposed to DBTDL lose weight and show a lethargic and dull behavior. An increase in the activity of heme oxygenase,<sup>27</sup> which suggests an increase of heme degradation, as well as a prolonged induction of hepatic heme,<sup>28</sup> leads to a decrease in cytochrome P-450 activity. This affects the biotransformation mechanism in hepatic microsomes. This alteration could modify the response to drugs and other pharmaceutical products. Like other organotin derivatives, DBTDL also shows differences in toxicant and drug metabolism due to hormonal influences.<sup>29,30</sup> In comparison to tertiary amines, DBTDL shows a higher cytotoxic potential.

### 4.2 Catalysts for PU polymerisation

In general the reaction rate between isocyanates and hydroxyl-groups is slow, thus the need for catalysts has been established in PU synthesis. Through catalyst choice, reaction time and resulting polymer architecture can be determined. Most catalysts work in a Lewis acid-base mechanism. The challenge is to choose the appropriate catalyst and in correct amounts to obtain the desired polymer properties. In industry, three classes of catalysts are used: tertiary amines, organometallic species, and aprotic salts.

### 4.2.1 Tertiary amine catalysts and non-tin metal complexes

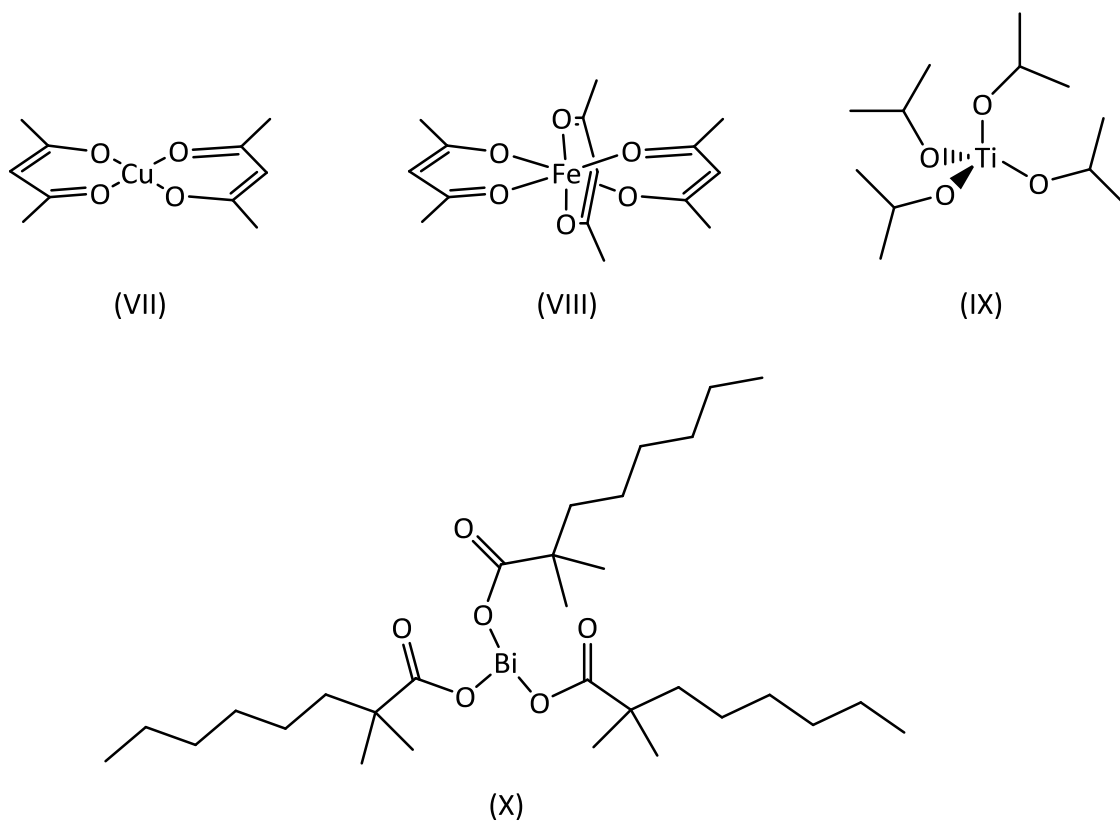
Tertiary amine catalysts (I-VI) are used for blowing and gelling reactions of polyurethane polymers.<sup>31</sup> In general, they are not very reactive towards isocyanate catalysts. Factors which influence the activity are the basicity of the nitrogen, catalyst molecular weight, steric hindrance and volatility. Increasing the basicity leads to a higher activity.



Scheme 2: Tetra amines as PU catalysts.

1,4-Diazabicyclo[2.2.2]octane (DABCO) (I) is the most common amine catalyst for PU production.<sup>31</sup> The disadvantage of tertiary amine catalysts is their strong fishlike odor and their high volatility, caused by the low molecular weight. They are considered to be a source of volatile organic compounds (VOCs) leading to environmental damage.

Current research also tries to determine environmentally friendly replacements (VII-X) for the common used catalyst DBTDL and DBTDA.<sup>32,33</sup>

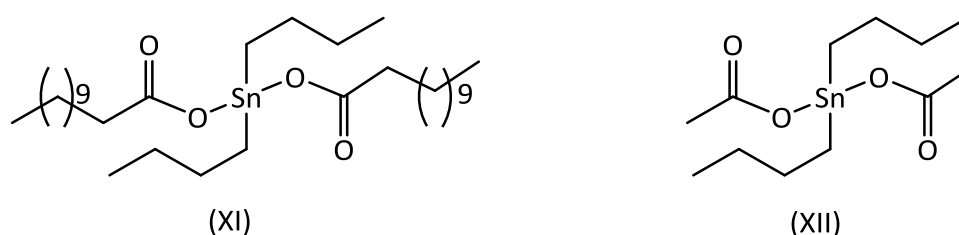


**Scheme 3: Catalysts for tin replacement.**

Promising compounds contain iron<sup>34</sup> (VIII), copper<sup>35</sup> (VII), titanium<sup>36</sup> (IX) or bismuth<sup>37</sup> (X) as the metal and occur as oxides, acac complexes, or carboxylates. However, these compounds show significant disadvantages due to their interaction with neighboring groups, decreasing the reaction rate.<sup>38</sup> In addition no acceptable candidate has been found due to issues including the catalyst color, their behavior as strong oxidants, or their toxicity. This limits the use of these compounds to a smaller set of applications.

#### 4.2.2 Organotin catalysts

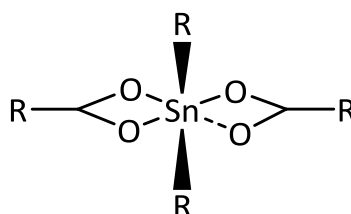
Organotin compounds have been extensively investigated for their catalytic activity in PU synthesis. The well-established common industrial catalysts are dibutyltin diacetate (DBTDA) (XII) and dibutyltin dilaurate (DBTDL) (XI), the working horse catalyst for PU formation. Not only does the high activity of DBTDL greatly increase the reaction rate in considerable small quantities, it shows particularly good compatibility in all sorts of used systems for PU synthesis. In addition, the catalyst reactivity is only marginal influenced by light and moisture.



Scheme 4: Common tin catalysts (DBTDL and DBTDA).

Structurally, in both tin(IV) derivatives, the carboxylate groups are bound through both oxygens displaying a bidentate bonding motif leading to a skewed trapezoid bipyramidal geometry instead of the usual tetrahedral structure.<sup>39-43</sup>

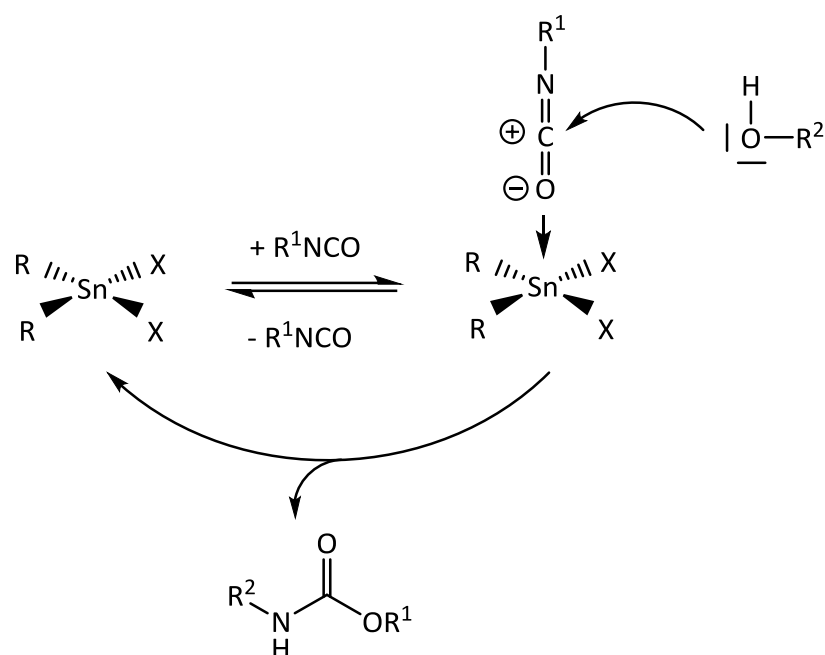
Due to the availability of the 5d orbitals in tin, an expansion of the coordination number is possible by hypervalent interaction between the tin and the carbonyl oxygen.



Scheme 5: Proposed structure of DBTDL and DBTDA.

The mechanism of catalyzed polyurethane synthesis by using tin catalysts, is still under investigation. Three mechanisms are discussed in literature: Insertion mechanism,<sup>44,45</sup> Ionic mechanism,<sup>46,47</sup> and the most supported Lewis acid mechanism.<sup>48</sup> In the latter, the tin compound reacts as a Lewis acid. In the initial step, the carbonyl oxygen is polarized by

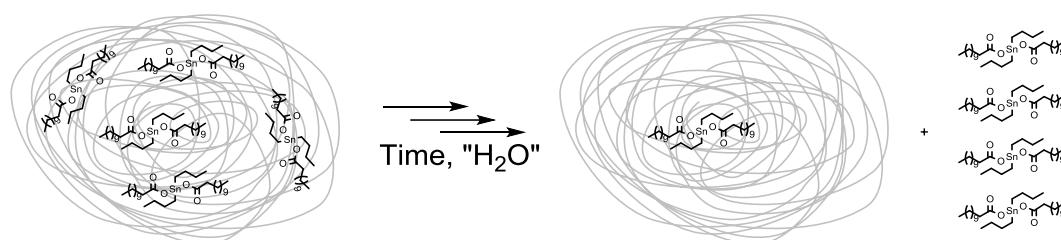
coordination to the tin center. Consequently, the isocyanate carbon is more electrophilic, as a result it can undergo nucleophilic attack by the alcohol.



Scheme 6: Suggested Lewis acid mechanism.

#### 4.2.3 Aim of Project

The main problem that occurs by using DBTDL as a catalyst in polyurethane synthesis is the leach out effect of the catalyst from the polymer due to weathering. Resulting in a lack of chemical bonding of the catalyst within the polymer bulk material.



Scheme 7: Catalyst leach out of the polymer.

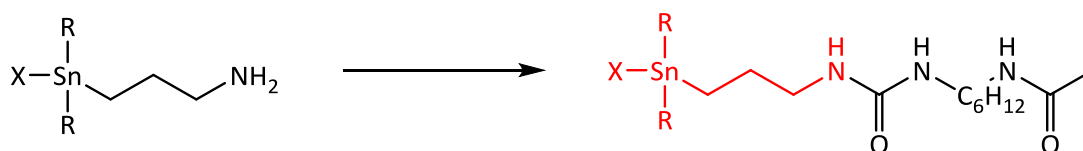
Therefore and due to the mentioned toxicity, DBTDL is partially banned in the EU under article (EU-Richtlinie 76/769/EG idgF).<sup>49</sup> Our aim is to synthesize organotin derivatives which display corresponding catalytic activity as DBTDL, but lack the negative effects associated with their use, by introducing aminopropyl side chains into the catalytically active molecules.

Due to the success of our working group in preparing monoaminoalkyltin compounds, this motivated us to synthesize diaminoalkyltin compounds.



**Scheme 8.** Structure typ of our aminoalkyl compounds.<sup>50-52</sup>

Via these amino groups, the derivatives can be incorporated into the target polymer through covalent bonding to avoid a possible leach-out effect.



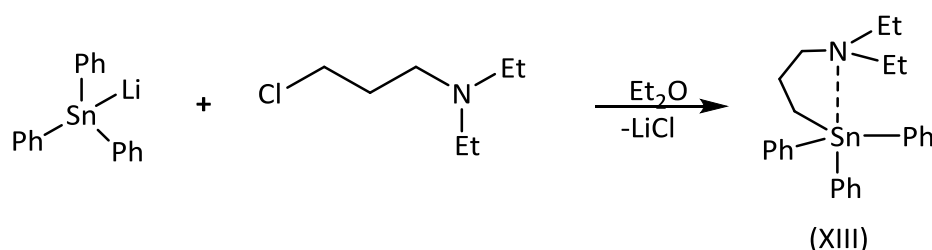
**Scheme 9:** Catalyst incorporation into the polymer.



### 4.3 Synthesis of literature known aminoalkyl tin compounds

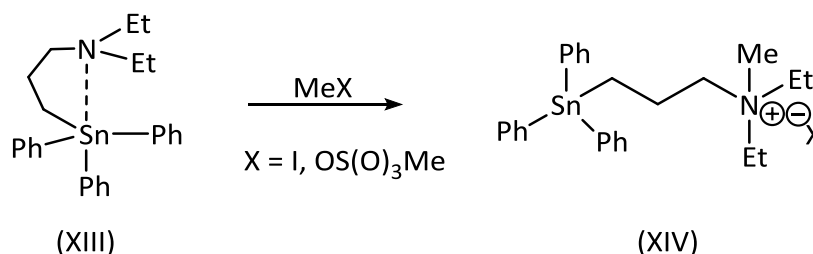
#### 4.3.1 Monoamino trialkyl tin compounds

One of the first examples of mono aminoalkyl tin derivatives was synthesized by Gilman in 1955, as a potential cytotoxic reagent.<sup>53</sup> Therefore, he reacted  $\text{Ph}_3\text{SnLi}$  with  $\gamma$ -diethylaminopropylchloride, leading to triphenyl- $\gamma$ -N,N-diethylaminopropyltin (XIII) by a salt-elimination reaction.



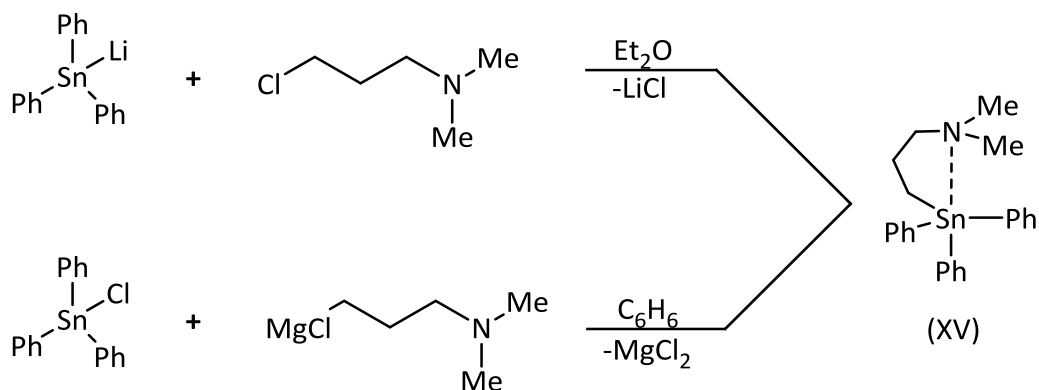
Scheme 10: Synthesis of triphenyl- $\gamma$ -N,N-diethylaminopropyltin.

To increase the water-solubility, Gilman derivated the nitrogen by converting it with methyl iodide or dimethylsulfate into a quaternary ammonium salt (XIV).<sup>53</sup>

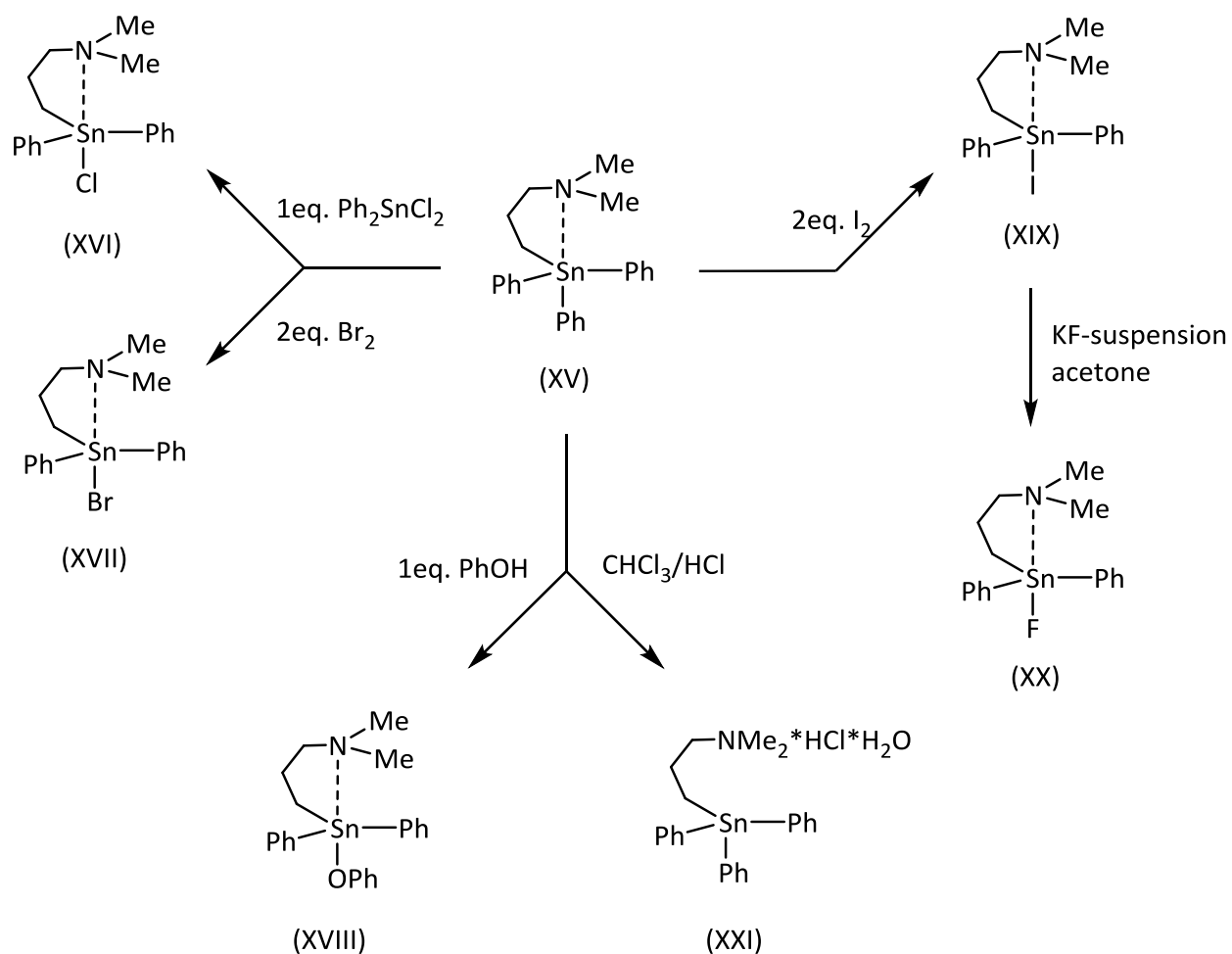


Scheme 11: Quaternization of triphenyl- $\gamma$ -N,N-diethylaminopropyltin.

Much more is known in literature about dimethylaminopropyl tin compounds. Triphenyl- $\gamma$ -N,N-dimethylaminopropyltin (XV) was described by Lequan in 1976.<sup>54</sup> Derivate (XV) was synthesized *via* the stannide reaction pathway of Gilman, as well as by using dimethylaminopropylmagnesium chloride as building block. Lequan was also the first to make a species with different alkyl substituents at the tin center.<sup>55</sup>

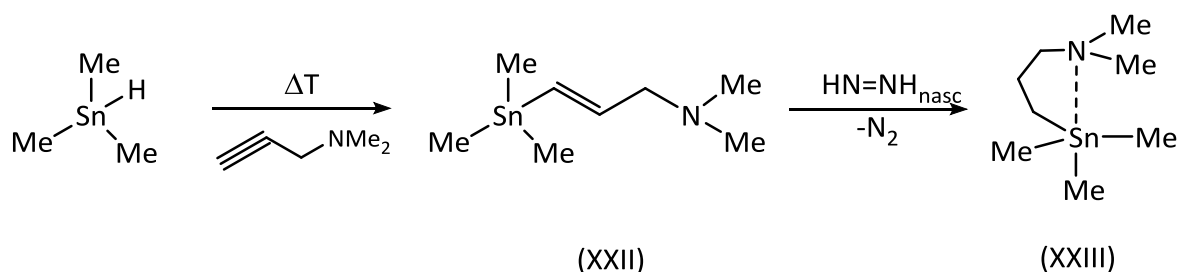
Scheme 12: Synthesis of triphenyl- $\gamma$ -N,N-dimethylaminopropyltin.

Jurkschat explored these compounds in the next two decades regarding reactivity, coordination behavior and structural chemistry. Jurkschat's working group also published a variety of derivatives with different alkyl and aryl substituents at the tin center.<sup>56</sup>

Scheme 13: Derivatization of triphenyl- $\gamma$ -N,N-dimethylaminopropyltin.

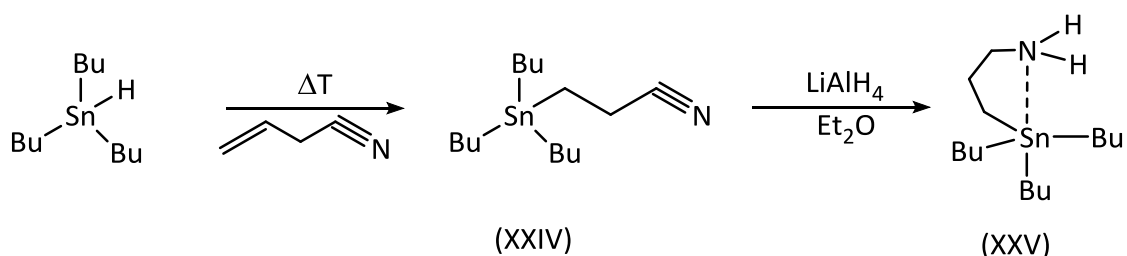
Starting from (XV), halogen derivatives (XVI-XVII and XIX-XX) can be prepared depending on the derivatization method. The chlorine (XVI) analogue can be achieved by a Kocheshkov reaction with one equivalent of  $\text{Ph}_2\text{SnCl}_2$ . The bromine (XVII) and iodine (XIX) can be isolated by reacting (XV) with elemental  $\text{I}_2$  or  $\text{Br}_2$ . The iodide derivative can then be converted *via* a Finkelstein type reaction to the fluoride (XX). A quaternization of the nitrogen (XXI) is also possible by reacting (XV) with etheric HCl.

Most of these aminoalkyl species were synthesized by a salt elimination reaction. In 2001 Han showed that these compounds can also be accessed by a hydrostannylation reaction, an activated triple bond is reacted with a tin hydride, yielding a E/Z mixture (XXII).<sup>57</sup> The mixture is then reduced with *in situ nascendi* hydrazine (XXIII).



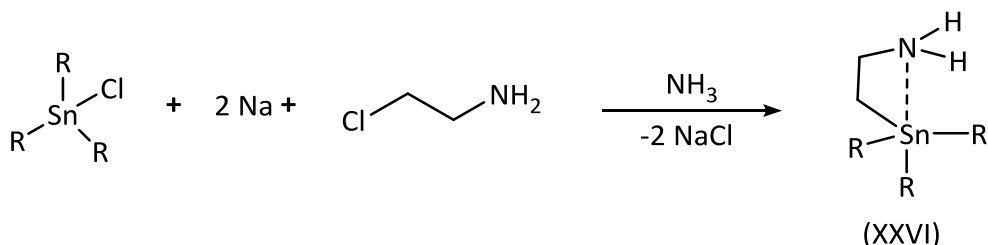
Scheme 14: Hydrostannylation as synthesis strategy to generate aminopropyltin compounds.

All compounds mentioned before have alkyl groups at the nitrogen. For tin species with two hydrogens at the nitrogen center, only a few examples are known in literature. The first synthesized derivative was tributyl- $\gamma$ -aminopropyltin (XXV). In the first step, acryl nitrile undergoes a hydrostannylation reaction with tributyltinhydride. Afterwards, the nitrile (XXIV) is reduced with  $\text{LiAlH}_4$  to the corresponding amine (XXV).



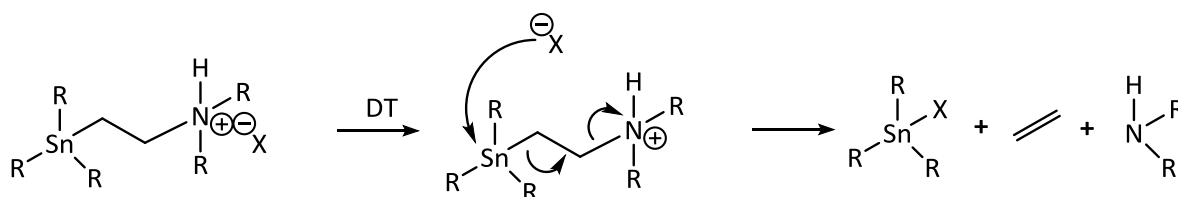
Scheme 15: Hydrostannylation as synthesis strategy to generate aminopropyltin compounds with acidic hydrogens.

Another way to achieve this class of compounds was made by Tzschach.<sup>58</sup>  $\beta$ -aminoethyl tin species (XXVI) was synthesized by solving triaryl- or trialkyltin chlorides in liquid ammonia, followed by adding two equivalent of sodium. Then 2-chlorethylamine is added to the sodiumstannide solution, leading to the product under salt elimination.



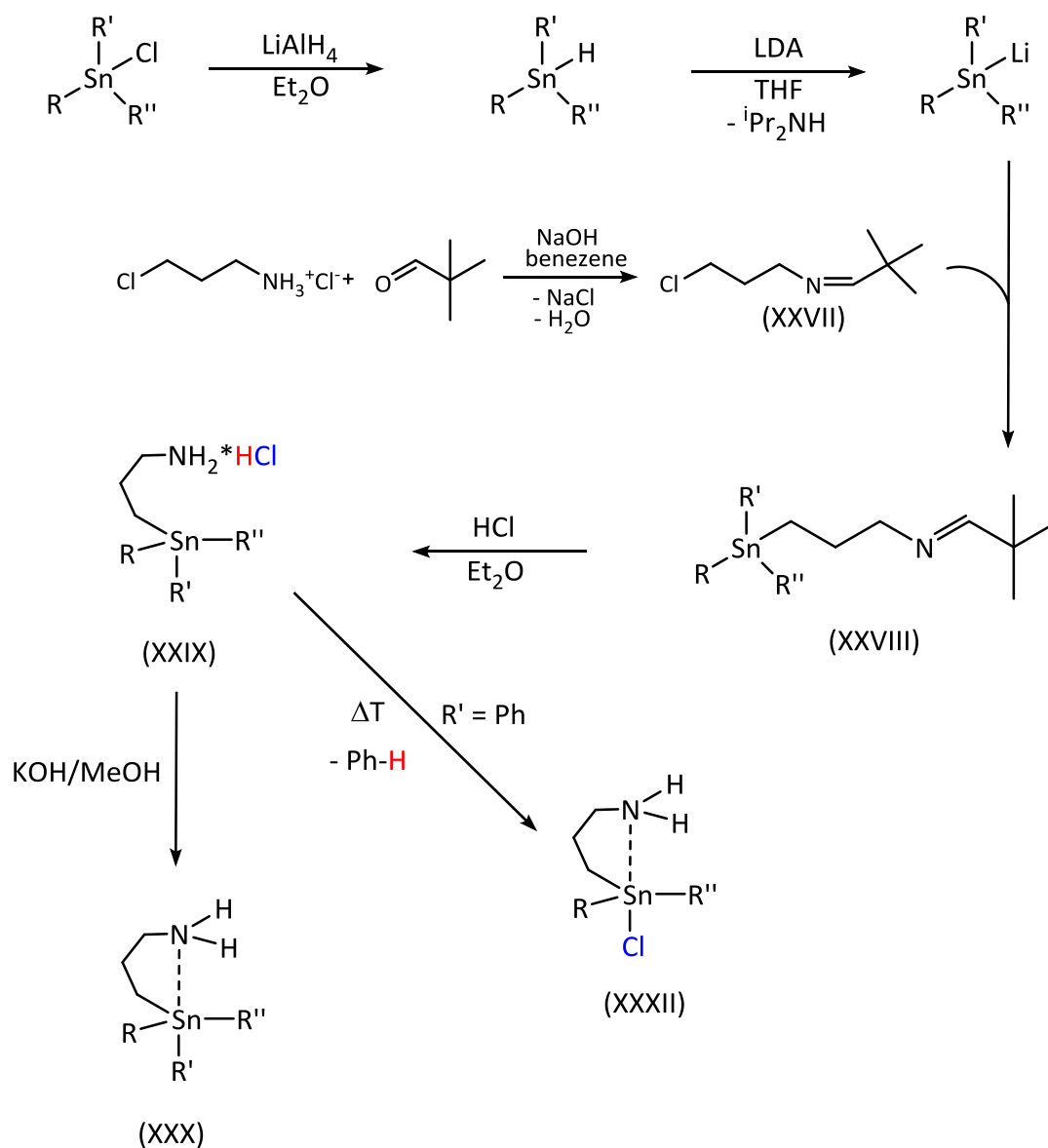
Scheme 16: Synthesis of  $\beta$ -aminoethyl tin species (XXVI)

The problem of this reaction is that it is limited to 2-chlorethylamine.<sup>58</sup> Lengthening the carbon chain of the  $\alpha,\omega$ -chloralkylamine spacer was without success. Quarternisation of the nitrogen leads to decomposition. These compounds undergo a Grob-fragmentation,<sup>59</sup> which depends on the substituent and already starts at 0°C with elimination of ethene.



Scheme 17: Mechanism of the Grob-fragmentation.

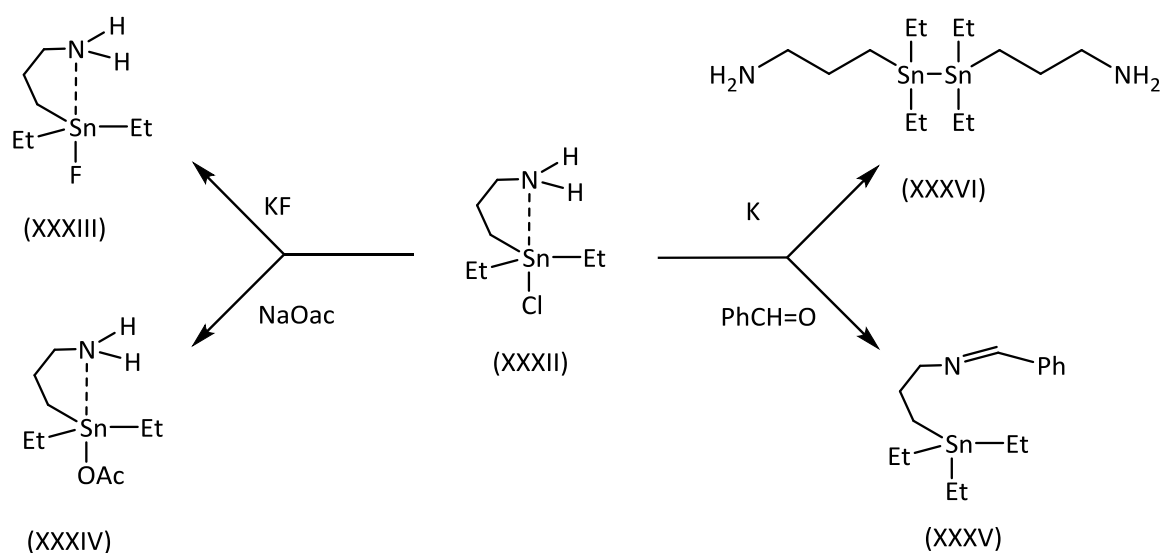
Our working group recently published a synthesis route to gain aminopropyl tin derivatives with two hydrogens atoms at the nitrogen. Protecting the chloramine by preparing the corresponding chloro imine (XXVII) derivative is necessary to preserve the active amino hydrogen successfully circumventing unwanted side reactions.<sup>60</sup>



Scheme 18: Synthesis route to achieve aminopropyl tin compounds with acidic nitrogen hydrogens.<sup>50</sup>

In the first step, the alkyl/aryl tin chloride is converted to the tin hydride with  $\text{LiAlH}_4$ . Then the stannide is generated by adding LDA, which afterwards is reacted with the chloro imine to produce (XXVIII). The imine is then converted to the ammonia chloride (XXIX) by adding etheric HCl. The final product (XXX) is obtained by adding KOH/MeOH. Pichler showed a

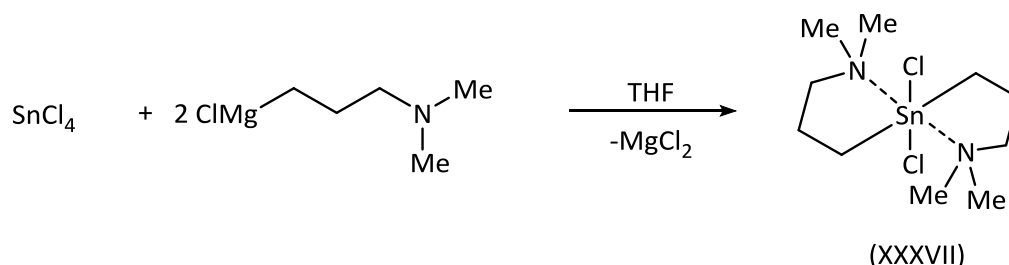
thermal rearrangement of the ammonia chloride (XXXI) is possible.<sup>60</sup> Hereby, benzene is released and the product (XXXII) is obtained pure in quantitative yield. The product (XXXII) then can also be derivatized at the tin center to the fluorine (XXXIII),<sup>50</sup> or the carboxylate (XXXIV). Also connecting two XXXIIs to the distannane (XXXVII) by adding potassium is possible. The amino group can be reconverted to the imine (XXXVI).<sup>51,52</sup>



Scheme 19: Derivatization possibilities of compound XXXII

#### 4.3.2 Diamino dialkyl tin compounds

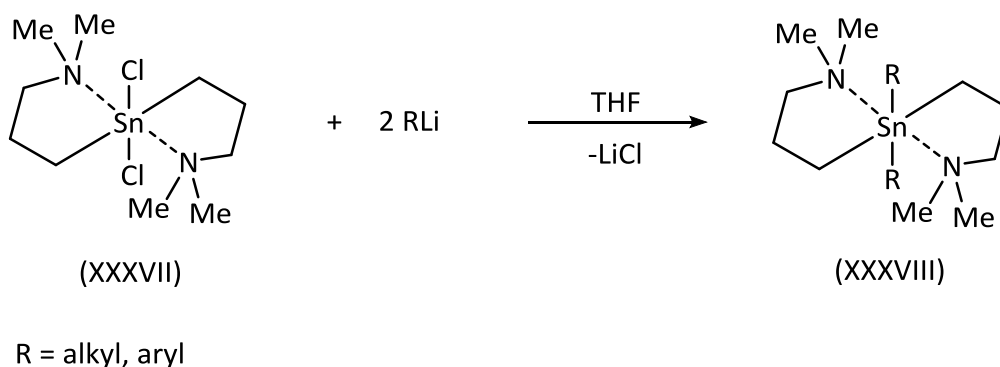
All compounds presented thus far have in common that they contain only one aminoalkyl group. However, there are also derivatives known with two aminoalkyl substituents. Jurkschat synthesized bis(3-(dimethylaminopropyl))tin dichloride (XXXVII).



Scheme 20: Synthesis of bis(3-(dimethylamino)propyl)tin dichloride

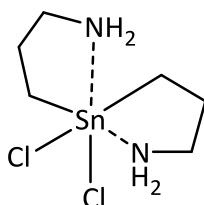
Using two equivalents of dimethylaminopropyl magnesium bromide as Grignard reagent, (XXXVII) can be obtained by reaction with  $\text{SnCl}_4$ . This compound can be converted to the

corresponding alkyl/aryl (XXXVIII) by treating (XXXVII) with organolithium reagents, undergoing a salt elimination reaction.



**Scheme 21: Alkyl/arylation of bis(3-(dimethylamino)propyl)tin dichloride**

The success in isolating non protected tin mono amino derivatives  $\text{Et}_2\text{SnX}(\text{CH}_2)_3\text{NH}_2$  (X = F, Cl, Br, I, acetate) in this working group has provided motivation for the preparation of the diamino analogues. These compounds bear hydrogen atoms instead of alkyl groups at the nitrogen atom, to bind the catalyst covalently into the polymer during the synthesis and are a promising class of substances for potential water soluble cytotoxic agents<sup>62-64</sup>.

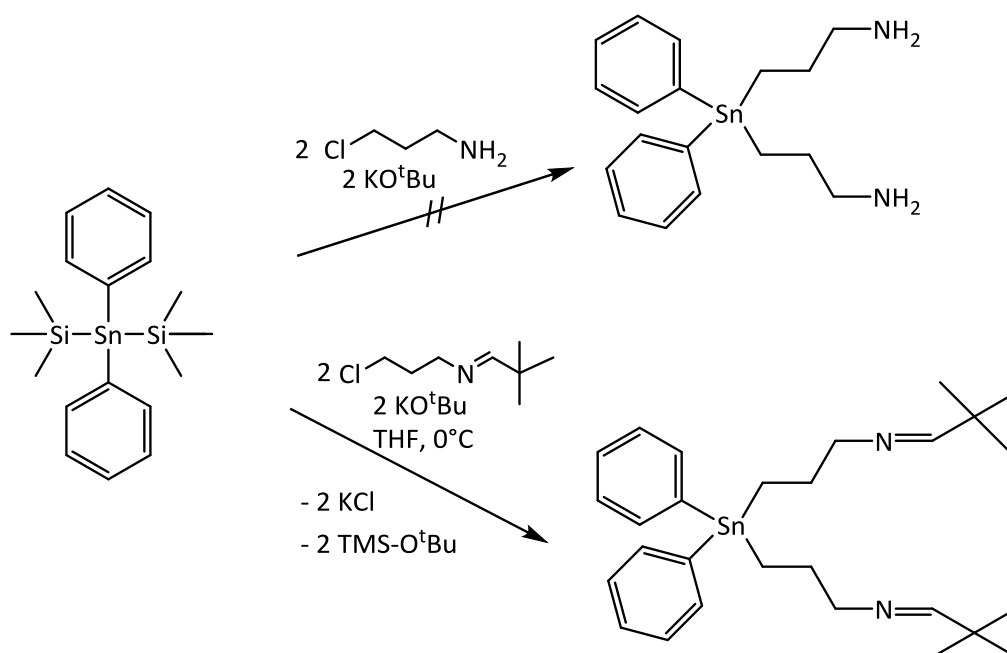


**Scheme 22: Target precursor molecule**

## 5 Results and Discussion

### 5.1 Synthesis of precursor

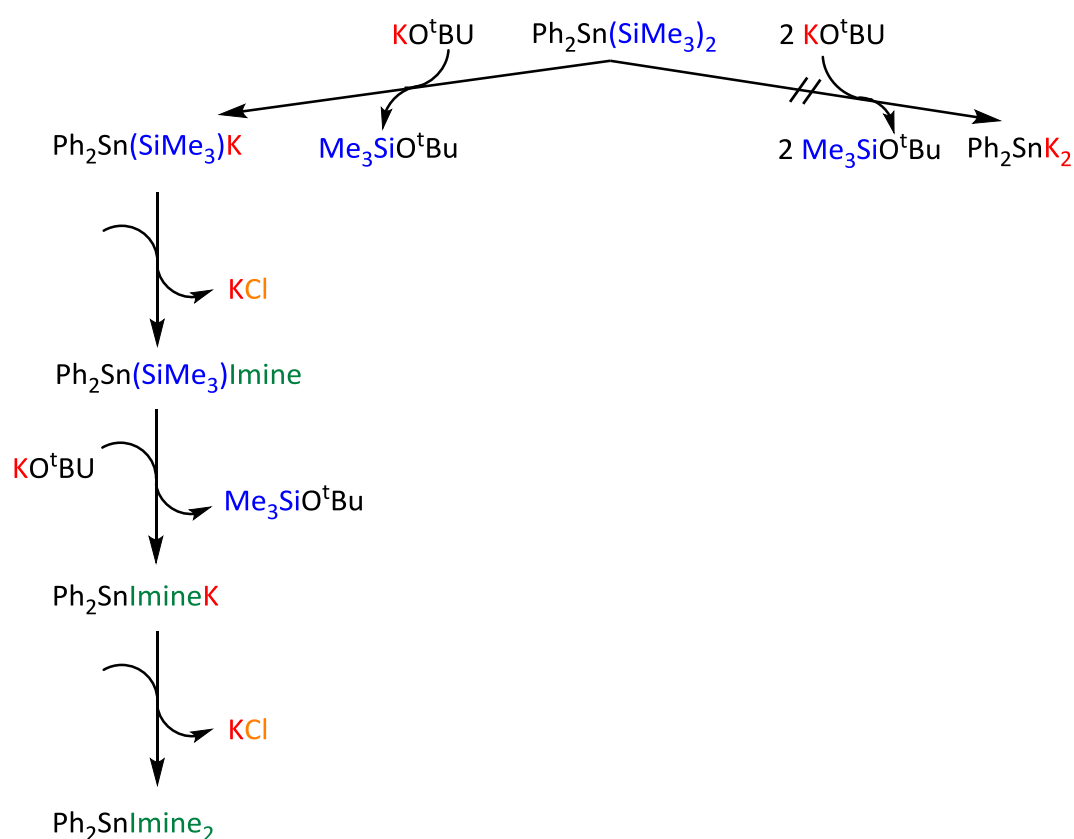
Previous reaction routes affording monoaminopropyltin derivatives entailed the synthesis of monohydrdestannane educts which were then deprotonated with LDA (lithium diisopropyl amide).<sup>60</sup> However, this route was not advantageous for the synthesis of the bis(aminopropyl)tin derivatives due to fact that tin dihydride precursors are much more difficult to synthesize and temperature labile, partially polymerizing. Therefore, an alternative reaction pathway was employed, using the literature known diphenylbis(trimethylsilyl)stannane ( $\text{Ph}_2\text{Sn}(\text{SiMe}_3)_2$ ).<sup>65</sup> This bis(silyl)stannane is more stable than the corresponding dihydrides and can be stored for long periods without decomposition. Diphenylbis(trimethylsilyl)stannane was desilylated (Scheme 24) using a one-pot variation of the well-established cleavage of trimethylsilyl residues with  $\text{KO}^t\text{Bu}$ .<sup>66-68</sup> As already shown by Pichler et al the  $\text{Cl}(\text{CH}_2)_3\text{NH}_2$  cannot be used directly. Instead the chloro imine was used. Adopting this procedure, diphenylbis(<sup>t</sup>butyliminopropyl)stannane was obtained in very good yield and purity through distillation after solvent removal and filtration of the potassium salt byproduct.



Scheme 23: Generating diphenylbis(<sup>t</sup>butyliminopropyl)stannane.

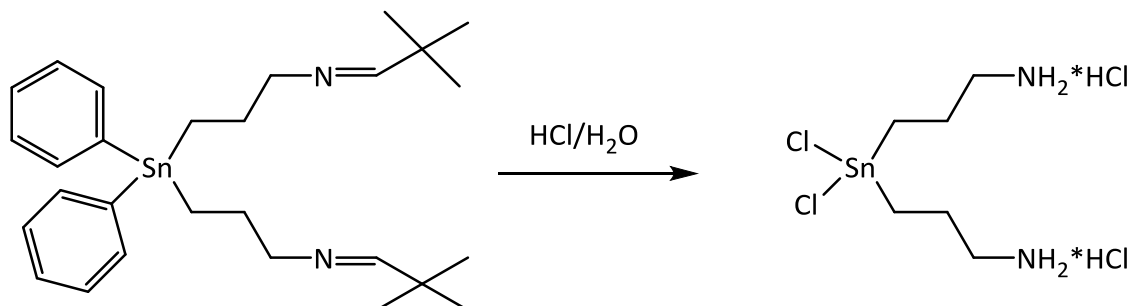


The reaction runs in a multiple step pathway, due to the fact, that dianionic stannides does not exist. In the first step,  $\text{Ph}_2\text{Sn}(\text{TMS})_2$  is reacted with  $\text{KO}^t\text{BU}$  and one of the trimethylsilyl (TMS) group is cleaved off in a desilylation reaction with  $\text{Me}_3\text{SiO}^t\text{Bu}$  as a side product. The resulting nucleophilic potassium stannide is then reacted with the electrophilic  $^t\text{butyliminopropylchloride}$  (XXVII) undergoing a salt-elimination reaction. The remaining TMS group is also cleaved off in the same way as above resulting in diphenylbis( $^t\text{butyliminopropyl}$ )stannane.



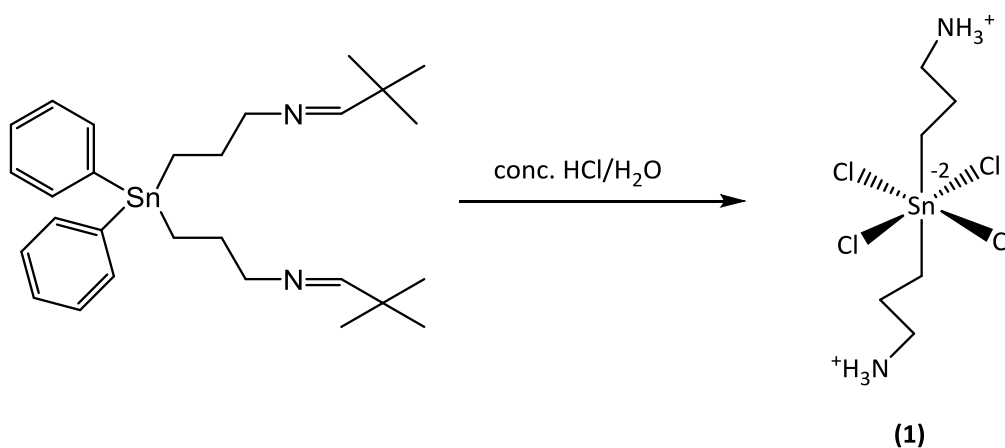
Scheme 24: Multistep mechanism for the cleavage of two trimethylsilyl groups

In the next step the aldehyde is removed by addition of an excess 0.5 M aqueous hydrochloric acid, leading to the corresponding dichlorobis(3-ammoniumchloridepropyl)stannane. At the same time the tin-phenyl bonds are cleaved.

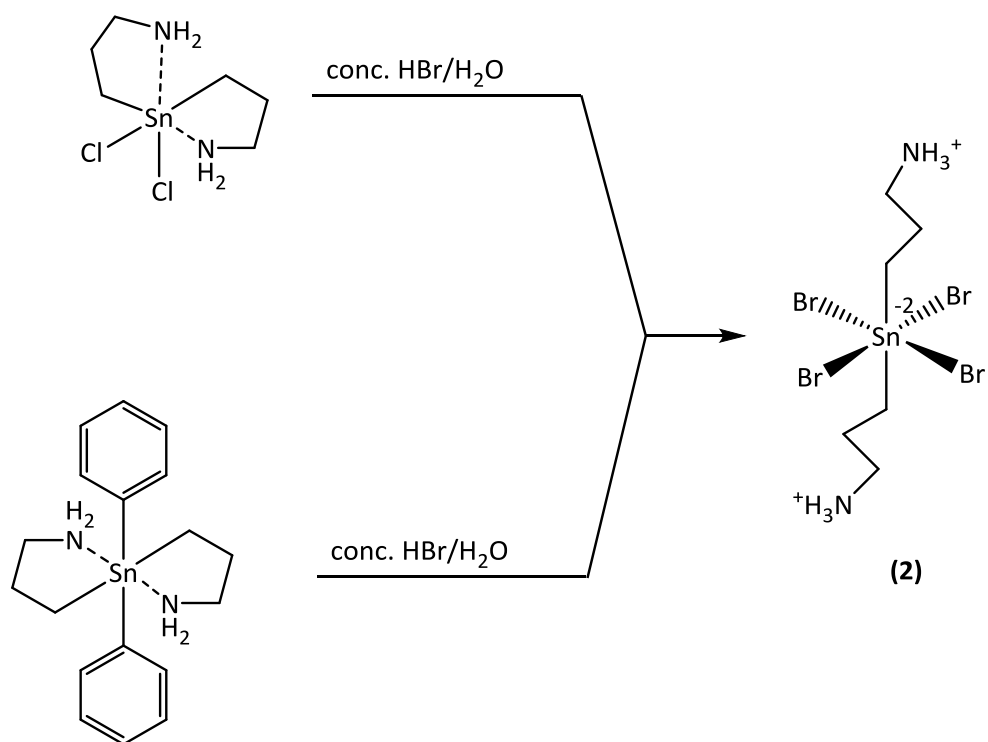


Scheme 25: Treating diphenylbis(3-(tert-butylimino)propyl)stannane with HCl/H<sub>2</sub>O.

By adding a 12 M aqueous hydrochloric acid, instead of obtaining dichlorodi-(3-ammoniumchloridepropyl)stannane, an overchlorination takes place, leading to bis(ammonio)propyl)tetrachlorostannate (**1**).



Scheme 26: Treating diphenylbis(3-(tert-butylimino)propyl)stannane with HCl/H<sub>2</sub>O.



Scheme 27: Synthesis of the bromo derivate (2).

In a similar way diphenylbis(3-aminopropyl)stannane can be converted to the bromine derivate of (2), by adding conc. HBr/H<sub>2</sub>O. By adding HBr/H<sub>2</sub>O to dichlorobis(3-aminopropyl)stannane, a chlorine/bromine halogen exchange takes place.

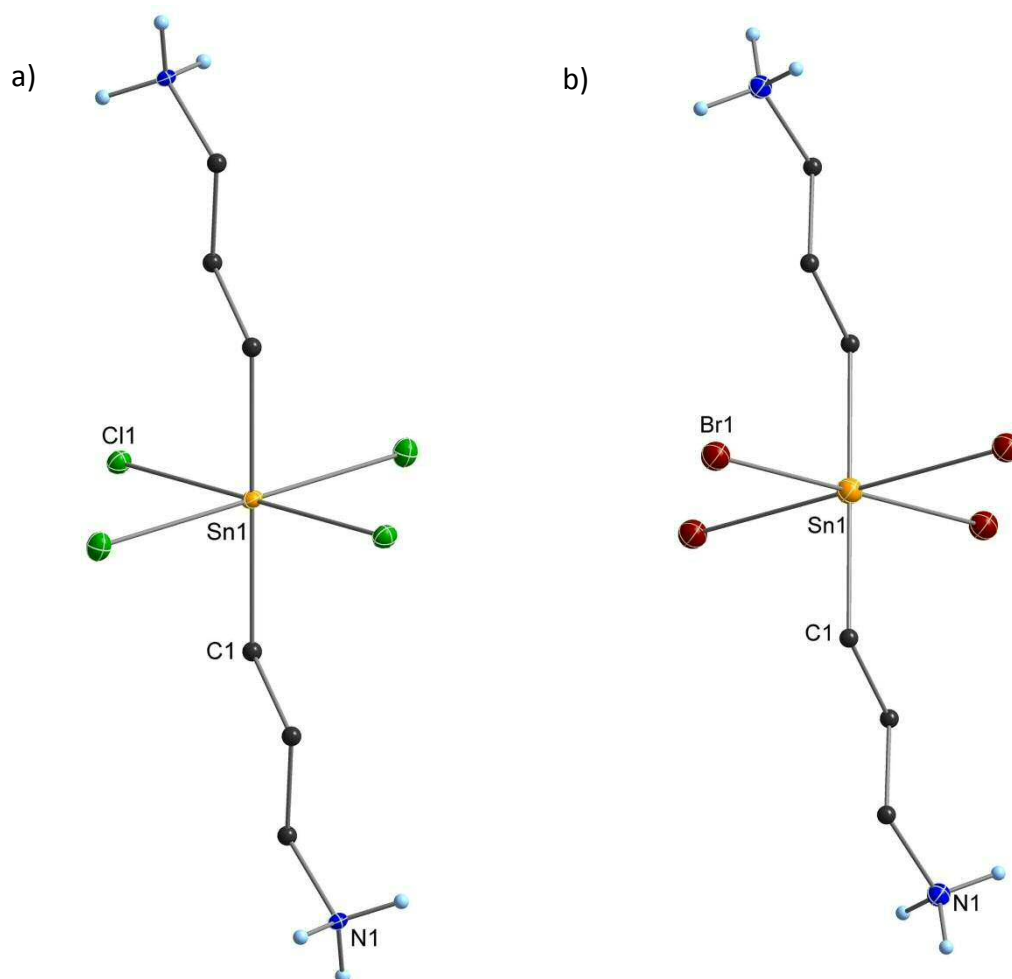


Figure 1: a) Crystal bis(propylammonia)tetrachlorostannate (**2**). b) Crystal bis(propylammonia)tetrabromostannate (**2**). All non-carbon atoms shown as 30% shaded ellipsoids. Hydrogen atoms removed for clarity.

Suitable crystals of (**1**) and (**2**) for x-ray diffraction were obtained from recrystallization from H<sub>2</sub>O. Both show an octahedral geometry, where four halogen atoms surrounding the tin center in the axial plane. The 3-aminopropyl moieties change from a *cis*-configuration into a *trans*-configuration. This behavior is similar to the in literature known anion di(butyl)-tetrachlorostannate<sup>69</sup> and di(methyl)-tetrabromostannate.<sup>70–73</sup> In contrast to these compounds, which have a counter cation to balance the charges, (**1** & **2**) show a betaine structure. Due to protonation of the amine, no lone pair is available for hypervalent interaction between nitrogen and tin center. Refluxing this reaction over a few hours, leads also to Sn-C bond cleavage, resulting in SnBr<sub>6</sub> and two equivalents of <sup>+</sup>H<sub>3</sub>N(CH<sub>2</sub>)<sub>3</sub>Br (**3**). H-Br interactions ranging from 2.82–3.12 Å are observed between the amine hydrogens and bromines. This side product can be circumvented by controlling the reaction conditions.

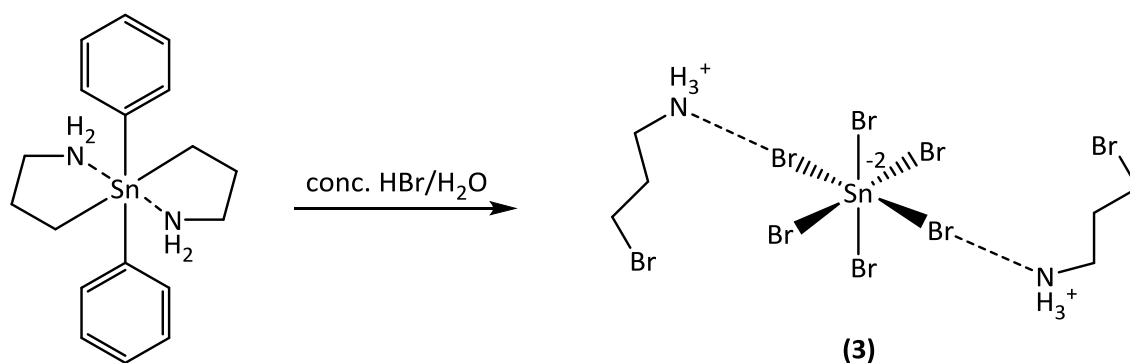
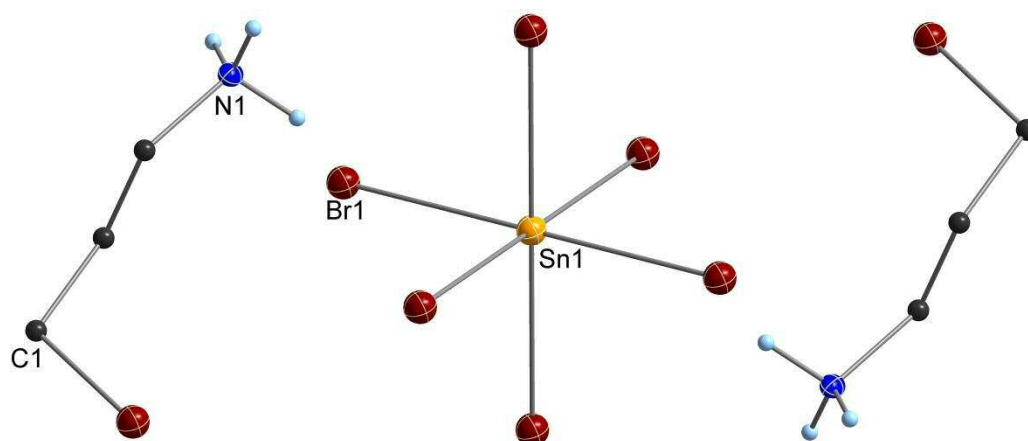
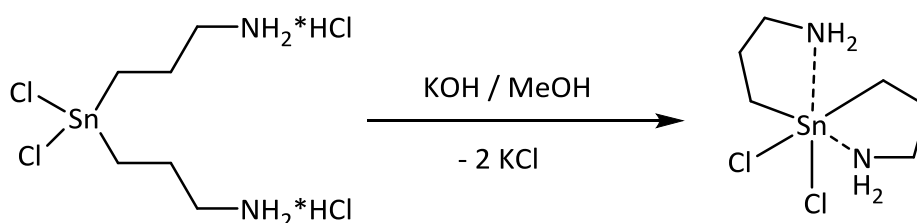
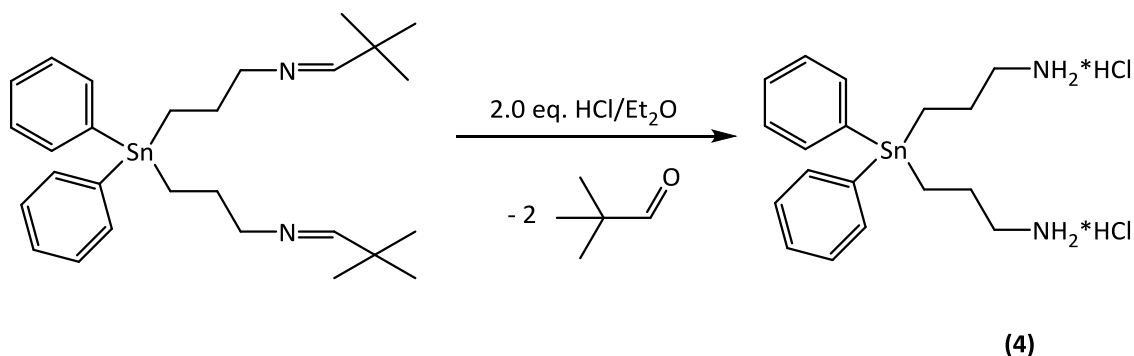
Scheme 28: Refluxing  $\text{Ph}_2\text{SnA}_2$  with  $\text{HBr}/\text{H}_2\text{O}$ .

Figure 2: Crystal structure of (3). All non-carbon atoms shown as 30% shaded ellipsoids. Hydrogen atoms removed for clarity.

To obtain the desired product, dichlorobis(3-ammoniumchloridepropyl)stannane is treated with two equivalents of  $\text{KOH}/\text{MeOH}$  (Scheme 29). As a side product,  $\text{KCl}$  is produced. The main drawback of this synthetic route is the same solubility of main and side product giving rise to problems with compound separation.

Scheme 29: Converting the ammonium chloride into the amine with  $\text{MeOH}/\text{KOH}$ .

The only way to separate the compounds is by sublimation. However, this is time consuming and only very small yields can be obtained. Therefore, an alternative way to obtain the dichlorobis(3-ammoniumchloridepropyl)stannane starting material had to be designed.



Scheme 30: Converting the imine to the corresponding ammonium chloride with HCl/Et<sub>2</sub>O.

An alternative method is to convert the imine to the corresponding ammonium chloride derivative. The deprotection was easily achieved by using diluted aqueous solutions of HCl in equimolar amounts. Diphenylbis(<sup>t</sup>butyliminopropyl)stannane was then hydrolyzed, and the liberated aldehyde was removed together with the water under vacuum. The labile Sn–C bond remains untouched under these conditions and leads to an almost quantitative isolation of diphenyldi(3-ammoniumchloridepropyl)stannane (**4**) as an amorphous solid. Crystallization was achieved in a mixture of methanol/water. The obtained structure shows an expected tetrahedral structure, without hypervalent interactions (Figure 3)

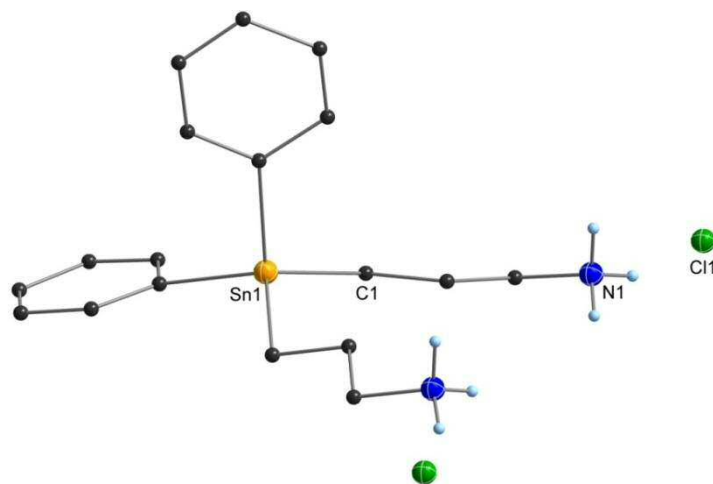
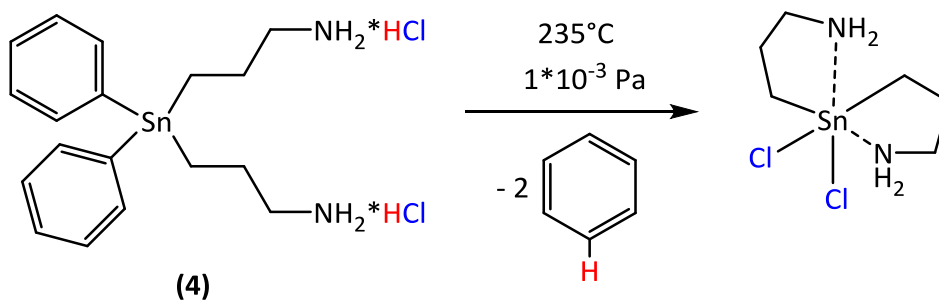


Figure 3: Crystal structure of diphenyldi(propyl-3-ammoniumchloride)stannane (**4**). All non-carbon atoms shown as 30% shaded ellipsoids. Hydrogen atoms removed for clarity.

Diphenylbis(3-ammoniumchloridepropyl)stannane (**4**) was then converted into the dichlorobis(3-aminopropyl)stannane *via* a thermally induced intramolecular proto-dearylation reaction (Scheme 29).

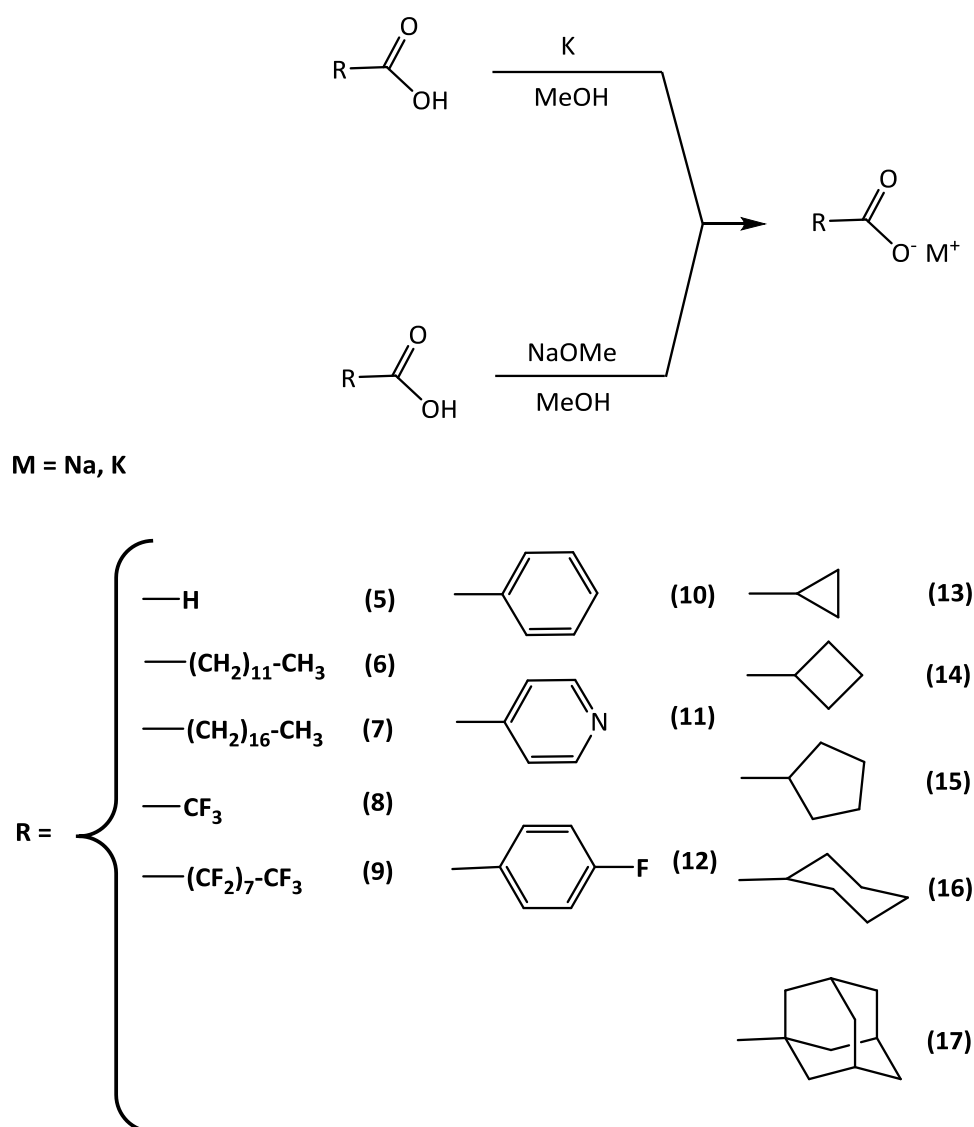


Scheme 31: Thermal rearrangement of (4) to dichlorobis(3-aminopropyl)stannane.

A TGA/DSC-MS measurement was first conducted to establish the optimal reaction temperature in order to avoid Grob fragmentation. According to this measurement, the first phenyl ring was liberated as benzene at around 190 °C and the second phenyl ring at around 225 °C. At 260 °C, no phenyl groups were observed, however, decomposition of the target molecule begins at 240 °C. Therefore, a heating temperature of 235 °C was chosen for the preparative synthesis of dichlorobis(3-aminopropyl)stannane (Scheme 31). After 1 h of heating, dichlorobis(3-aminopropyl)stannane was obtained as a solid and recrystallized out of methanol. Sequencing reactions have to be performed in methanol or water, due to the low solubility of dichlorobis(3-aminopropyl)stannane in organic solvents.

## 5.2 Synthesis of tin dicarboxy compounds

In previous work conversion of the carboxyl acid into the carboxylate was done by weighting the equimolar amount of potassium, and solving it in methanol to generate potassium methanolate, followed by adding the carboxylic acid to obtain the carboxylate. This way is very time consuming, and also includes with handing of harmful chemicals, such as potassium. An easier and safer route is by taking commercially available NaOMe, dissolving in methanol and adding the carboxylic acid in equimolar amounts (Scheme 32).



Scheme 32: Overview of all used carboxylic acids and the synthesis route to carboxylates.

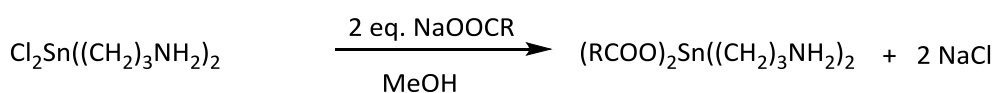


Depending on the nature of the carboxylic acid, the solution was refluxed until all the educts went into solution. This was done for carboxylic acids with long alkyl chains (**6**, **7**) due to their lipophilic behaviour.

We have chosen structurally and chemically different carboxylic acids (Scheme 30). Starting from the shortest carboxylic acid (**5**) with C<sub>1</sub>, to acetic acid with C<sub>2</sub>, up to lauric acid (**6**) C<sub>12</sub> and stearic acid (**7**) C<sub>18</sub>.

Also, the perfluorinated analogues trifluoroacetic acid (**8**) C<sub>2</sub> and the longer perfluoro-*n*-nonanoic acid C<sub>9</sub> were used to observe if they differ in their catalytic activity in comparison to the non-fluorinated ones. Also, cycloalkyl systems with different ring strains, starting from the highly strained cyclopropanecarboxylic (**13**) (27.5 kcal/mol) and cyclobutanecarboxylic acid (**14**) (26.3 kcal/mol) to the lower strained cyclopentanecarboxylic (**15**) (6.2 kcal/mol) and the strainless cyclohexanecarboxylic acid (**16**) (0.1 kcal/mol) were studied.<sup>74</sup> Furthermore, aromatic system like the simplest six membered ring benzoic acid was investigated. Also, aromatic ring systems with introduced hetero atoms inside the ring (**11**) and outside the ring (**12**) were considered.

Dichlorobis(3-aminopropyl)stannane was then converted into the corresponding biscarboxylbis(3-aminopropyl)stannane *via* a salt metathesis reaction by adding dichlorobis(3-aminopropyl)stannane to the alkali carboxylate salt in methanol. The solvent was removed under vacuum, the residue suspended in THF and filtered through a PTFE syringe filter. Afterwards, the solvent was completely removed under vacuum. Depending on the carboxylate residue, different solvents were used to obtain crystals.



**Scheme 33: Synthesis of dicarboxylates by salt elimination.**

X-ray structures reveals, depending on the R group, the tin center can display a six- or seven-membered coordination sphere (chapter 5.3).

The six- or seven-membered coordination sphere can only be observed in the solid state. In solution  $^{119}\text{Sn}$ -NMR measurements showed that all compounds are in a range of -293 ppm to -341.4 ppm.

**Table 1:**  $^{119}\text{Sn}$ -NMR shift of dicarboxy tin compounds

Compounds	$^{119}\text{Sn}$ NMR ( $\text{CDCl}_3$ , 112 MHz) in ppm
Bis(formate)-bis(3-aminopropyl)stannane ( <b>5</b> )	-293
Bis(acetate)-bis(3-aminopropyl)stannane <sup>60</sup>	-330.2
Bis(laurate)-bis(3-aminopropyl)stannane ( <b>6</b> )	-330.1
Bis(stereate)-bis(3-aminopropyl)stannane ( <b>7</b> )	-336.5
Bis(benzylcarboxyl)-bis(3-aminopropyl)stannane ( <b>10</b> )	-328.2
Bis-(4-pyribisnecarboxyl)-bis(3-aminopropyl)stannane ( <b>11</b> )	-334
Bis(p-fluorobenzylcarboxyl)-bis(3-aminopropyl)stannane ( <b>12</b> )	-341.4
Bis(cyclopropylcarboxyl)-bis(3-aminopropyl)stannane ( <b>13</b> )	-326
Bis(cyclobutylcarboxyl)-bis(3-aminopropyl)stannane ( <b>14</b> )	-310
Bis(cyclopentylcarboxyl)-bis(3-aminopropyl)stannane ( <b>15</b> )	-315.9
Bis(cyclohexylcarboxyl)-bis(3-aminopropyl)stannane ( <b>16</b> )	-321.3
Bis(adamantylcarboxyl)-bis(3-aminopropyl)stannane ( <b>17</b> )	-327.3

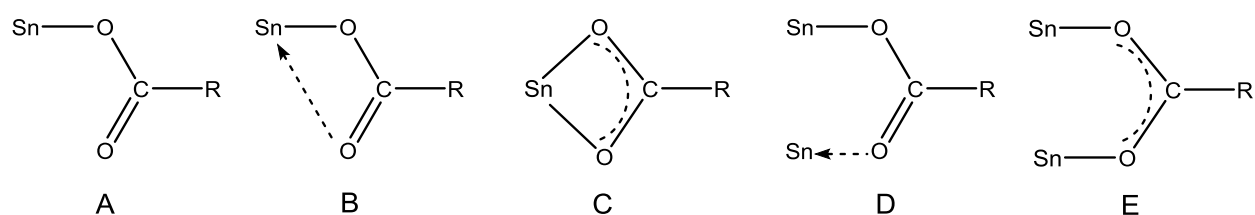
**Table 2:**  $^{13}\text{C}$ -NMR shift of 3-aminopropyl substituents of all dicarboxy tin compounds.

Compounds	$^{13}\text{C}$ NMR ( $\text{CDCl}_3$ , 75.5 MHz) in ppm		
	Sn- $\text{CH}_2$	- $\text{CH}_2$ - [ $^2J(^{13}\text{C}-^{119}\text{Sn})$ in Hz]	- $\text{CH}_2$ - $\text{NH}_2$ [ $^3J(^{13}\text{C}-^{119}\text{Sn})$ in Hz]
Bis(formate)-bis(3-aminopropyl)stannane ( <b>5</b> )	19.2	23.5 [52]	39 [72]
Bis(acetate)-bis(3-aminopropyl)stannane <sup>60</sup>	20.5	23.6 [54]	40.4 [70]
Bis(laurate)-bis(3-aminopropyl)stannane ( <b>6</b> )	20.0	23.9 [55]	39.9 [68]
Bis(stereate)-bis(3-aminopropyl)stannane ( <b>7</b> )	20.3	24.1 [52]	40.1 [71]
Bis(benzylcarboxyl)-bis(3-aminopropyl)stannane ( <b>10</b> )	20.2	25.1 [53]	40.9 [74]
Bis-(4-pyribisnecarboxyl)-bis(3-aminopropyl)stannane ( <b>11</b> )	20.3	24.1 [53]	40.2 [71]
Bis(p-fluorobenzylcarboxyl)-bis(3-aminopropyl)stannane ( <b>12</b> )	20.2	24.2 [52]	40.9 [74]
Bis(cyclopropylcarboxyl)-bis(3-aminopropyl)stannane ( <b>13</b> )	20.1	24 [54]	40.2 [73]
Bis(cyclobutylcarboxyl)-bis(3-aminopropyl)stannane ( <b>14</b> )	19.8	24.1 [53]	40.1 [70]
Bis(cyclopentylcarboxyl)-bis(3-aminopropyl)stannane ( <b>15</b> )	21	24.2 [50]	40.4 [72]
Bis(cyclohexylcarboxyl)-bis(3-aminopropyl)stannane ( <b>16</b> )	20.6	23.9 [53]	40.2 [70]
Bis(adamantylcarboxyl)-bis(3-aminopropyl)stannane ( <b>17</b> )	20	24.5 [54]	40.1 [72]

Furthermore the  $^{13}\text{C}$  and  $^1\text{H}$  NMR chemical shifts in solution are in the expected range. The  $\text{Sn}-\underline{\text{C}}\text{H}_2\text{CH}_2\text{CH}_2\text{NH}_2$  carbon shows a broad signal with a full width at half maximum of approximately 16 Hz. In addition the  $^1J(^{13}\text{C}-^{119}\text{Sn})$  coupling constant, which can be expected in a range of 500 Hz,<sup>74</sup> is not observed. For the  $\text{Sn}-\text{CH}_2-\underline{\text{C}}\text{H}_2\text{CH}_2\text{NH}_2$  carbon, all shifts for the compounds **5-16** are in a range from 23.4 to 24.3 ppm with a  $^2J(^{13}\text{C}-^{119}\text{Sn})$  coupling constant of 51-54 Hz. The  $\text{Sn}-\text{CH}_2\text{CH}_2-\underline{\text{C}}\text{H}_2-\text{NH}_2$  signal can be found between 39 - 41 ppm with a  $^3J(^{13}\text{C}-^{119}\text{Sn})$  coupling constant of 69.6 - 74 Hz. The amine hydrogens show a broad singlet in a range from 3.15 to 3.39 ppm. This signal cannot be detected in deuterated protic solvents such as  $d^4$ -MeOH and  $\text{D}_2\text{O}$  due to exchange processes between the amine hydrogens and the deuteriums of the solvent. Summarized, it can be said, that no correlation between the solid state structure modes and the coordination mode in solution can be identified.

### 5.3 Bonding situation in the solid state

The variety of bonding modes available to carboxylate anions in the solid state of organotin dicarboxylates is quite diverse and well-established (Scheme 34). These varied structural motifs are possible due to the ability of tin to have valency requirements satisfied by four bonds, but additionally the capacity of the Lewis acidic tin centers to increase their coordination numbers by *intra-* and/or *intermolecular* hypervalent interactions,<sup>75</sup> allowing coordination numbers up to 7 in organotin carboxylates. In literature, the most common bonding motif for the carboxylate substituent in diorganotin dicarboxylates involves bonding of the central tin atom through both oxygen atoms in a bidentate fashion (Scheme 34 C), resulting in a delocalized system. In some cases, the carbonyl oxygen is only weakly interacting with the central tin atom (Scheme 34 B).<sup>76–78</sup> Also in some cases there is no interaction between the carbonyl and the tin center. (Scheme 34 A).<sup>79,80</sup> Finally, the carbonyl oxygen on the carboxylate substituent can also bridge neighboring tin atoms (Scheme 34 D, E) forming oligo- and polymeric species. The propensity towards a particular bonding mode is dependent on several factors including the nature of the carboxylic acid, stoichiometry of reactants, but most importantly, the number and nature of the organo substituents on the tin atom.<sup>81,82</sup> In other words, the steric contribution from the organo substituent onto the Sn atom has a marked effect on the type of coordination mode presented.



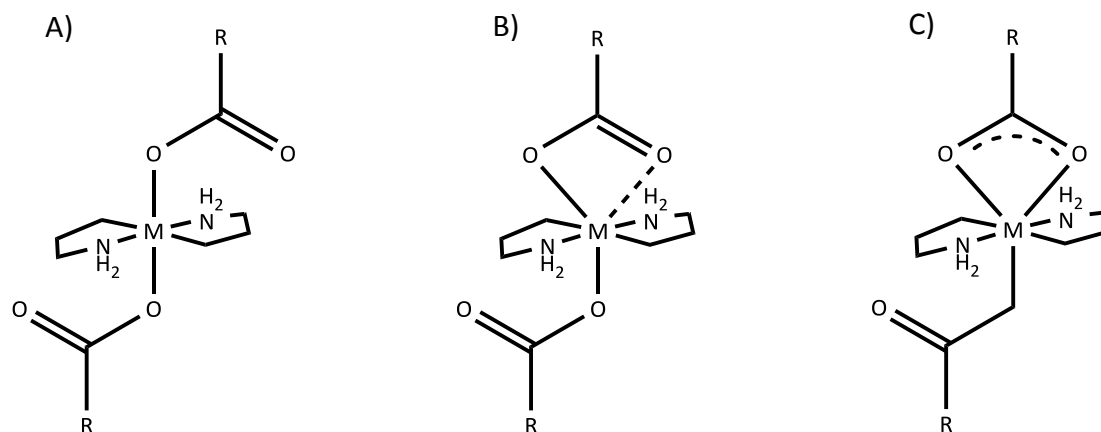
Scheme 34: Possible structural motifs for organotin(IV) esters of carboxylic acids.

However, a not so well established binding mode of the carboxylic substituents (Scheme 33A) is the monodentate mode, where only one oxygen is bound to the tin center and no interaction from the carbonyl oxygen to either the central or neighboring tin atom is observed. This mode is prevalent in cases where, in addition to the electronic contribution afforded by the carboxylate substituents, the coordinating organo substituents offer significant intramolecular contact through atoms within the substituent itself or steric saturation to the central tin atom effectively circumventing oligo- or polymerization. These compounds include di- and triorganotin(IV) compounds containing the 2-(*N,N*-dimethylaminomethyl)phenyl group as a *C,N*-chelating substituent.<sup>83,84</sup> All compounds of this type reveal significant intramolecular contact between tin and nitrogen and a monodentate bonding mode of the carboxylate substituents is observed. By the chelating ligand effectively saturating the metal center, the carbonyl oxygen from the carboxylic substituent is not capable of binding to the central tin atom.

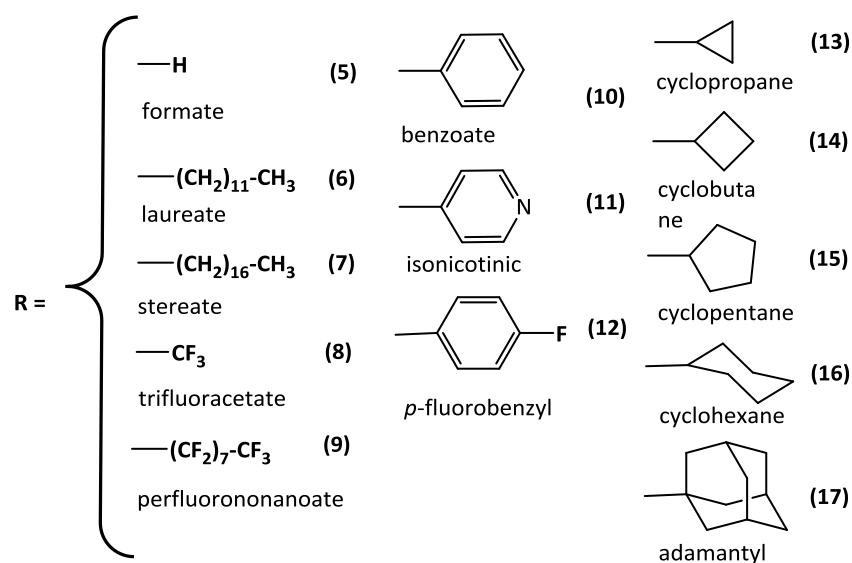
In the interest of expanding the list of diorgano substituted dicarboxylates exhibiting organo substituents with intramolecular chelating effects, a series of diaminopropyltin compounds were characterized with single crystal X-ray diffraction. These compounds exhibit carboxylic acids with a wide variety organic groups ranging from short to long chains, alkanes, cycloalkanes, aromatic rings, fluorinated chains, and functionalized benzyls. The effects of the nature of the carboxylic acid on the central tin atom geometry including the observed carboxylic bonding mode will be presented. In addition, the effects of the nature of the carboxylic acid on the packing effects of these molecules and the secondary electrostatic interactions present in the extended solid state will be highlighted and discussed.

### 5.3.1 Diaminopropyltin Dicarboxylates

All presented diaminopropyltin dicarboxylates,  $(\text{RCOO})_2\text{Sn}((\text{CH}_2)_3\text{NH}_2)_2$ , (Scheme 35) exclusively display *trans* coordination of the carboxylic substituent, despite exhibiting various carboxylic bonding motifs depending on the nature of the carboxylate used. These will be compared and contrasted based on the coordination modes exhibited by the carboxylic substituents. In each case, the chelating aminopropyl substituent displays close Sn—N dative bonds between the tin metal center and the deprotected amine and coordinates to the tin center in the equatorial plane. In addition, the deprotected amine is involved in hydrogen bonding in the solid state giving rise to interesting packing arrangements which will be described in detail below.



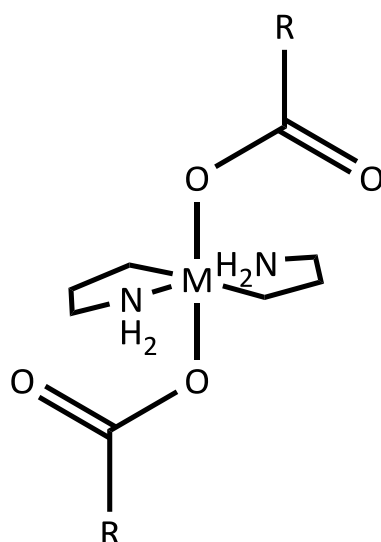
Scheme 35: Coordination modes 6, 6.5, 7.



Scheme 36: Overview of all used carboxylic acid.

### 5.3.2 Diaminopropyltin Monodentate Dicarboxylates – Coordination Number 6

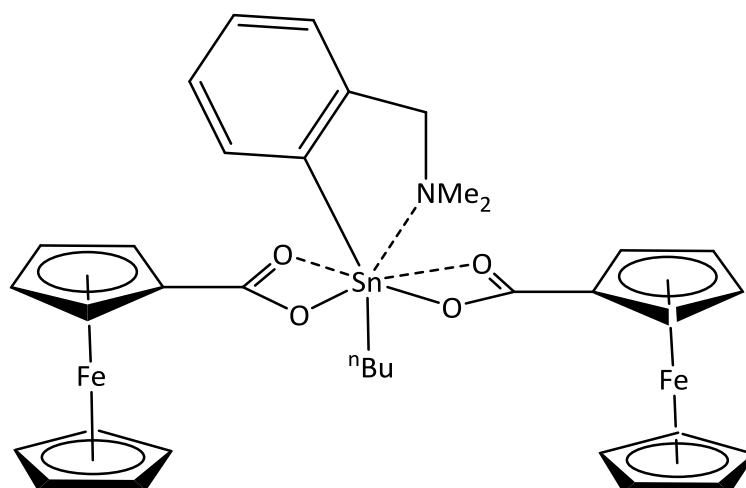
Compounds formate<sub>2</sub>SnA<sub>2</sub> (**5**) (A = -(CH<sub>2</sub>)<sub>3</sub>NH<sub>2</sub>), laurate<sub>2</sub>SnA<sub>2</sub> (**6**), stearate<sub>2</sub>SnA<sub>2</sub> (**7**), trifluoroacetate<sub>2</sub>SnA<sub>2</sub> (**8**), perfluorononanoate<sub>2</sub>SnA<sub>2</sub> (**9**), benzoate<sub>2</sub>SnA<sub>2</sub> (**10**), *p*-fluorobenzoate<sub>2</sub>SnA<sub>2</sub> (**12**), cyclopentanecarboxylate<sub>2</sub>SnA<sub>2</sub> (**15**), cyclohexanecarboxylate<sub>2</sub>SnA<sub>2</sub> (**16**), and adamantanecarboxylate<sub>2</sub>SnA<sub>2</sub> (**17**) all crystallize in a near octahedral geometry (Scheme 35A, Table 3) with the dicarboxylate substituents coordinating in a *trans* configuration with a monodentate bonding mode (Scheme 35A). With respect to Sn–O bonds, these fall within an expected range of 2.18 – 2.25 Å and are dependent more on the potential electronic withdrawing nature of the carboxylate ligand than that of its relative bulkiness. This is observed for the fluorinated carboxylic acids in trifluoroacetate<sub>2</sub>SnA<sub>2</sub> (**8**) and perfluorononanoate<sub>2</sub>SnA<sub>2</sub> (**9**), which show the longest Sn–O bonds of 2.246(13) and 2.248(10) Å respectively, as compared to the large adamantane organic group in adamantanecarboxylate<sub>2</sub>SnA<sub>2</sub> (**17**), which curiously has the shortest Sn–O bond of 2.182(2) Å. Accordingly with a monodentate bonding mode, the carbonyl oxygen for all monodentate diaminopropyltin dicarboxylates is at a distance above that of an interaction between oxygen and the Sn central atom, falling within the range of 3.29 – 3.56 Å. Nonetheless, a degree of electron delocalization is observed in the COO<sup>-</sup> moiety of the carboxylate ligand with an averaged difference between bound and free C–O bond lengths of 0.05 Å. The closest to double bond nature in the carboxylic moiety is found in perfluorononanoate<sub>2</sub>SnA<sub>2</sub> (**9**) with a C–O bond distance of 1.17(2) Å. This is also the carboxylic substituent with one of the lowest pK<sub>a</sub> of its corresponding acid (Perfluorononanoic acid, pK<sub>a</sub> = 0)<sup>85,86</sup> along with trifluoroacetate<sub>2</sub>SnA<sub>2</sub> (**8**) (Trifluoroacetic acid, pK<sub>a</sub> = -0.25).<sup>87</sup> All other corresponding carboxylic acids used range in pK<sub>a</sub> from 3.77 – 5.3.<sup>85–91</sup> Despite this delocalized nature of the carboxylic moiety, no interaction between the carbonyl oxygen with a Sn atom of a neighboring molecule is observed, rather close hydrogen bonds between neighboring NH<sub>2</sub> moieties (N–H⋯O) and the carbonyl oxygen are preferred in the extended solid state. With respect to Sn–C bonds, these fall within such a narrow range (2.13 – 2.15 Å), that statements related to steric or electronic effects of the carboxylic substituents on this bond cannot be stated.



**Scheme 37: Near octahedral geometry coordinating in a *trans* configuration with a monodentate bonding mode Monodentate Diaminopropyltin Dicarboxylates.**

Seemingly, bidentate coordination from the carboxylate substituents for these compounds is directly prevented by the chelating ability of the aminopropyl substituent which displays close Sn $\cdots$ N dative bonds to the tin center (Table 3). These Sn $\cdots$ N interactions range from 2.28 – 2.32 Å and fall within expected ranges for previously reported diaminopropyltin species with Sn $\cdots$ N dative bond lengths of 2.292(2) Å in acetate<sub>2</sub>SnA<sub>2</sub> and 2.326(4) Å in Cl<sub>2</sub>SnA<sub>2</sub>. These chelating substituents arrange themselves in the equatorial position around the tin atom effectively saturating the metal center, allowing for symmetrical and ideal octahedral geometry in nearly all monodentate diaminopropyltin dicarboxylates with all C–Sn–C, N–Sn–N, O–Sn–O angles being close to 180°, with the largest deviation observed for trifluoroacetate<sub>2</sub>SnA<sub>2</sub> (**8**). The *trans* configuration for the diaminopropyltin dicarboxylates is in stark contrast to the diorganotin dicarboxylates containing the 2-(*N,N*-dimethylaminomethyl)phenyl group as a *C,N*-chelating substituent which arrange themselves in a *cis* motif with exclusive monodentate binding of the carboxylate (Table 3). This preferred *cis* coordination is due to the sterically encumbered 2-(*N,N*-dimethylaminomethyl)phenyl not being able to comfortably lie in the equatorial plane. Trifluoroacetate<sub>2</sub>SnA<sub>2</sub><sup>\*</sup> and ferrocenoate<sub>2</sub>SnA<sub>2</sub><sup>\*</sup> (A<sup>\*</sup> = -Ph(CH<sub>2</sub>)NMe<sub>2</sub>) (Scheme 38) display on average shorter Sn–O bonds, 2.194(3) Å and 2.202(4) Å respectively, than that for the aminopropyl substituted tin dicarboxylates (2.18 – 2.25 Å).<sup>83,84</sup>





Scheme 38: Structure of ferrocenoate<sub>2</sub>SnA\*<sub>2</sub> (A\* = -Ph(CH<sub>2</sub>NMe<sub>2</sub>))<sup>83,84</sup>

Also, shorter Sn–C bonds, 2.115(3) Å and 2.125(3) Å, are observed as compared to the diaminopropyltin derivatives (2.13 – 2.15 Å). However, the protecting methyl groups on the nitrogen in the 2-(*N,N*-dimethylaminomethyl)phenyl substituent cause an elongation of the Sn⋯N dative bond in trifluoroacetate<sub>2</sub>SnA\*<sub>2</sub> (2.511(3) Å) and ferrocenoate<sub>2</sub>SnA\*<sub>2</sub> (2.579(5) Å) as compared to the range of Sn⋯N interactions in the diaminopropyltin derivatives (2.28 – 2.32 Å).

As discussed, the nature of the carboxylic acid has some small effects on the geometry around the central tin atom. However, more obvious differences can be observed when comparing the organic groups on the carboxylic acid and how their characteristics affect their orientation relative to the tin atom. First, no appreciable differences can be observed between functionalization the chains through fluorination as observed in acetate<sub>2</sub>SnA<sub>2</sub> (Figure 7a) and its fluorinated counterpart, trifluoroacetate<sub>2</sub>SnA<sub>2</sub> (**8**) (Figure 7b) and benzoate<sub>2</sub>SnA<sub>2</sub> (**10**) (Figure 8a), and its fluorinated derivative *p*-fluorobenzoate<sub>2</sub>SnA<sub>2</sub> (**12**) (Figure 8b).

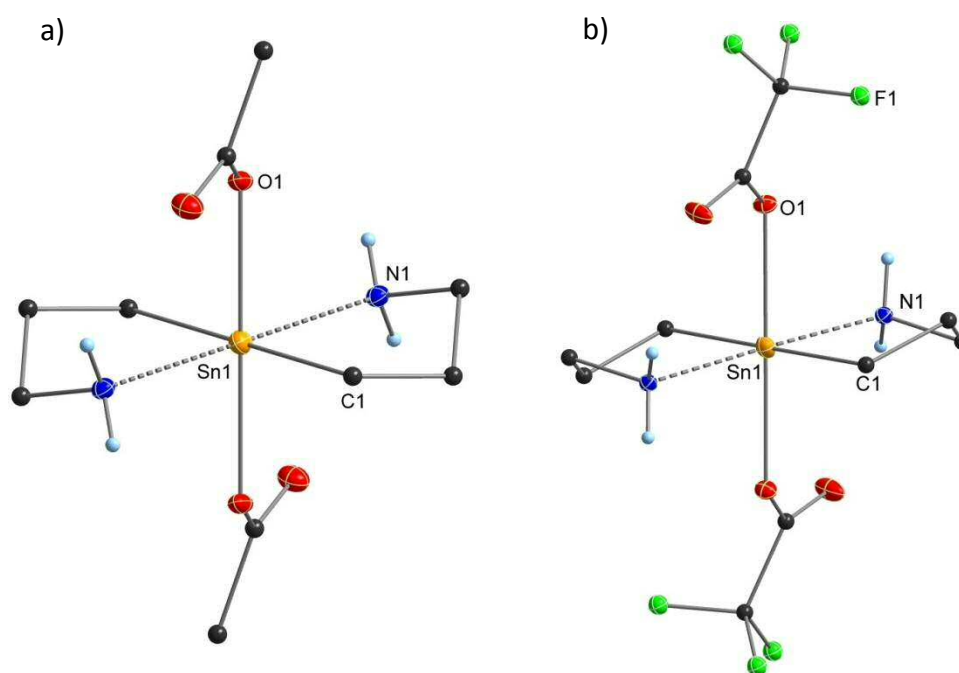


Figure 4: a) Crystal structure of acetate<sub>2</sub>SnA<sub>2</sub>.<sup>60</sup> b) Crystal structure of trifluoroacetate<sub>2</sub>SnA<sub>2</sub> (8). All non-carbon atoms shown as 30% shaded ellipsoids. Hydrogen atoms removed for clarity.

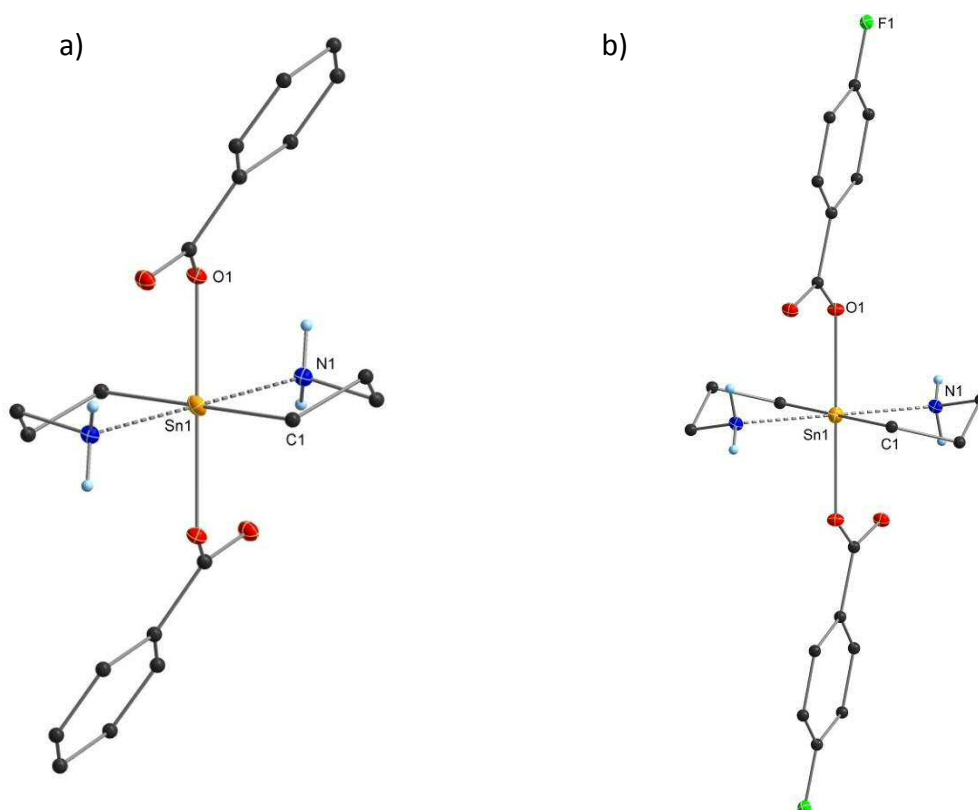


Figure 5: a) Crystal structure of benzoate<sub>2</sub>SnA<sub>2</sub> (10). b) Crystal structure of *p*-fluorobenzoate<sub>2</sub>SnA<sub>2</sub> (12). All non-carbon atoms shown as 30% shaded ellipsoids. Hydrogen atoms removed for clarity.

However, if comparing the compounds with organic groups comprised of alkyl chains, laurate<sub>2</sub>SnA<sub>2</sub> (6), stearate<sub>2</sub>SnA<sub>2</sub> (7), and perfluorononanoate<sub>2</sub>SnA<sub>2</sub> (9), we can see that chain

length has an effect on the molecular geometry. Both laurate<sub>2</sub>SnA<sub>2</sub> (**6**) and perfluorononanoate<sub>2</sub>SnA<sub>2</sub> (**9**) derivatives show the alkyl chains in the carboxylate substituents in a Z conformation (Figure 6a, b), with the alkyl chain almost perpendicular to the plane of the Sn–O bond with averaged torsion angles ( $O_1-C_\gamma-C_\alpha-C_\beta$ ) of 85.16° and 102.57°, respectively. This is in stark contrast to stearate<sub>2</sub>SnA<sub>2</sub> (**7**) which display the alkyl chains in a linear conformation (Figure 6c) in plane with the Sn–O bond with an averaged torsion angle ( $O_1-C_\gamma-C_\alpha-C_\beta$ ) of 171.93°. This linear conformation of the stearate chain is quite remarkable due to the fact that despite having the longest chain length, which should have the highest degree of freedom through the carbons in the chain, manages to remain relatively linear. While all bond lengths and angles for both the laurate<sub>2</sub>SnA<sub>2</sub> (**6**) and stearate<sub>2</sub>SnA<sub>2</sub> (**7**) derivatives are quite similar, the difference in alkyl chain orientation can be better addressed upon considering the extended solid state. These differences are highlighted and discussed below (5.4 extended structures).

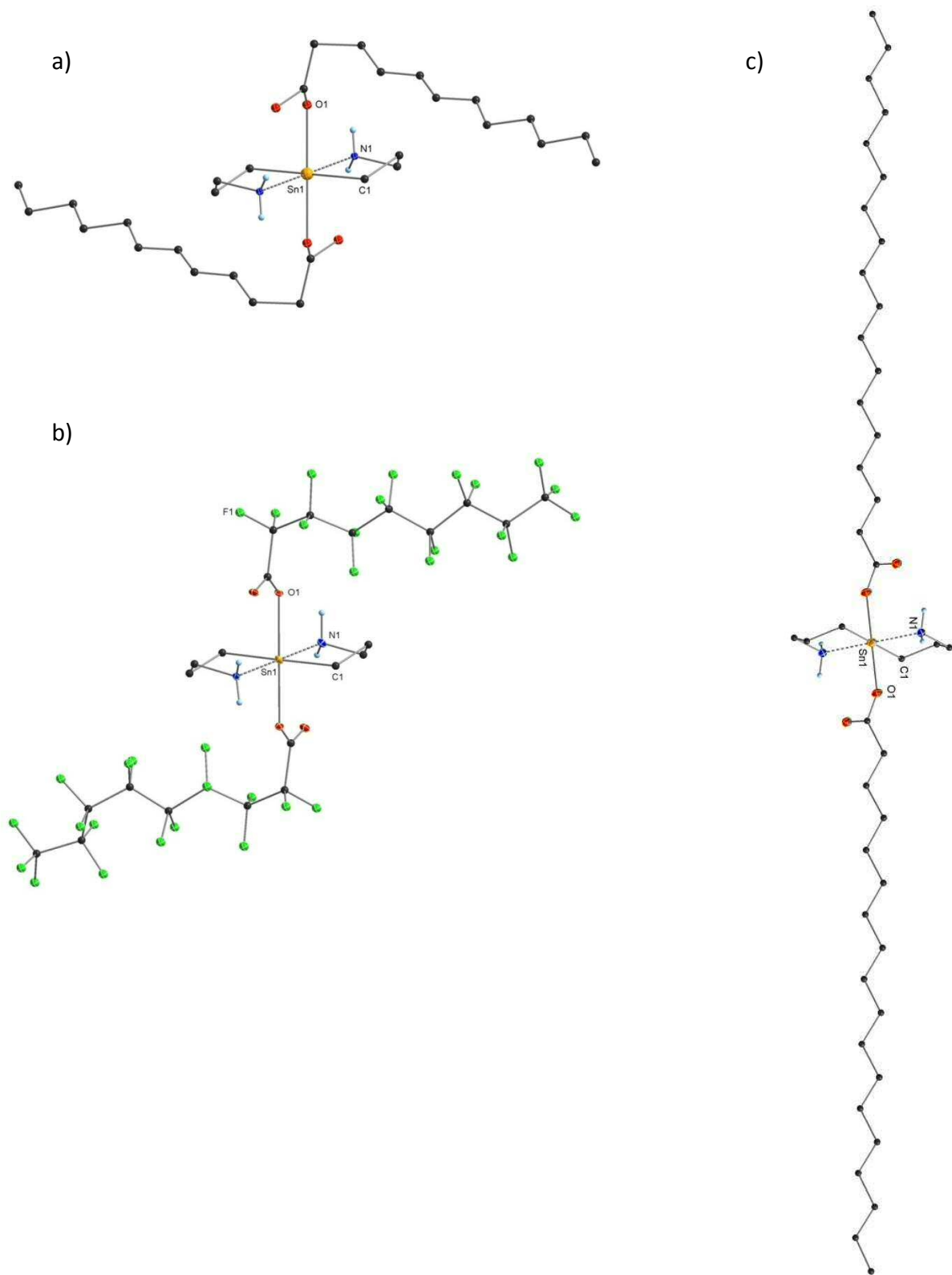


Figure 6: a) Crystal structure of laurate<sub>2</sub>SnA<sub>2</sub> (6). b) Crystal structure of perfluorononanoate<sub>2</sub>SnA<sub>2</sub> (9) c) Crystal structure of stearate<sub>2</sub>SnA<sub>2</sub> (7). All non-carbon atoms shown as 30% shaded ellipsoids. Hydrogen atoms removed for clarity.

Between cyclopentanecarboxylate<sub>2</sub>SnA<sub>2</sub> (**15**) (Figure 7a), cyclohexanecarboxylate<sub>2</sub>SnA<sub>2</sub> (**16**) (Figure 7b), and adamantanecarboxylate<sub>2</sub>SnA<sub>2</sub> (**17**) (Figure 7c) which contain cycloalkane organic groups on the carboxylate substituents, a similar discrepancy in torsion angles can also be observed. The smaller cycloalkane in cyclopentanecarboxylate<sub>2</sub>SnA<sub>2</sub> (**15**) also results in a Z conformation of the ring relative to the plane of the Sn–O bond with an averaged torsion angle ( $O_1-C_r-C_\alpha-C_\beta$ ) of  $103.65^\circ$ , while cyclohexanecarboxylate<sub>2</sub>SnA<sub>2</sub> (**16**) and adamantanecarboxylate<sub>2</sub>SnA<sub>2</sub> (**17**) show torsion angles closer to linear orientations with averaged torsion angle ( $O_1-C_r-C_\alpha-C_\beta$ ) of  $147.27^\circ$  and  $167.33^\circ$ , respectively. Finally, both benzoate<sub>2</sub>SnA<sub>2</sub> (**10**) and *p*-fluorobenzoate<sub>2</sub>SnA<sub>2</sub> (**12**) (Figure 8a, b) show linear orientations with averaged torsion angles ( $O_1-C_r-C_\alpha-C_\beta$ ) of  $178.36^\circ$  and  $175.01^\circ$ , respectively.

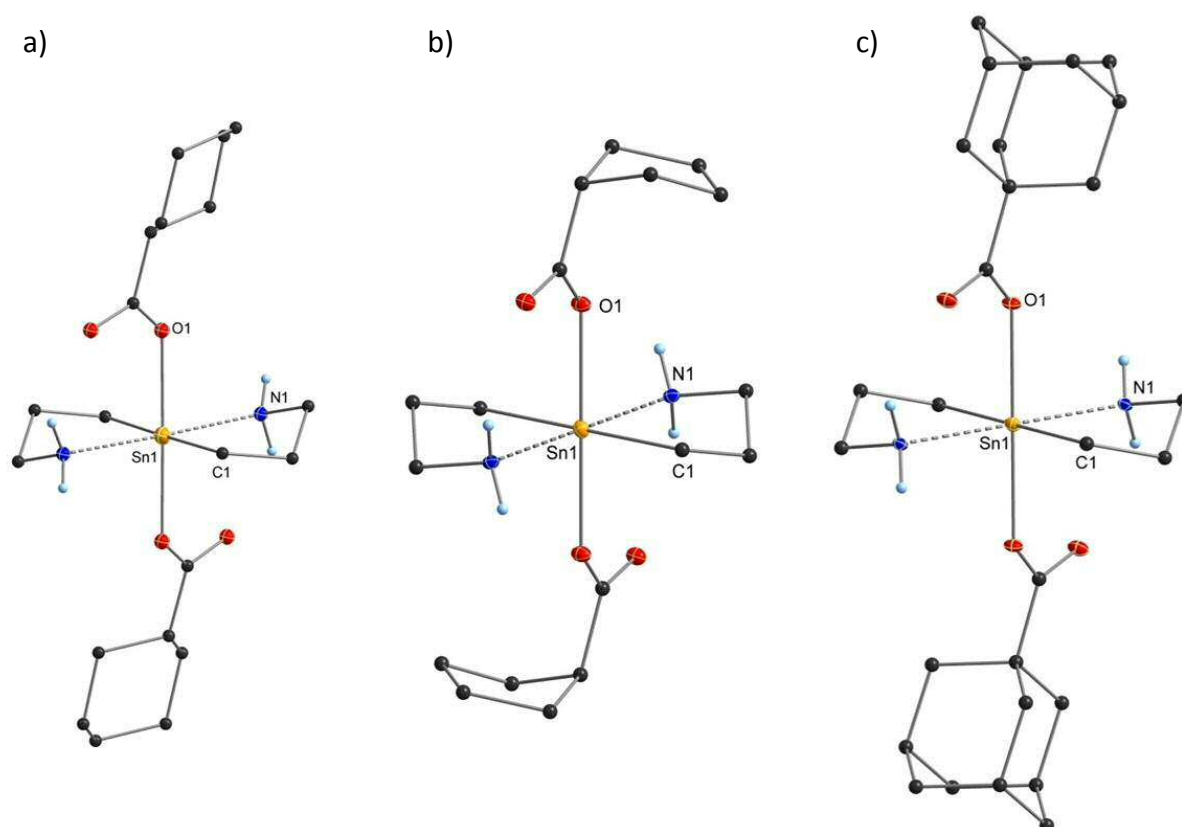


Figure 7: a) Crystal structure of cyclopentanecarboxylate<sub>2</sub>SnA<sub>2</sub> (**15**). b) Crystal structure of cyclohexanecarboxylate<sub>2</sub>SnA<sub>2</sub> (**16**). c) Crystal structure of adamantanecarboxylate<sub>2</sub>SnA<sub>2</sub> (**17**). All non-carbon atoms shown as 30% shaded ellipsoids. Hydrogen atoms removed for clarity.

Table 3: Selected bond lengths and angles for Monodentate Diaminopropyltin Dicarboxylates.

Compounds	Space Group	Sn-C (Å) (avg.)	Sn...N (Å) (avg.)	Sn-O (Å) (avg.)	Sn...O (Å) (avg.)	C-Sn-C (°)	N-Sn-N (°)	O-Sn-O (°)
acetate <sub>2</sub> SnA <sub>2</sub> <sup>11</sup>	<i>P</i> -1	2.152(2)	2.292(2)	2.242(2)	3.29	180.00(5)	180.0	180.0
laurate <sub>2</sub> SnA <sub>2</sub> ( <b>6</b> )	<i>P</i> 2 <sub>1</sub> / <i>c</i>	2.147(3)	2.292(2)	2.207(2)	3.35	180.0	180.0	180.00(4)
stearate <sub>2</sub> SnA <sub>2</sub> ( <b>7</b> )	<i>P</i> -1	2.135(7)	2.300(5)	2.226(4)	3.34	180.0	180.0	180.0
trifluoroacetate <sub>2</sub> SnA <sub>2</sub> ( <b>8</b> )	<i>P</i> 2 <sub>1</sub> / <i>n</i>	2.135(15)	2.303(13)	2.246(13)	3.44	179.58(7)	178.34(5)	178.88(4)
perfluorononanoate <sub>2</sub> SnA <sub>2</sub> ( <b>9</b> )	<i>P</i> -1	2.144(14)	2.318(12)	2.248(10)	3.56	180.0(8)	180.0	180.0
benzoate <sub>2</sub> SnA <sub>2</sub> ( <b>10</b> )	<i>P</i> 2 <sub>1</sub> / <i>c</i>	2.139(2)	2.311(2)	2.215(2)	3.39	180.0	180.0	180.0
<i>p</i> -fluorobenzoate <sub>2</sub> SnA <sub>2</sub> ( <b>12</b> )	<i>P</i> -1	2.133(2)	2.304(2)	2.228(2)	3.29	180.0	180.0	180.00(6)
cyclopentanecarboxylate <sub>2</sub> SnA <sub>2</sub> ( <b>15</b> )	<i>P</i> 2 <sub>1</sub> / <i>c</i>	2.141(4)	2.288(3)	2.194(3)	3.48	180.0	180.0	180.0
cyclohexanecarboxylate <sub>2</sub> SnA <sub>2</sub> ( <b>16</b> )	<i>P</i> -1	2.142(5)	2.279(5)	2.201(4)	3.33	180.0	180.00(15)	180.0(3)
adamantanecarboxylate <sub>2</sub> SnA <sub>2</sub> ( <b>17</b> )	<i>P</i> -1	2.150(3)	2.296(3)	2.182(2)	3.38	180.0	180.0	180.0
trifluoroacetate <sub>2</sub> SnA <sub>2</sub> <sup>2</sup>	<i>P</i> 2 <sub>1</sub> 2 <sub>1</sub> 2 <sub>1</sub>	2.115(3)	2.511(3)	2.111(3)	3.42	154.68(17)	106.70(12)	85.35(12)
ferrocenoate <sub>2</sub> SnA <sub>2</sub> <sup>3</sup>	<i>C</i> <sub>c</sub>	2.125(3)	2.579(5)	2.065(3)	3.27	155.17(19)	102.70(12)	99.83(13)

A = -(CH<sub>2</sub>)<sub>3</sub>NH<sub>2</sub>, A<sup>2</sup> = -Ph(CH<sub>2</sub>)NMe<sub>2</sub>

### 5.3.3 Mixed Diaminopropyltin Dicarboxylates –Coordination Number 7

Compounds isonicotinate<sub>2</sub>SnA<sub>2</sub> (**11**), cyclopropanecarboxylate<sub>2</sub>SnA<sub>2</sub> (**13**), and cyclobutanecarboxylate<sub>2</sub>SnA<sub>2</sub> (**14**) all crystallize in a pseudo octahedral geometry (Scheme 35A, Table 4) with the dicarboxylate substituents coordinating in a *trans* configuration as was observed with the monodentate diaminopropyltin dicarboxylates. However, in the case of isonicotinate<sub>2</sub>SnA (**11**), cyclopropanecarboxylate<sub>2</sub>SnA<sub>2</sub> (**13**), and cyclobutanecarboxylate<sub>2</sub>SnA<sub>2</sub> (**14**), mixed coordination modes of the carboxylic substituents is observed, where one substituent is coordinated through only one oxygen atom to the central tin atom (Scheme 34B), while the second carboxylate substituent displays bidentate coordination to the tin atom (Scheme 35C). This results in an overall increase in the formal coordination number around the tin atom from 6 in the monodentate diaminopropyltin dicarboxylates to 7 in isonicotinate<sub>2</sub>SnA<sub>2</sub> (**11**) (Figure 8c), cyclopropanecarboxylate<sub>2</sub>SnA<sub>2</sub> (**13**) (Figure 8a), and cyclobutanecarboxylate<sub>2</sub>SnA<sub>2</sub> (**14**) (Figure 8b).

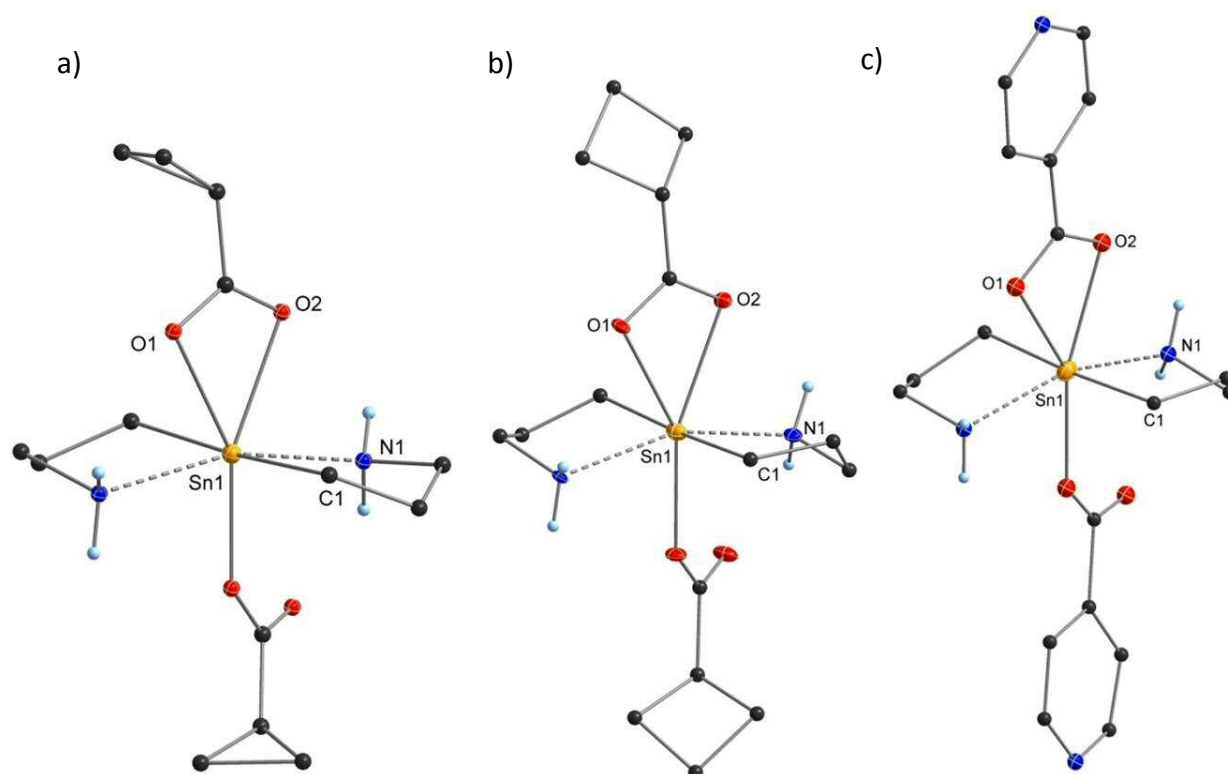
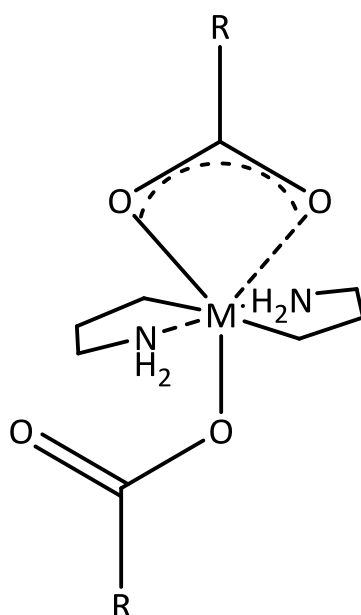


Figure 8: a) Crystal structure of cyclopropanecarboxylate<sub>2</sub>SnA<sub>2</sub> (**13**). b) Crystal structure of cyclobutanecarboxylate<sub>2</sub>SnA<sub>2</sub> (**14**). c) Crystal structure of isonicotinate<sub>2</sub>SnA<sub>2</sub> (**11**). All non-carbon atoms shown as 30% shaded ellipsoids. Hydrogen atoms removed for clarity.



**Scheme 39: pseudo octahedral geometry coordinating in a *trans* configuration with both mono- and bidentate bonding mode in mixed dentate Diaminopropyltin Dicarboxylates**

With respect to Sn–C bonds, these fall within the same narrow range (2.13 – 2.15 Å) as was observed for the monodentate dicarboxylates derivatives, thus, statements related to steric or electronic effects of the carboxylic substituents on this bond cannot be stated. However, as expected, the Sn–O bonds corresponding to the bidentate carboxylic substituents are on average longer (2.45 Å) than that for the monodentate Sn–O bonds in either the monodentate carboxylate substituents of the 6 coordinate (2.18 Å) or 7 coordinate (2.23 Å) derivatives. This is consistent with a higher degree of electron delocalization in the COO<sup>-</sup> moiety in the bidentate ligand and also consistent with a higher coordination number around the central tin atom. Nonetheless, as was observed in the monodentate dicarboxylates derivatives, a degree of electron delocalization is observed in both the mono- and bidentate COO<sup>-</sup> moieties of the carboxylates with an averaged difference between bound and free C–O bond lengths of 0.04 Å in the monodentate carboxylate and between the bidentate C–O bond lengths of 0.02 Å. No pKa effects on the binding of the carboxylic substituents were observed as all the corresponding acids of the three compounds isonicotinate<sub>2</sub>SnA<sub>2</sub> (**11**) (isonicotinic acid, pKa = 4.58), cyclopropanecarboxylate<sub>2</sub>SnA<sub>2</sub> (**13**) (cyclopropanecarboxylic acid, pKa = 4.78), and cyclobutanecarboxylate<sub>2</sub>SnA<sub>2</sub> (**14**) (cyclobutanecarboxylic acid, pKa = 4.80) have similar values.<sup>85–91</sup> In addition, the carbonyl oxygen for all the mixed dentate diaminopropyltin dicarboxylates are also at a distance above that of an interaction between oxygen and the Sn central atom, falling within the



range of 3.55 – 3.68 Å. These are on average longer than distances found for the monodentate diaminopropyltin dicarboxylates (3.29 – 3.56 Å). Despite this delocalized nature of the carboxylic moiety, no interaction between the carbonyl oxygen with a Sn atom of a neighboring molecule is observed, rather close hydrogen bonds between neighboring NH<sub>2</sub> moieties (N–H···O) and the carbonyl oxygen are preferred in the extended solid state.

In accordance with the increased coordination number, the mixed dentate diaminopropyltin dicarboxylates show longer Sn···N dative bond lengths, as compared to the monodentate derivatives with averaged Sn···N dative bond lengths of 2.321 Å in isonicotinate<sub>2</sub>SnA<sub>2</sub> (**11**), 2.331 Å in cyclopropanecarboxylate<sub>2</sub>SnA<sub>2</sub> (**13**), and 2.342 Å in and cyclobutanecarboxylate<sub>2</sub>SnA<sub>2</sub> (**14**) (Figure 11b). Despite these chelating substituents arranging themselves in the equatorial position around the tin atom effectively saturating the metal center, the bidentate carboxylate substituent forces a pseudo octahedral geometry in all mixed dentate diaminopropyltin dicarboxylates in contrast to the near perfect octahedral environment for tin found in the monodentate diaminopropyltin dicarboxylates. In the mixed dentate diaminopropyltin dicarboxylates, while the C–Sn–C angles show the highest degree of linearity with C–Sn–C angles of 176.9(4)° in isonicotinate<sub>2</sub>SnA<sub>2</sub> (**11**), 177.1(2)° in cyclopropanecarboxylate<sub>2</sub>SnA<sub>2</sub> (**13**), and 175.45(8)° in cyclobutanecarboxylate<sub>2</sub>SnA<sub>2</sub> (**14**). However, deviations from ideal octahedral geometry begin to arise with respect to the chelating aminopropyl moiety with compounds isonicotinate<sub>2</sub>SnA<sub>2</sub> (**11**), cyclopropanecarboxylate<sub>2</sub>SnA<sub>2</sub> (**13**), and cyclobutanecarboxylate<sub>2</sub>SnA<sub>2</sub> (**14**) displaying N–Sn–N angles of 158.7(3)°, 160.81(17)°, and 158.28(6)°, respectively. These deviations result in the aminopropyl substituent puckering towards the monodentate substituent as a result of the higher steric contribution provided by the bidentate carboxylate substituent and the resulting higher coordination number on the Sn. Accordingly, with the nonsymmetrical O–Sn–O angles as a result of the mixed dentate bonding modes, these show the largest deviations from octahedral geometry with angles ranging from 144.4(2)° – 161.3(2)°.

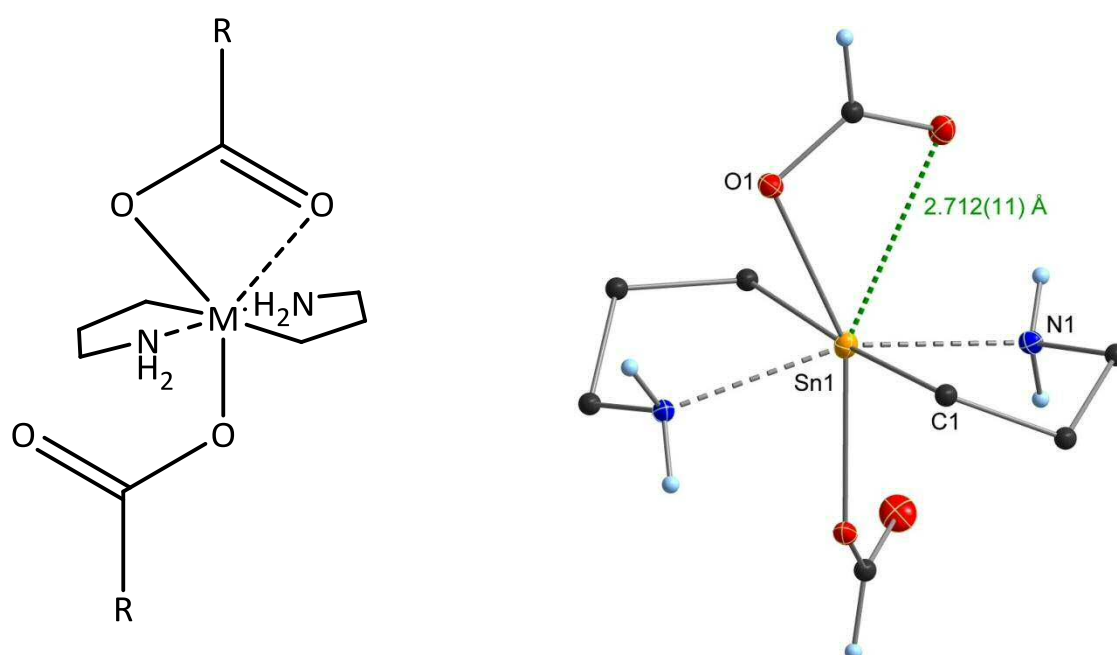
Table 4: Selected bond lengths and angles for mixed Mono and bidentate Diaminopropyltin

Compounds	Space Group	Sn-C (Å)	Sn...N (Å)	Sn-O (bidentate) (Å)	Sn-O (monodentate) (Å)	Sn...O (Å)	C-Sn-C (°)	N-Sn-N (°)	O-Sn-O (°)
formate <sub>2</sub> SnA <sub>2</sub> (5)	<i>P2<sub>1</sub>/n</i>	2.138(4) 2.136(4)	2.312(4) 2.307(3)	2.354(2) 2.249(2)	2.712(11)	3.46	175.15(6)	160.53(5)	153.02(4) 155.10(4)
isonicotinate <sub>2</sub> SnA <sub>2</sub> (11)	<i>P2<sub>1</sub></i>	2.126(8) 2.154(8)	2.308(8) 2.333(7)	2.434(6) 2.478(6)	2.247(6)	3.68	176.9(4)	158.7(3)	144.4(2) 161.3(2)
cyclopropanecarboxylate <sub>2</sub> SnA <sub>2</sub> (13)	<i>P2<sub>1</sub>/c</i>	2.145(5) 2.147(6)	2.313(5) 2.348(5)	2.441(4) 2.450(4)	2.218(4)	3.60	177.1(2)	160.81(17)	149.15(15) 157.05(15)
cyclobutanecarboxylate <sub>2</sub> SnA <sub>2</sub> (14)	<i>P2<sub>1</sub>/n</i>	2.131(2) 2.132(2)	2.332(7) 2.348(7)	2.426(4) 2.484(5)	2.225(4)	3.55	175.45(8)	158.28(6)	149.89(5) 156.78(5)

A = -(CH<sub>2</sub>)<sub>3</sub>NH<sub>2</sub>

### 5.3.4 Mixed Diaminopropyltin Dicarboxylate – Coordination Number 6.5

Due to the unique bonding situation in formate<sub>2</sub>SnA<sub>2</sub> (**5**), it is described separately. This compound crystallizes in a pseudo octahedral geometry with the dicarboxylate substituents coordinating in a *trans* configuration as was observed with the monodentate diaminopropyltin dicarboxylates. However, mixed coordination modes of the carboxylic substituents is observed, where one substituent is coordinated through only one oxygen atom to the central tin atom (Scheme 35A). In contrast to the Mixed Mono- and Bidentate Diaminopropyltin Dicarboxylates, the second carboxylate substituent displays a much weaker bidentate coordination to the tin atom (Scheme 39) resulting from a longer carbonyl oxygen to tin bond length of 2.712(11) Å as compared to the averaged Sn–O bond length of 2.45 Å for isonicotinate<sub>2</sub>SnA<sub>2</sub> (**11**), cyclopropanecarboxylate<sub>2</sub>SnA<sub>2</sub> (**13**), and cyclobutanecarboxylate<sub>2</sub>SnA<sub>2</sub> (**14**). This can then be better described as a pseudo bidentate coordination mode through a Sn⋯O dative bond between the carbonyl oxygen and the tin atom (Scheme 35B).



Scheme 40: a) Mixed Mono- and Pseudo Bidentate Diaminopropyltin Dicarboxylate – Coordination Number 6.5 pseudo octahedral geometry coordinating in a *trans* configuration with both mono- and bidentate bonding mode in mixed dentate Diaminopropyltin Dicarboxylates. b) Crystal structure of formate<sub>2</sub>SnA<sub>2</sub> (**5**). All non-carbon atoms shown as 30% shaded ellipsoids. Hydrogen atoms removed for clarity.

Only a few other diorganotin dicarboxylates were shown to have such a weak Sn–O bidentate bond length ranging from 2.71–2.81 Å.<sup>92–95</sup> However, these cannot be compared directly to formate<sub>2</sub>SnA<sub>2</sub> (**5**) due to vastly different organosubstituents and carboxylic substituents between compounds. Nevertheless, all other bond lengths and angles for formate<sub>2</sub>SnA<sub>2</sub> (**5**) (Scheme 40) fall within expected ranges (Table 4). Also, no pKa effects on the binding of the formate substituents were observed as the pKa of the corresponding acid of formate<sub>2</sub>SnA<sub>2</sub> (**5**) (formic acid, pKa = 3.77) is similar to all other carboxylic acids presented, ranging in pKa from 3.77 – 5.3. In addition, the carbonyl oxygen in formate<sub>2</sub>SnA<sub>2</sub> (**5**) is at a distance of 3.46 Å. Also, no interaction between the carbonyl oxygen with a tin atom of a neighboring molecule is observed, rather close hydrogen bonds between neighboring NH<sub>2</sub> moieties (N–H···O) and the carbonyl oxygen are preferred in the extended solid state.

### 5.3.5 Aminopropyltin Bidentate Dicarboxylate – Coordination Number 6

Compound laurate<sub>2</sub><sup>n</sup>propylSnA (**18**) (figure 13) crystallizes in a distorted trigonal bipyramidal geometry with the nitrogen from the chelating aminopropyltin and the bidentate carboxylate substituents in the basal plane. In contrast to all other species discussed, both the carboxylate substituents bind to the tin atom in a bidentate fashion (Scheme 35B) and are in a *cis* configuration, resulting from the substitution of an aminopropyl substituent by an <sup>n</sup>propyl organosubstituent (Table 3). A slight deviation in bond lengths in laurate<sub>2</sub><sup>n</sup>propylSnA (**18**) as compared to all other presented compounds is related to the Sn–C bond lengths of the different organosubstituents. The Sn–C bond length for the aminopropyl substituent falls within expected ranges with a distance of 2.124(13) Å. A slightly longer Sn–C bond length is observed for the <sup>n</sup>propyl with a bond length of 2.183(16). All other bond lengths are within expected ranges. Curiously, one of the alkyl chains remains in the plane of the carboxylate moiety and the tin atom, while the other is perpendicular to the basal plane (91.2°).

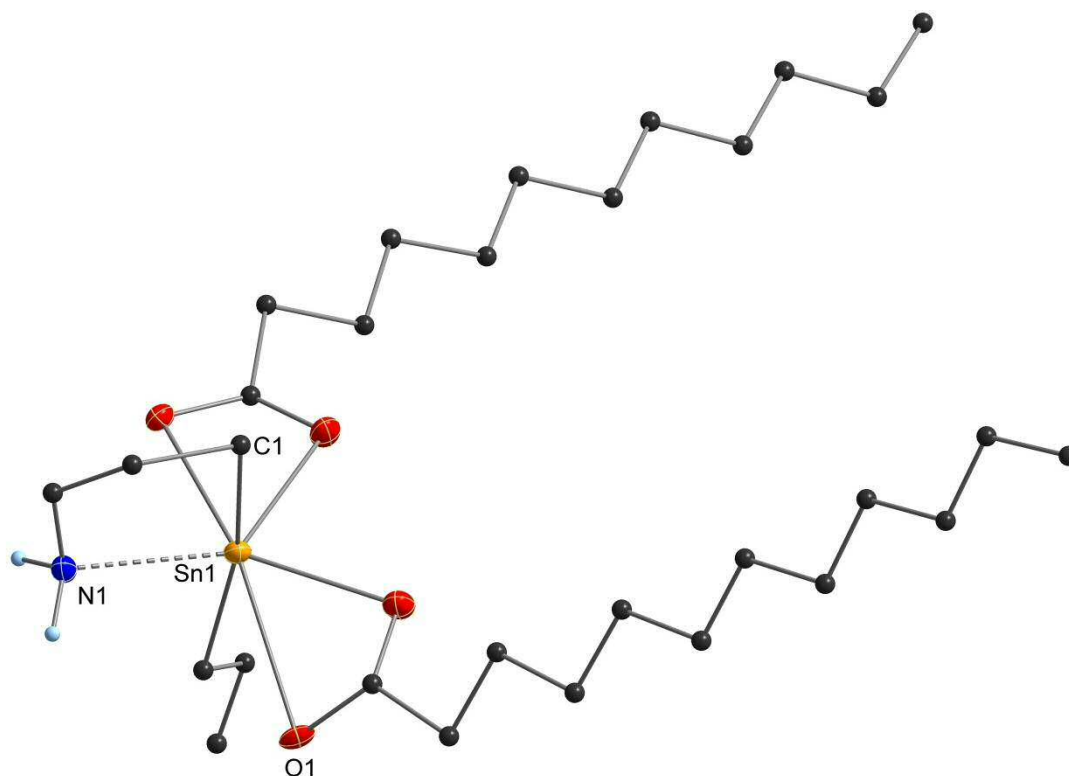


Figure 9: Crystal structure of laurate<sub>2</sub><sup>n</sup>propylSnA (18). All non-carbon atoms shown as 30% shaded ellipsoids. Hydrogen atoms removed for clarity.

As mentioned above, despite all monodentate diaminopropyltin dicarboxylates displaying *trans* coordination of the carboxylate substituents, marked differences can be observed in the orientation of the organic group of these substituents in the molecular structure depending on their nature i.e. chain length, alkyl or aryl, functionalization, conjugation and fluorination. In addition, the nature of these organic groups on the carboxylate substituents has a direct consequence on the packing effects and the intermolecular interactions these molecules use to optimize their arrangement in the extended solid state.

## 5.4 Extended structures

As mentioned above, despite all monodentate diaminopropyltin dicarboxylates displaying *trans* coordination of the carboxylate substituents, marked differences can be observed in the orientation of the organic group of these substituents in the molecular structure depending on their nature i.e. chain length, alkyl or aryl, functionalization, conjugation and fluorination. In addition, the nature of these organic groups on the carboxylate substituents has a direct consequence on the packing effects and the intermolecular interactions these molecules use to optimize their arrangement in the extended solid state. These include a variety of hydrogen bonding interactions (C/N–H···O),<sup>96–101</sup> electrostatic non-covalent intermolecular interactions<sup>102–105</sup> in the form of  $\pi$ -stacking stemming from the aromatic substituents and van der Waals contacts<sup>106,107</sup> from the halogenide substituent and adjacent hydrogens, C–H···F. While individually these are weak interactions, combined they offer an overall stabilizing effect to these molecules in the solid state and aid in their crystallization.

All presented compounds display N–H···O hydrogen bonds between the hydrogens from the amino group and the oxygens from the carboxylate substituents of a neighboring molecule. While through the aid of these interactions discrete orientations in the solid state are observed, not all compounds display the same degree of dimensionality. The degree of propagation is then more dependent on the nature of the substituent i.e. chain length, alkyl or aryl, functionalization, conjugation and fluorination and the additional interactions that these substituents can provide. The three main types of network propagation for the monodentate diaminopropyltin dicarboxylates will be described below and the additional interactions present will be highlighted and discussed.

### 5.4.1 1D Chains

The simplest method that these monodentate diaminopropyltin dicarboxylates propagate in the extended solid state is through N–H···O hydrogen bonds between the amino group and the carbonyl oxygen from the carboxylate substituents of a neighboring molecule creating a 1D chain. This motif is adopted by compounds cyclohexanecarboxylate<sub>2</sub>SnA<sub>2</sub> (**16**) (2.06 – 2.18 Å) and adamantanecarboxylate<sub>2</sub>SnA<sub>2</sub> (**17**) (2.08 – 2.20 Å) (Figure 10) where no other interactions between the chains is observed.

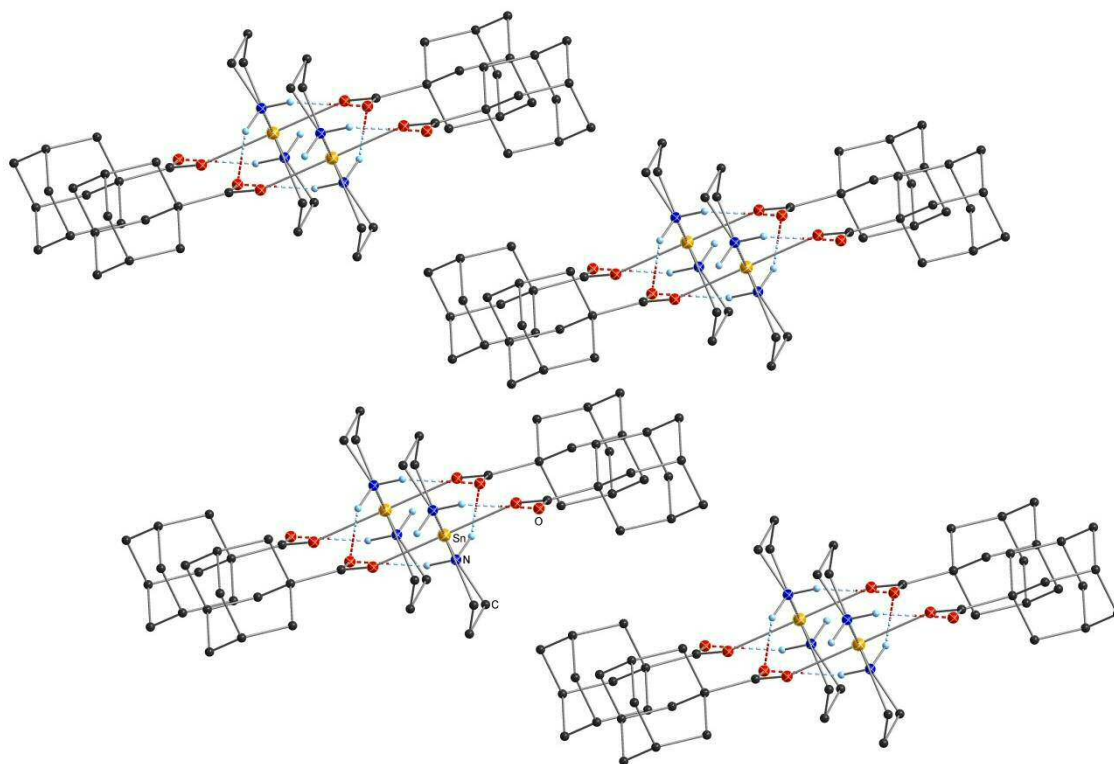


Figure 10: Crystal packing diagram for adamantanecarboxylate<sub>2</sub>SnA<sub>2</sub> (**17**). N–H···O hydrogen bonds highlighted by dashed bonds. All non-carbon atoms shown as 30% shaded ellipsoids. Hydrogen atoms not involved in intermolecular interactions removed for clarity.

### 5.4.2 2D Sheets

While in 1D chains the N–H···O hydrogen bonds are exclusively found between the amino group and the carbonyl oxygen from the carboxylate substituents of a neighboring molecule, additional N–H···O hydrogen bonds arising between the carbonyl as well as the metal bound carboxylate oxygen allows for propagation of molecules in a continuous plane. These sheets can also be propagated by C–H···O interactions arising from the organic substituent and even van der Waals contacts from the halogenide substituent and adjacent fluorides, C–H···F depending on the nature of the substituent and bonding motif of the carboxylate moiety. However, no interaction between these sheets is observed resulting in 2D networks. In the case of formate<sub>2</sub>SnA<sub>2</sub> (**5**) (Figure 11), all hydrogens from the amino moieties are involved in N–H···O hydrogen bonding with either the carbonyl oxygen or the metal bound oxygen from the carboxylate substituent (2.13 – 2.45 Å). This bonding motif is also observed for acetate<sub>2</sub>SnA<sub>2</sub>. No interaction is observed from the hydrogen atom on the formate substituent with neighboring molecules.

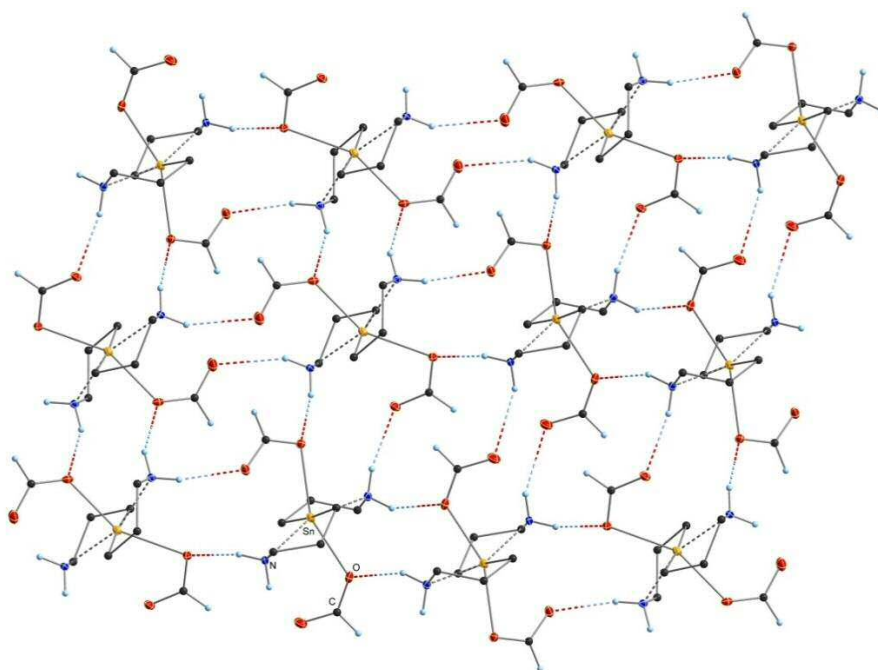
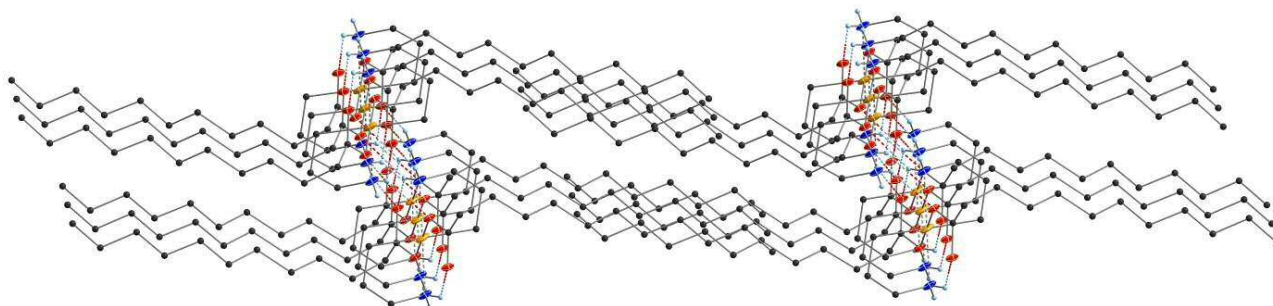


Figure 11: Crystal packing diagram for formate<sub>2</sub>SnA<sub>2</sub> (**5**). N–H···O hydrogen bonds highlighted by dashed bonds. All non-carbon atoms shown as 30% shaded ellipsoids. Hydrogen atoms not involved in intermolecular interactions removed for clarity.



In the case of laurate<sub>2</sub>SnA<sub>2</sub> (**6**) (2.02 – 2.56 Å) (Figure 12) and cyclopentanecarboxylate<sub>2</sub>SnA<sub>2</sub> (**15**) (2.03 – 2.59 Å), N–H···O hydrogen bonding interactions are occurring between hydrogens from the amino moieties and to the carbonyl oxygens. These carbonyl oxygens are involved in two N–H···O hydrogen bonding interactions and effectively propagate into sheets through these bridging interactions. Again, no interaction between these sheets is observed resulting in 2D networks. This bridging capacity from the carbonyl oxygen is also observed in compound stearate<sub>2</sub>SnA<sub>2</sub> (**7**) (2.18 – 2.25 Å) (Figure 13), but in this case the hydrogen bond is not exclusively to the amino hydrogens, rather C–H···O interactions are occurring between the stearate chain and the carbonyl oxygen from a neighboring molecule propagating the sheet (2.57 Å). In addition to N–H···O interactions observed for cyclopropanecarboxylate<sub>2</sub>SnA<sub>2</sub> (**13**) (2.03 – 2.28 Å), and cyclobutanecarboxylate<sub>2</sub>SnA<sub>2</sub> (**14**) (2.07 – 2.30 Å) (Figure 14), C–H···O hydrogen bonding interactions are also present. However, these occur intramolecularly between the aminopropyl chain and the bidentate carboxylate moiety in cyclopropanecarboxylate<sub>2</sub>SnA<sub>2</sub> (**13**) (2.53 – 2.59 Å), and cyclobutanecarboxylate<sub>2</sub>SnA<sub>2</sub> (**14**) (2.55 Å).



**Figure 12: Crystal packing diagram of laurate<sub>2</sub>SnA<sub>2</sub> (**6**) displaying 2D sheet intercalation through the laurate moiety creating layers. N–H···O interactions highlighted by dashed bonds. All non-carbon atoms shown as 30% shaded ellipsoids. Hydrogen atoms not involved in intermolecular interactions removed for clarity.**

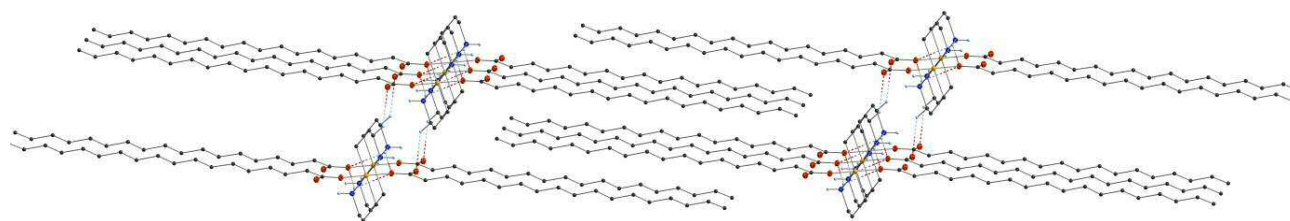


Figure 13: Crystal packing diagram of stearate<sub>2</sub>SnA<sub>2</sub> (**7**) displaying 2D sheet intercalation through the laurate moiety creating layers. N–H···O and C–H···O interactions highlighted by dashed bonds. All non-carbon atoms shown as 30% shaded ellipsoids. Hydrogen atoms not involved in intermolecular interactions removed for clarity.

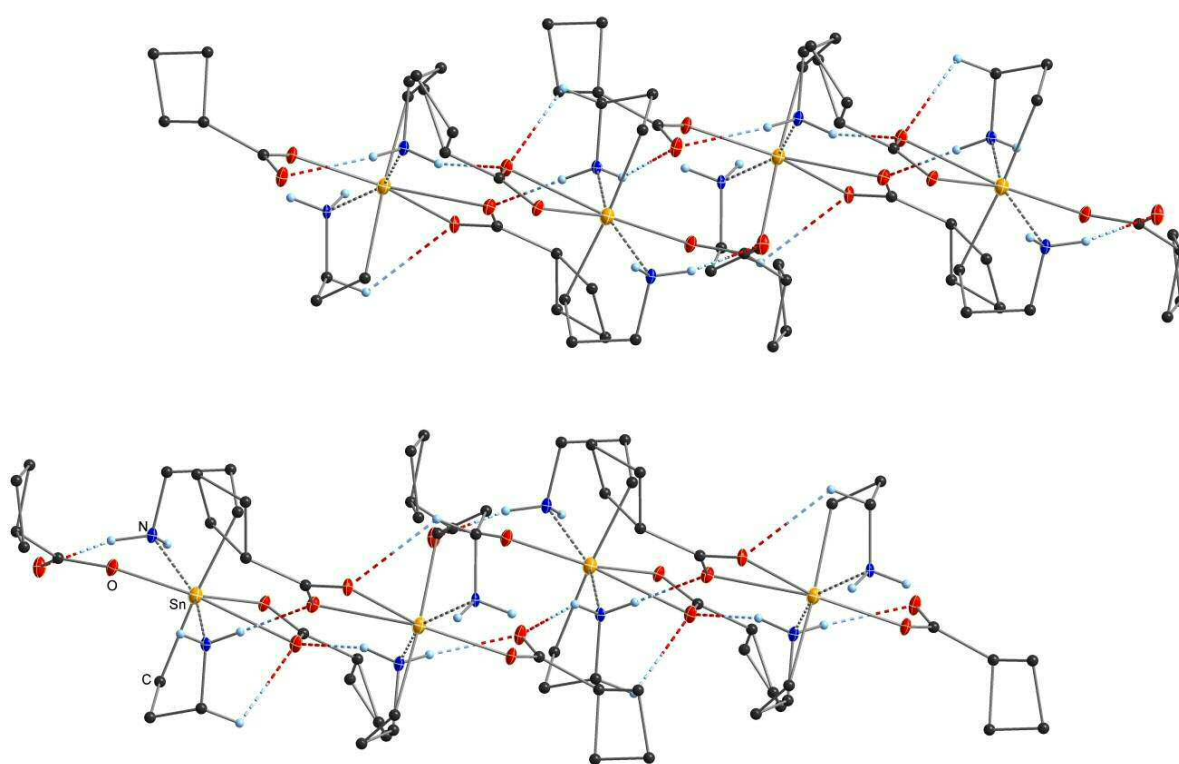
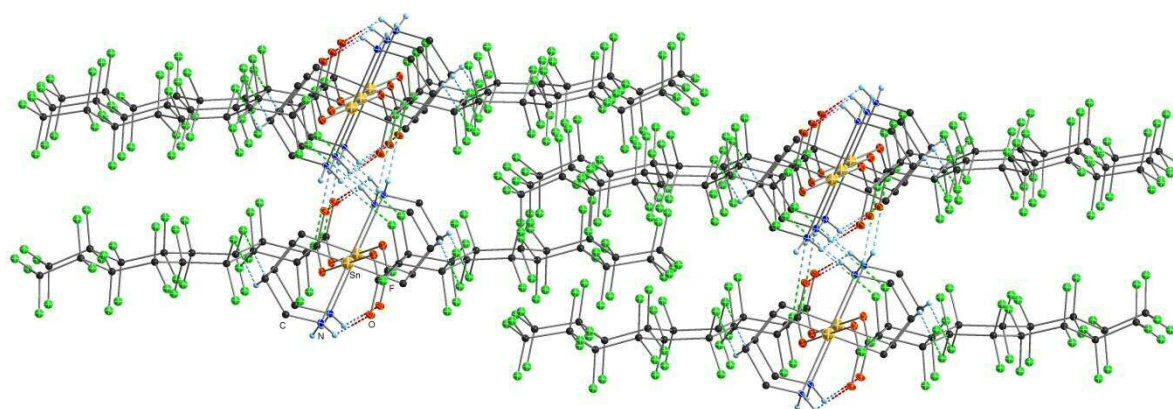


Figure 14: Crystal packing diagram for cyclobutanecarboxylate<sub>2</sub>SnA<sub>2</sub> (**14**). N–H···O and intramolecular C–H···O hydrogen bonds highlighted by dashed bonds. All non-carbon atoms shown as 30% shaded ellipsoids. Hydrogen atoms not involved in intermolecular interactions removed for clarity.

While there is a clear separation of the planar sheets in formate<sub>2</sub>SnA<sub>2</sub> (**5**), acetate<sub>2</sub>SnA<sub>2</sub>, cyclopropanecarboxylate<sub>2</sub>SnA<sub>2</sub> (**13**), cyclobutanecarboxylate<sub>2</sub>SnA<sub>2</sub> (**14**) and cyclopentanecarboxylate<sub>2</sub>SnA<sub>2</sub> (**15**), the longer alkyl chains in laurate<sub>2</sub>SnA<sub>2</sub> (**6**) and stearate<sub>2</sub>SnA<sub>2</sub> (**7**) create intercalated layers exhibiting discrete hydrophilic and hydrophobic

regions. This intercalation is occurring despite the different conformations of the alkyl chains in the carboxylate substituents of these long chain carboxylate compounds. laurate<sub>2</sub>SnA<sub>2</sub> (**6**) with the alkyl chain almost perpendicular to the plane of the Sn–O bond in a Z conformation and in stark contrast to stearate<sub>2</sub>SnA<sub>2</sub> (**7**) which displays the alkyl chains in a linear conformation. A similar type of arrangement or interdigitation can also be observed in the arrangement of membrane lipids which form the surface of all cells.

Perfluorononanoate<sub>2</sub>SnA<sub>2</sub> (**9**) (Figure 15), also arranges the alkyl chains in the carboxylate substituents in a Z conformation despite the exchange of all hydrogens in the alkyl chain by fluoride atoms. Similar to laurate<sub>2</sub>SnA<sub>2</sub> (**6**) the perfluorinated alkyl chains in perfluorononanoate<sub>2</sub>SnA<sub>2</sub> (**9**) intercalate to create layers exhibiting discrete hydrophilic and hydrophobic regions. In addition, similar to laurate<sub>2</sub>SnA<sub>2</sub> (**6**), N–H···O hydrogen bonding interactions are occurring between hydrogens from the amino moieties and to the carbonyl oxygens. These carbonyl oxygens are involved in two N–H···O hydrogen bonding interactions and effectively propagate into sheets through these bridging interactions. Additional C–H···F hydrogen bonding interactions (2.55 – 2.59 Å) and N–H···F (2.39 Å) hydrogen bonding interactions are present. The additional van der Waals interactions C–H···F (2.58 – 2.64 Å) and N–H···F (2.49 – 2.60 Å), in addition to N–H···O hydrogen bonding (2.11 – 2.37 Å), is also observed in the fluorinated formate derivative trifluoroacetate<sub>2</sub>SnA<sub>2</sub> (**8**).



**Figure 15: Crystal packing diagram of perfluorononanoate<sub>2</sub>SnA<sub>2</sub> (**9**) displaying 2D sheet intercalation through the laurate moiety creating layers. N–H···O, C–H···F, N–H···F interactions highlighted by dashed bonds. All non-carbon atoms shown as 30% shaded ellipsoids. Hydrogen atoms not involved in intermolecular interactions removed for clarity.**

### 5.4.3 3D Networks

As discussed above, all monodentate diaminopropyltin dicarboxylates propagate in the extended solid state through N–H···O hydrogen bonding interactions. This was shown for long chain alkanes, cycloalkanes, and even fluorinated substituents. However, in the case of benzoate<sub>2</sub>SnA<sub>2</sub> (**10**), isonicotinate<sub>2</sub>SnA<sub>2</sub> (**11**), and *p*-fluorobenzoate<sub>2</sub>SnA<sub>2</sub> (**12**), 3D networks are able to be obtained through the functionalization of the organic moiety on the carboxylate substituent. In the case of benzoate<sub>2</sub>SnA<sub>2</sub> (**10**) (Figure 16), the expected N–H···O hydrogen bonding interactions are present, creating 2D sheets. These 2D sheets are also propagated by secondary noncovalent CH<sub>3</sub>···π interactions (2.69 Å) between a hydrogen from the propylamino chain and the aromatic ring of a neighboring molecule. In addition, the aromatic phenyl groups on the backbone of the carboxylate substituents between 2D sheets are involved in edge to face interactions (3.15 Å) creating a 3D network.

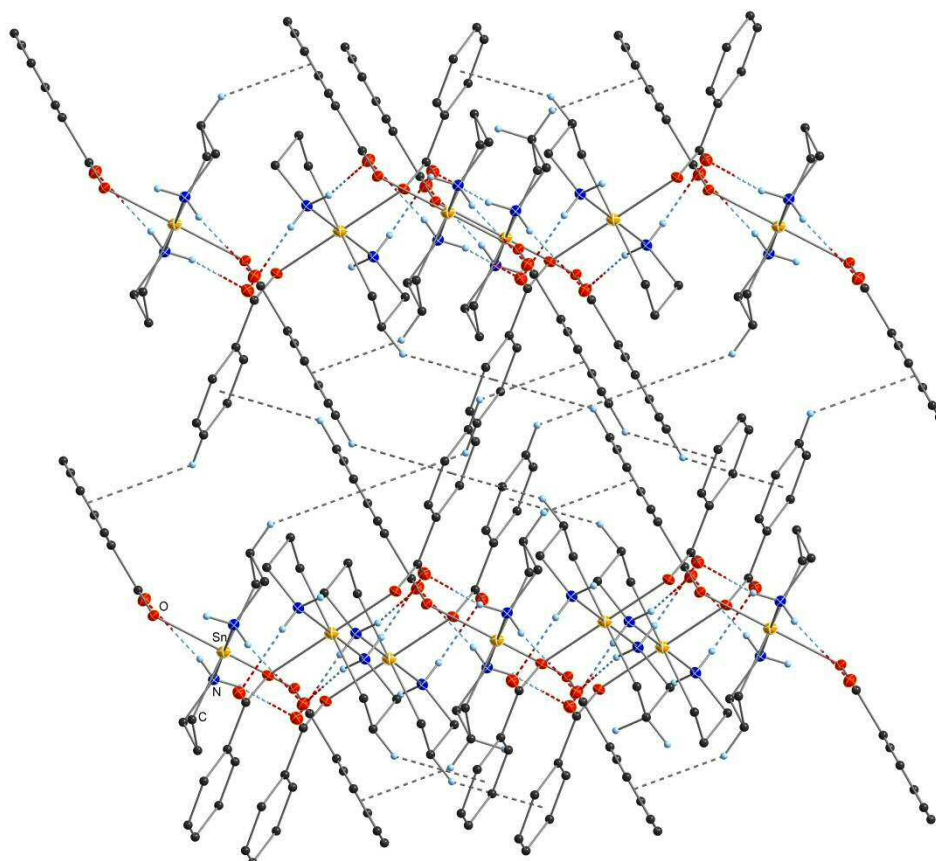


Figure 16: Crystal packing diagram for benzoate<sub>2</sub>SnA<sub>2</sub> (**10**). N–H···O hydrogen bonds, CH<sub>3</sub>···π and edge to face interactions highlighted by dashed bonds. All non-carbon atoms shown as 30% shaded ellipsoids. Hydrogen atoms not involved in intermolecular interactions removed for clarity.

Secondary interactions are also responsible for the propagation of a 3D network in *p*-fluoro-benzoate<sub>2</sub>SnA<sub>2</sub> (**12**) (Figure 17). In this case, 1D chains are propagated through N–H···O hydrogen bonding interactions (2.18 – 2.24 Å). 2D sheets are then created through  $\pi$ – $\pi$  ( $d = 3.41$ ,  $R = 1.58$  Å) interactions through the *p*-fluorobenzoate rings of adjacent 1D chains. Finally, a 3D network is created by N–H···F hydrogen bonding interactions (2.75 Å) between the fluorine atom at the *para* position on the phenyl ring of the carboxylate substituent and an amino hydrogen from a neighboring 2D sheet. A substituent in the *para* position is also responsible for the propagation of a 3D network in isonicotinate<sub>2</sub>SnA<sub>2</sub> (**11**) (Figure 18). In addition to N–H···O (2.18 – 2.24 Å) and C–H···O (2.62 Å) hydrogen bonding interactions, the nitrogen at 6 position in the isonicotinate ring is involved in N–H···N interactions with the amino hydrogens of neighboring molecules (2.34 Å).

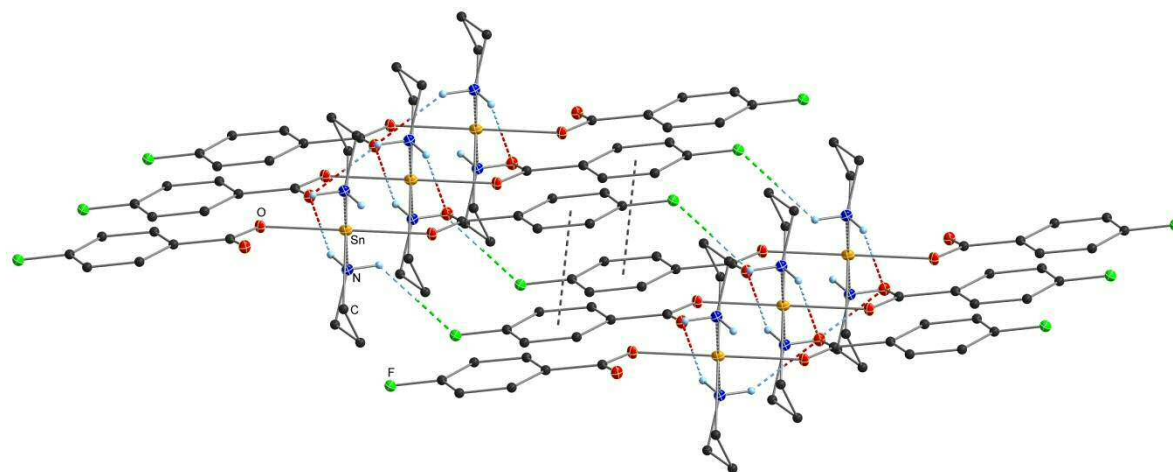


Figure 17: Crystal packing diagram for *p*-fluorobenzoate<sub>2</sub>SnA<sub>2</sub> (**12**). N–H···O and N–H···F hydrogen bonds, and  $\pi$ – $\pi$  interactions highlighted by dashed bonds. All non-carbon atoms shown as 30% shaded ellipsoids. Hydrogen atoms not involved in intermolecular interactions removed for clarity.



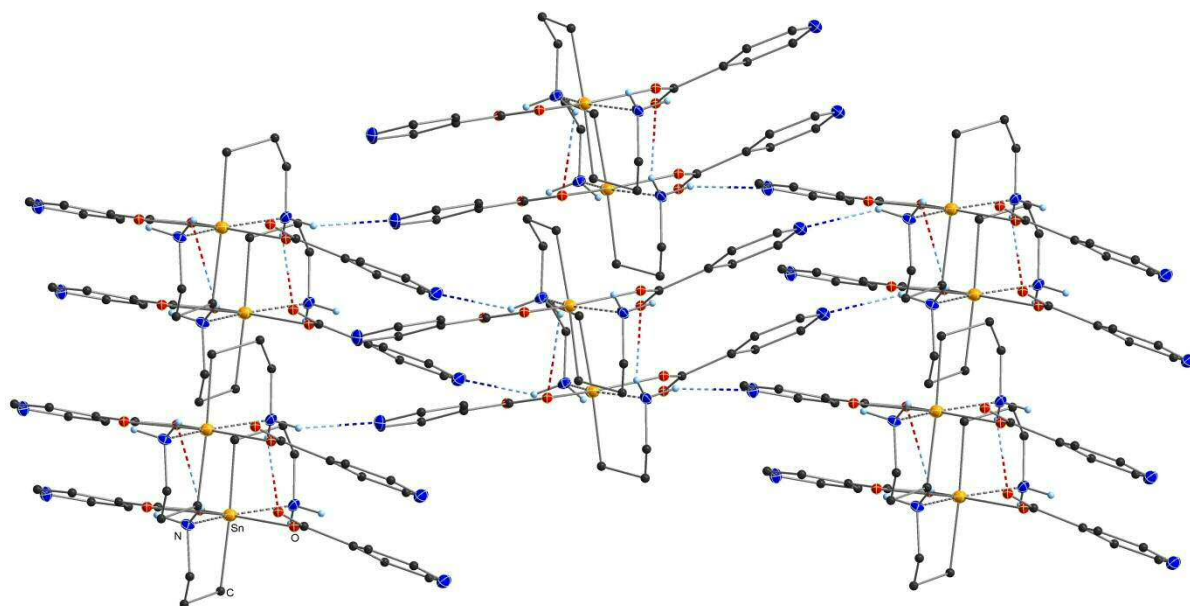


Figure 18: Crystal packing diagram for isonicotinate<sub>2</sub>SnA<sub>2</sub> (11). N–H···O and N–H···N hydrogen bonds interactions highlighted by dashed bonds. All non-carbon atoms shown as 30% shaded ellipsoids. Hydrogen atoms not involved in intermolecular interactions removed for clarity.

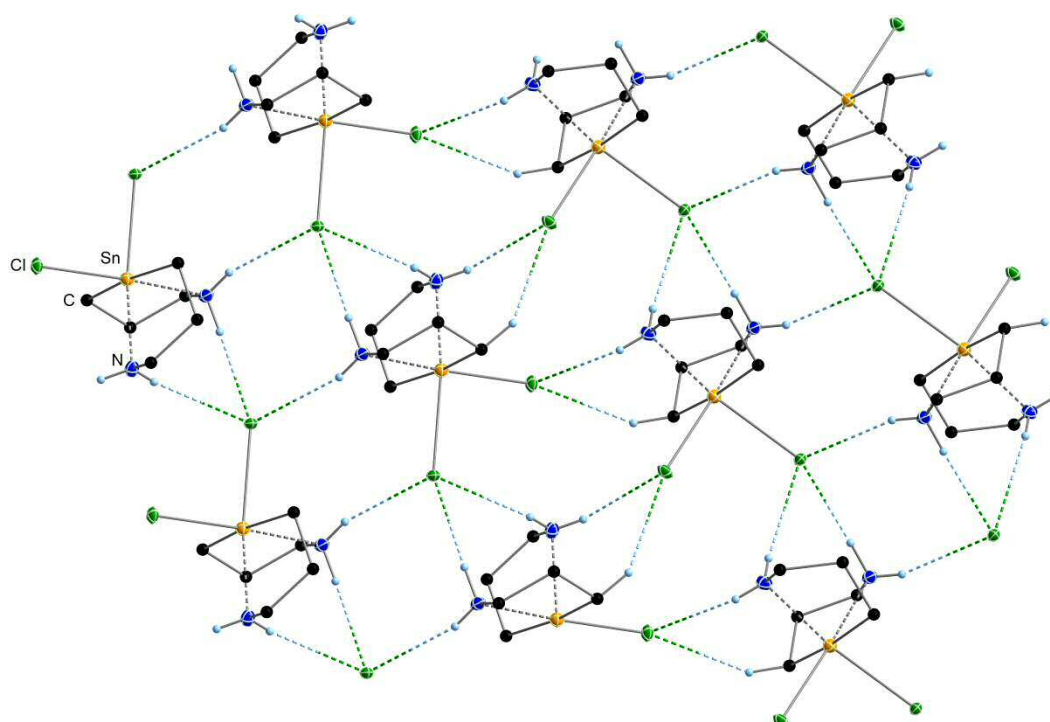


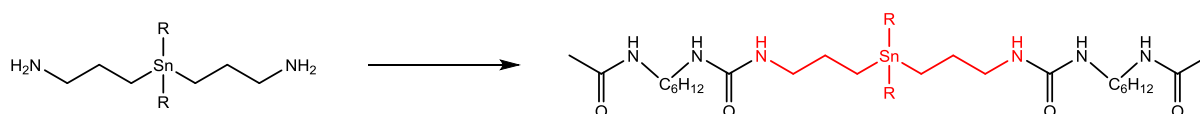
Figure 19: Crystal packing diagram of dichlorobis(3-aminopropyl)stannane. Sn–N, N–H···Cl and C–H···Cl interactions highlighted by dashed bonds. All non-carbon atoms shown as 30% shaded ellipsoids. Hydrogen atoms not involved in intermolecular interactions removed for clarity.

---

Similar to the dichlorobis(3-aminopropyl)stannane, bis(acetate)-bis(3-aminopropyl)stannane and **(6)** show intermolecular interactions in the form of N–H···O (2.09(3)–2.57(3) Å) hydrogen bonds in the solid state. However, the dichloride (Figure 19) exhibits a 3D polymeric structure in the solid state, whilst the acetate and laurate moieties only allow for 2D networks to form. The diacetate and dilaurate **(6)** (Figure 12) diamino-stannanes compounds arrange themselves to form planar sheets of intermolecularly hydrogen bonded molecules. While there is a separation of the planar sheets in the diacetate, the longer chains in the dilaurate diamino-stannane **(6)** create intercalated layers exhibiting discrete hydrophilic and hydrophobic regions. A similar type of arrangement or interdigitation can also be observed in the arrangement of membrane lipids which form the surface of all cells.

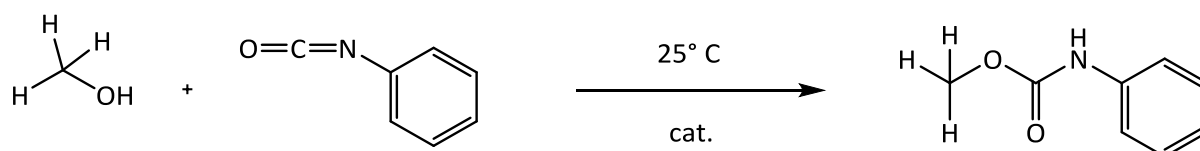
## 6 Conclusion and Outlook

We were able to extend the synthetic procedure reported for monoaminopropyltin compounds successfully to bis(3-amino)propyltin derivatives employing the desilylation of a tin trimethylsilyl species ( $\text{Ph}_2\text{Sn}(\text{SiMe}_3)_2$ ). Also, the synthesis of bis(amino)propyltin dichloride *via* a thermochemical procedure similar to the already published monoamine derivatives could be demonstrated. Diaminopropyltin dichloride was also converted into the corresponding acetate and laurate derivative *via* a salt-metathesis reaction. Single crystal structure analysis reveals discrete crystal packing effects depending on the nature of the substituent on the tin central atom. While the dichloride and diacetate diaminostannane display only extensive hydrogen bonding, the arrangement of the long hydrocarbon chains of the dilaurate carboxylate moiety allows the formation of discrete hydrophilic and hydrophobic layers. The synthesized compounds are highly interesting candidates for biological or catalytic applications and for avoidance of the leach out effect.



**Scheme 41: Incorporation of a diamino catalyst into the polymer.**

In future investigations, it will be tested if the incorporation into polymer (Scheme 41) works. Also catalytic tests will be made with a variety of tin compounds concerning different carboxylate moieties and alkyl or aryl substituent, as well as the comparison between monoamino and diamino compounds. The model reaction for the catalytic tests will be methanol with phenylisocyanate in  $\text{CDCl}_3$ . The reaction progress will be observed with a 60MHz Benchtop NMR.



**Scheme 42: Model reaction used for catalytic activity tests**



## 7 Experimental Section

### 7.1 Materials and Methods

All moisture and air sensitive reactions were carried out under inert atmosphere using Schlenk line techniques unless otherwise stated. Nitrogen was used as inert gas and passed through molecular-sieve 4Å and P<sub>5</sub>O<sub>10</sub> with moisture indicator (Sicapent<sup>®</sup> by Merck) to remove trace water. Solvents were stored over a drying agent (lithium aluminum hydride (LDA) in case of THF, P<sub>5</sub>O<sub>10</sub> for CH<sub>2</sub>Cl<sub>2</sub> and (MeO)<sub>2</sub>Mg for methanol) under N<sub>2</sub> and distilled prior to use or taken directly from an Innovative Technology<sup>®</sup> solvent drying system (benzene). CDCl<sub>3</sub> was distilled over P<sub>5</sub>O<sub>10</sub> and stored under N<sub>2</sub>, MeOH-d<sub>4</sub> was purchased water free. All chemicals were used as received from various chemical suppliers without any further purification. All elemental analyses were performed on a Heraeus VARIO ELEMENTAR EL analyzer. Melting points were determined with a STUART SCIENTIFIC SMP 10, no temperature corrections were applied.

### 7.2 X-ray Crystallography

All crystals suitable for single crystal X-ray diffractometry were removed from a vial or a Schlenk under N<sub>2</sub> and immediately covered with a layer of silicone oil. A single crystal was selected, mounted on a glass rod on a copper pin, and placed in the cold N<sub>2</sub> stream provided by an Oxford Cryosystems cryostream. XRD data collection was performed on a Bruker APEX II diffractometer with use of an Incoatec microfocus sealed tube of Mo K $\alpha$  radiation ( $\lambda$ = 0.71073 Å) and a CCD area detector. Empirical absorption corrections were applied using SADABS or TWINABS.<sup>108,109</sup> The structures were solved with use of the intrinsic phasing option in SHELXT and refined by the full-matrix least-squares procedures in SHELXL.<sup>110–113</sup> The space group assignments and structural solutions were evaluated using PLATON.<sup>114,115</sup>

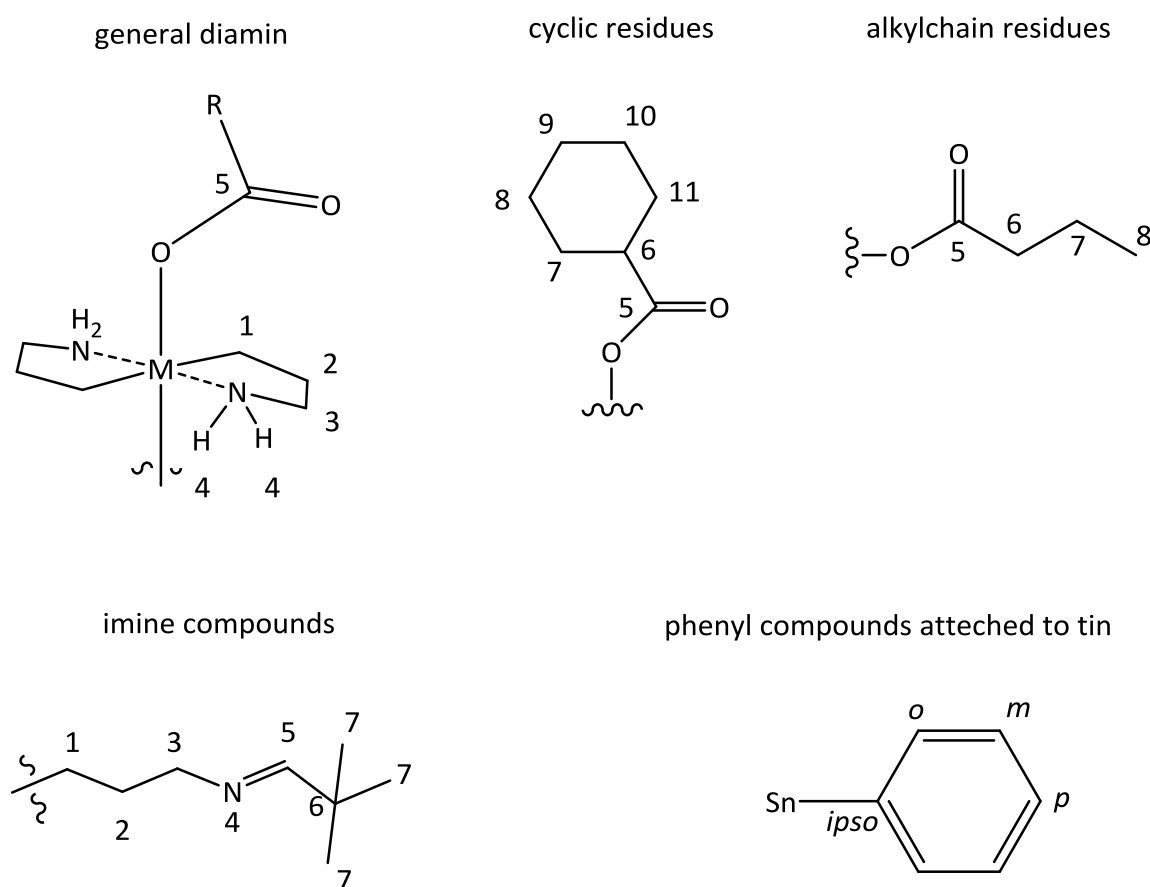
Non-hydrogen atoms were refined anisotropically. When possible, hydrogen atoms bonded to nitrogen atoms were located in a difference map and refined isotropically. All other hydrogen atoms were located in calculated positions corresponding to standard bond lengths and angles and refined using a riding model.

Disorder was handled by modeling the occupancies of the individual orientations using free variables to refine the respective occupancy of the affected fragments (PART)<sup>116</sup>. In some cases, the similarity SAME restraint, the similar-ADP restraint SIMU and the rigid-bond restraint DELU, as well as the constraints EXYZ and EADP were used in modelling disorder to make the ADP values of the disordered atoms more reasonable. In some cases, the distances between arbitrary atom pairs were restrained to possess the same value using the SADI instruction and in some cases distance restraints (DFIX) to certain target values were used. In some tough cases of disorder, anisotropic  $U^{ij}$ -values of the atoms were restrained (ISOR) to behave more isotropically. In compound laurate<sub>2</sub>SnA<sub>2</sub> (6), disordered positions for one of the laurate chain residues were refined using 65/35 positions. In compound laurate<sub>2</sub><sup>n</sup>propylSnA (18), disordered positions for the central Sn atom, ethylamine chain and second oxygen of the Laurate chain residues were refined using 50/50, 55/45, and 50/50 split positions.

Compound cyclopentanecarboxylate<sub>2</sub>SnA<sub>2</sub> (15) was twinned and was refined using the TWIN option in SHELXL. Compound adamantanecarboxylate<sub>2</sub>SnA<sub>2</sub> (17) was twinned and was refined using the TWIN option in SHELXL. Electrostatic non-covalent intermolecular interactions,<sup>117-120</sup> van der Waals contacts (CH...X),<sup>121,122</sup> and hydrogen bonds for presented and published compounds were based on a Cambridge Structural Database<sup>123</sup> search and fall within expected ranges. Centroids and planes were determined by features of the programs Mercury<sup>124</sup> and Diamond.<sup>125</sup> All crystal structures representations were made with the program Diamond. Table x contains crystallographic data and details of measurements and refinement for compounds 5-17.

### 7.3 NMR-spectroscopy

$^1\text{H}$  (300.22 MHz),  $^{13}\text{C}$  (75.50 MHz) and  $^{119}\text{Sn}$  (111.92 MHz) NMR spectra were recorded on a Mercury 300 MHz spectrometer from Varian at 25 °C. Chemical shifts are given in parts per million (ppm) relative to TMS ( $\delta = 0$  ppm) regarding  $^{13}\text{C}$  and  $^1\text{H}$  and relative to  $\text{SnMe}_4$  in the case of  $^{119}\text{Sn}$ . Coupling constants ( $J$ ) are reported in Hertz (Hz). For complete peak assignment, multinuclear NMR experiments were also carried out (H,H-COSY and C,H-HETCOR). Processing of the data was carried out using MestReNova7 (Mestrelab research).



Scheme 43: Schematic numbering of synthesized compounds

## 7.4 Synthesis

### 7.4.1 Literature known compounds

#### (*E*)-*N*-(3-chloropropyl)-2,2-dimethylpropan-1-imine<sup>60</sup>

In a 500 mL flask with a Dean-Stark-trap, 3-chloro-propan-1-amine hydrochloride (6.5 g, 0.05 Mol) 2,2-dimethylpropanal (4.3 g, 0.05 Mol) and KOH (2.8 g, 0.05 Mol) were suspended in 250 mL of Benzene. The suspension was heated under reflux until no more H<sub>2</sub>O was generated. The solvent was pumped. The crude product was distilled affording (*E*)-*N*-(3-chloropropyl)-2,2-dimethylpropan-1-imine as colourless liquid (4.4 g, 52%). B.p.: 63°C at 15 mbar. The product is stored under at -15°C.

<sup>1</sup>H NMR (CDCl<sub>3</sub>, 300 MHz) δ: 7.48 (t, 1H, <sup>1,4</sup>J = 2.53, **5**); 3.44 (t, 2H, <sup>1,3</sup>J = 12.9, **1**); 3.41 (td, 2H, <sup>1,3</sup>J = 14.1 Hz, **3**); 1.96 (p, 2H, **2**); 0.98 (s, 9H, **7**)

<sup>13</sup>C NMR (CDCl<sub>3</sub>, 75.5 MHz) δ: 42.6 (1C, **1**); 33.2 (1C, **2**); 57.6 (1C, **3**); 36.3 (1C, **6**); 173.3 (1C, **5**); 27.0 (3C, **7**)

#### Diphenyl-bis(trimethylsilyl)stannan

60g (174 mmol) diphenyltindichloride are suspended in 1.5L and cooled to 0°C. Afterwards 13 g (535 mmol) magnesium are added. The start of the reaction can be observed by changing the reaction colour to a green/black solution. At this point 45 mL (37,8 g; 348 mmol) TMS-Cl are added. Then the solution is warmed up to room temperature and stirred for 48 hours. Afterwards, the solvent was removed under vacuum and the residue suspended in 50 mL pentane and filtered over Celite<sup>®</sup> 512. Yield: 62,13 g (85 %),

<sup>1</sup>H NMR (CDCl<sub>3</sub>, 300 MHz) δ: 7.70-7.45 (m, 4H, *o*-Ph); 7.45-7.10 (m, 6H, *m/p*-Ph); 0.60-0.30 (m, 18H, Si(CH<sub>3</sub>)<sub>3</sub>)

<sup>13</sup>C-NMR (CDCl<sub>3</sub>) δ: 139.6 (2C, *isop*-Ph); 137.9 (4C, *o*-Ph); 128.3 (4C, *m*-Ph); 127.4 (2C, *p*-Ph); 1.8 (6C, Si(CH<sub>3</sub>)<sub>3</sub>)

<sup>119</sup>Sn-NMR (CDCl<sub>3</sub>) δ: -253.7 (<sup>1</sup>J(<sup>29</sup>Si-<sup>119</sup>Sn) = 513)

**Diphenyl-bis(<sup>t</sup>butyliminopropyl)stannane**

A 200 mL Schlenk tube was charged with 5.0 g (12 mmol) of diphenylbis(trimethylsilyl)stannane and 100 mL THF. The solution was chilled to 0 °C and 3.0 g (26 mmol) KO<sup>t</sup>Bu were added under stirring. After 5 min, 3.9 g (24 mmol) of (*E*)-*N*-(3-chloropropyl)-2,2-dimethylpropan-1-imine was added *via* a syringe and the reaction mixture stirred for another 20 min. Afterwards, the solvent was removed under vacuum and the residue suspended in 50 mL CH<sub>2</sub>Cl<sub>2</sub> and filtered over Celite<sup>®</sup> 512. The crude product was distilled under vacuum. Bp.: 175 °C at 4x10<sup>-2</sup> mbar. Yield: 5.6 g (89%).

<sup>1</sup>H NMR (CDCl<sub>3</sub>, 300 MHz) δ: 7.65-7.46 (m, 4H, *o*-Ph), 7.46-7.40 (s, 2H, **5**), 7.40-7.25 (m, 6H, *m/p*-Ph); 3.38 (t, 4H, **1**), 1.92 (m, 4H, **2**), 1.25 (m, 4H, **3**), 1.07 (s, 18H, **7**) ppm.

<sup>13</sup>C NMR (CDCl<sub>3</sub>, 75.5 MHz) δ: 172.0 (2C, **5**), 139.6 (2C, *i*-Ph), 136.7 (4C, *o*-Ph), 128.4 (2C, *p*-Ph), 128.2 (4C, *m*-Ph), 64.8 (2C, **3**), 35.8 (2C, **6**), 27.7 (2C, **2**), 26.9 (6C, **7**), 7.3 (2C, <sup>1</sup>J(<sup>13</sup>C-<sup>119</sup>Sn) = 366 Hz, <sup>1</sup>J(<sup>13</sup>C-<sup>117</sup>Sn) = 350 Hz, **1**) ppm.

<sup>119</sup>Sn NMR (CDCl<sub>3</sub>, 112 MHz) δ: -71.5 ppm.

**Diphenyl-bis(propyl-3-ammoniumchloride)stannane**

A 250 mL round bottom flask was charged with 5.0 g (9.5 mmol) of diphenylbis(<sup>t</sup>butyliminopropyl)stannane. 95 mL (19 mmol) of 0.5 M HCl were added while stirring. Once all of the educt went into solution, the solvent was removed under vacuum at 60 °C. Mp: 178-180 °C. Yield: 4.3 g (98.3%).

<sup>1</sup>H NMR (CDCl<sub>3</sub>, 300 MHz) δ: 7.58-7.50 (m, 4H, <sup>3</sup>J(<sup>1</sup>H-<sup>119/117</sup>Sn) = 46.1 Hz, *o*-Ph), 7.42-7.34 (m, 6H, *m/p*-Ph), 2.95 (t, 4H, <sup>3</sup>J(<sup>1</sup>H-<sup>1</sup>H) = 7.47 Hz, **3**), 2.07-1.89 (m, 4H, **2**), 1.41-1.30 (m, 4H, **1**) ppm.

<sup>13</sup>C NMR (CDCl<sub>3</sub>, 75.5 MHz) δ: 139.2 (2C, *i*-Ph), 137.8 (4C, <sup>2</sup>J(<sup>13</sup>C-<sup>119</sup>Sn) = 35.2 Hz, 130.1 (2C, <sup>3</sup>J(<sup>13</sup>C-<sup>119</sup>Sn) = 11.3 Hz, *p*-Ph), 129.7 (4C, <sup>3</sup>J(<sup>13</sup>C-<sup>119</sup>Sn) = 48.2 Hz, *m*-Ph), 44.0 (2C, <sup>3</sup>J(<sup>13</sup>C-<sup>119</sup>Sn) = 83.3 Hz, **3**), 25.9 (2C, <sup>2</sup>J(<sup>13</sup>C-<sup>119</sup>Sn) = 16.4 Hz, **2**), 6.9 (2C, <sup>1</sup>J(<sup>13</sup>C-<sup>119</sup>Sn) = 362 Hz, **1**) ppm.

<sup>119</sup>Sn NMR (CDCl<sub>3</sub>, 112 MHz) δ: -70.6 ppm.

### Dichloro-bis(3-aminopropyl)stannane

A 100 mL Schlenk tube was charged with 3.5 g (7.6 mmol) of diphenylbis(propyl-3-ammonium chloride)stannane and placed under vacuum in an oil bath. The oil bath was heated to 235 °C and the temperature was kept for 1 h. The oil bath was removed and the colorless product which had sublimed into the upper part of the Schlenk tube was dissolved in hot methanol, filtered through a 0.20 µm PTFE syringe filter and afterwards the solvent removed under vacuum. The crude product was recrystallized from methanol. Mp: 270-272 °C. Yield: 2.3 g (98.2%).

$^1\text{H NMR}$  (65 °C, MeOH- $d_4$ )  $\delta$ : 3.35 (t, 4H,  $^3J(^1\text{H}-^1\text{H})= 5.9$  Hz, **3**), 2.49-2.38 (m, 4H,  $^3J(^1\text{H}-^{119}\text{Sn})= 175.2$  Hz,  $^3J(^1\text{H}-^{117}\text{Sn})= 169.1$  Hz, **2**), 1.84 (t, 4H,  $^3J(^1\text{H}-^1\text{H})= 7.1$  Hz,  $^2J(^1\text{H}-^{119}\text{Sn})= 96.2$  Hz,  $^2J(^1\text{H}-^{117}\text{Sn})= 91.4$  Hz, **1**) ppm.

$^{13}\text{C NMR}$  (65 °C, MeOH- $d_4$ )  $\delta$ : 41.2 (2C,  $^3J(^{13}\text{C}-^{119}\text{Sn})= 74.4$  Hz,  $^3J(^{13}\text{C}-^{117}\text{Sn})= 71.1$  Hz, **3**), 25.3 (2C,  $^1J(^{13}\text{C}-^{119}\text{Sn})= 908$  Hz,  $^1J(^{13}\text{C}-^{117}\text{Sn})= 863$  Hz, **1**), 25.2 (2C,  $^2J(^{13}\text{C}-^{119}\text{Sn})= 51.3$  Hz, **2**) ppm.

$^{119}\text{Sn NMR}$  (65 °C, MeOH- $d_4$ )  $\delta$ : -186.6 ppm.

### Bis(acetate)-bis(3-aminopropyl)stannane

A 100 mL Schlenk tube was charged with 2.0 g (6.5 mmol) of dichlorodi(3-aminopropyl)stannane and 50 mL methanol. 1.1 g (13 mmol) sodium acetate was added to the suspension under stirring. After 5 min, the solvent was removed under vacuum, the residue suspended in 50 mL  $\text{CH}_2\text{Cl}_2$  and filtered through a 0.20 µm PTFE syringe filter. The solvent was removed under vacuum and the crude product recrystallized from benzene.

$^1\text{H NMR}$  ( $\text{CDCl}_3$ , 300 MHz)  $\delta$ : 3.13 (bs, 4H, **4**), 2.88 (t, 4H, **3**), 1.92 (s, 6H, **6**), 1.90-1.81 (m, 4H,  $^3J(^1\text{H}-^{119/117}\text{Sn})= 175.3$  Hz, **2**), 1.05 (t, 4H,  $^3J(^1\text{H}-^1\text{H})= 6.7$  Hz,  $^2J(^1\text{H}-^{119/117}\text{Sn})= 100.9$  Hz, **1**) ppm.

$^{13}\text{C NMR}$  ( $\text{CDCl}_3$ , 75.5 MHz)  $\delta$ : 178.9 (2C, **5**), 40.1 (2C,  $^3J(^{13}\text{C}-^{119}\text{Sn})= 69.6$  Hz, **3**), 24.1 (2C,  $^2J(^{13}\text{C}-^{119}\text{Sn})= 53.6$  Hz, **2**), 23.6 (2C, **6**), 20.5 (2C, **1**) ppm.

$^{119}\text{Sn NMR}$  ( $\text{CDCl}_3$ , 112 MHz)  $\delta$ : -330.2 ppm

**Bis(laurate)-bis(3-aminopropyl)stannane (6)**

A 100 mL Schlenk tube was charged with 0.51 g (13 mmol) freshly cut (in dry box) potassium and 50 mL methanol. After the metal was dissolved, 2.6 g (13 mmol) lauric acid was added. After a clear solution was obtained, 2.0 g (6.5 mmol) of dichlorodi(3-aminopropyl)stannane were added. After 5 min the solvent was removed under vacuum, the residue suspended in 50 mL CH<sub>2</sub>Cl<sub>2</sub> and filtered through a 0.20 μm PTFE syringe filter. The solvent was pumped down under vacuum and the product was dried under oil vacuum for 2 h at 60 °C. The crude product was recrystallized from heptane. Mp: 84-85 °C. Yield: 3.7 g (98%).

<sup>1</sup>H NMR (CDCl<sub>3</sub>, 300 MHz) δ: 2.88 (m, 4H), 2.19 (m, 4H), 1.88 (m, 3H), 1.56 (m, 4H), 1.24 (m, 30H), 1.04 (m, 3H), 0.87 (t, 6H).

<sup>13</sup>C NMR (CDCl<sub>3</sub>, 75.5 MHz) δ: 23.9 (2C, <sup>2</sup>J(<sup>13</sup>C-<sup>119</sup>Sn)= 55 Hz **2**) 39.9 (2C, <sup>3</sup>J(<sup>13</sup>C-<sup>119</sup>Sn)= 68.2 Hz, **3**), 181.5, 36.2, 31.9, 29.6, 29.5, 29.4, 29.4, 29.0, 20.0, 22.7, 14.1.

<sup>119</sup>Sn NMR (CDCl<sub>3</sub>, 112 MHz) δ: -330.1ppm

## 7.4.2 New synthesized compounds

### General Procedure for tin carboxylate

A 100 mL roundflask tube was charged with NaOMe (13 mmol) and Carboxylic (13 mmol) (in dry box) potassium and 15 mL methanol. After a clear solution was obtained, 2.0 g (6.5 mmol) of tin chloride were added drop wise. After 60 min the solvent was removed under vacuum, the residue suspended in 20 mL THF and filtered through a 0.20  $\mu\text{m}$  PTFE syringe filter. The solvent was pumped down under vacuum and the product was dried under oil vacuum. Depending of the carboxylate residue different solvents were used to obtain crystals.

### Bis(propylammonia)-tinteratrachlorid (**1**)

A 250 mL round bottom flask was charged with 2.0 g (3.8 mmol) of diphenylbis(<sup>t</sup>butyliminopropyl)stannane was solved in methanol and a highly excess of 12 M HCl was added while stirring. Once all of the educt went into solution, the solvent was removed under vacuum at 60 °C. Mp: 178-180 °C. Yield: 1.85g (98.%).

<sup>1</sup>H NMR (D<sub>2</sub>O, 300 MHz)  $\delta$ : 3.35 (t, 4H,  $^3J(^1\text{H}-^1\text{H})= 5.9$  Hz, **3**), 2.49-2.38 (m, 4H,  $^3J(^1\text{H}-^{119}\text{Sn})= 175.2$  Hz,  $^3J(^1\text{H}-^{117}\text{Sn})= 169.1$  Hz, **2**), 1.84 (t, 4H,  $^3J(^1\text{H}-^1\text{H})= 7.1$  Hz,  $^2J(^1\text{H}-^{119}\text{Sn})= 96.2$  Hz,  $^2J(^1\text{H}-^{117}\text{Sn})= 91.4$  Hz, **1**) ppm.

<sup>13</sup>C NMR (D<sub>2</sub>O, 75.5 MHz)  $\delta$ : 41.2 (2C,  $^3J(^{13}\text{C}-^{119}\text{Sn})= 74.4$  Hz,  $^3J(^{13}\text{C}-^{117}\text{Sn})= 71.1$  Hz, **3**), 25.3 **1**), 25.2 (2C,  $^2J(^{13}\text{C}-^{119/117}\text{Sn})= 51.3$  Hz, **2**) ppm.

<sup>119</sup>Sn NMR (D<sub>2</sub>O, 112 MHz)  $\delta$ : -192.3 ppm



**Bis(propylammonia)-tinteratrabromo (2)**

A 250 mL round bottom flask was charged with 1.0 g (1.9 mmol) of diphenylbis(<sup>t</sup>butyliminopropyl)stannane was solved in methanol and a highly excess of M HBr was added while stirring. Once all of the educt went into solution, the solvent was removed under vacuum at 60 °C. Yield: 2.2g (95%).

<sup>1</sup>H NMR (D<sub>2</sub>O, 300 MHz)δ: 1.53 (t, 4H, **1**) 2.03-1.86 (m, 4H, **2**), 2.92 (t, 4H, **3**) ppm.

<sup>13</sup>C NMR (D<sub>2</sub>O, 75.5 MHz) δ: 41.2 (2C, <sup>3</sup>J(<sup>13</sup>C-<sup>119</sup>Sn)= 74.4 Hz, <sup>3</sup>J(<sup>13</sup>C-<sup>117</sup>Sn)= 71.1 Hz, **3**), 25.3 **1**), 25.2 (2C, <sup>2</sup>J(<sup>13</sup>C-<sup>119/117</sup>Sn)= 51.3 Hz, **2**) ppm.

<sup>119</sup>Sn NMR (D<sub>2</sub>O, 112 MHz) δ: -191.7 ppm

**(Br(CH<sub>2</sub>)<sub>3</sub>NH<sub>3</sub><sup>+</sup>)<sub>2</sub>SnBr<sub>6</sub> (3)**

A 100 mL round bottom flask was charged with 500 mg (0.9 mmol) of diphenylbis(<sup>t</sup>butyliminopropyl)stannane was solved in methanol and a highly excess of HBr was added while stirring and the solutions was refluxed for three hours. Then the solvent was removed under vacuum at 60 °C. Yield: 2.45 g (91%).

<sup>1</sup>H NMR (D<sub>2</sub>O, 300 MHz)δ: 3.35 (t, 4H **3**), 2.49-2.38 (m, 4H, **2**), 1.84 (t, 4H, **1**) ppm.

<sup>13</sup>C NMR (D<sub>2</sub>O, 75.5 MHz) δ: 41.2 (2C **3**), 25.3 (2C, **1**), 25.2 (2C, **2**) ppm.

<sup>119</sup>Sn NMR (D<sub>2</sub>O, 112 MHz) δ: -286.3 ppm

**Bis(formiate)-bis(3-aminopropyl)stannane (5)**

44 mg (0.6 mmol) of NaOMe and 83 mg (0.6 mmol) Carboxylic acid are dissolved in 15 ml methanol. 138 mg (0.3 mmol) dichloro-bis(3-aminopropyl)stannane solved in 10 ml methanol was added. Crystals were obtained out of THF. Mp: 232-235 °C. Yield: 244 mg (76%)

$^1\text{H NMR}$  ( $\text{CDCl}_3$ , 300 MHz)  $\delta$ : 1.2 (t, 4H,  $^3J(^1\text{H}-^1\text{H})= 6.7$  Hz,  $^2J(^1\text{H}-^{119}\text{Sn})= 96.4$  Hz **1**), 1.97-1.83 (m, 4H,  $^3J(^1\text{H}-^{119}\text{Sn})= 172.2$  Hz, **2**), 2.86 (t, 4H,  $^3J(^1\text{H}-^1\text{H})= 6.5$  Hz, **3**), 3.3 (bs, 4H, **4**), 8.4 (s, 1H, **6**) ppm.

$^{13}\text{C NMR}$  ( $\text{CDCl}_3$ , 75.5 MHz)  $\delta$ : 19.2 (2C, **1**), 23.5 (2C,  $^2J(^{13}\text{C}-^{119}\text{Sn})= 51.6$  Hz, **2**), 39 (2C,  $^3J(^{13}\text{C}-^{119}\text{Sn})= 72.2$ , **3**), 168.4 (2C, **5**) ppm

$^{119}\text{Sn NMR}$  ( $\text{CDCl}_3$ , 112 MHz)  $\delta$ : -293 ppm

**Bis(stereate)-bis(3-aminopropyl)stannane (7)**

38 mg (0.7 mmol) of NaOMe and 132 mg (0.7 mmol) stearinic acid are dissolved in 100 ml methanol. 100 mg (0.3 mmol) dichloro-bis(3-aminopropyl)stannane solved in 10 ml methanol was added. Crystals were obtained out of hexane/benzene. Mp: 95-98°C. Yield: 476 mg (91%)

$^1\text{H NMR}$  ( $\text{CDCl}_3$ , 300 MHz)  $\delta$ : 2.8 (m, 4H), 2.1 (m, 4H), 1.38 (m, 3H), 1.47 (m, 4H), 1.18 (m, 56H), 0.96 (m, 3H), 0.81 (t, 6H) ppm

$^{13}\text{C NMR}$  ( $\text{CDCl}_3$ , 75.5 MHz)  $\delta$ : 24.1 (2C,  $^2J(^{13}\text{C}-^{119}\text{Sn})= 52.3$  Hz **2**) 40.1 (2C,  $^3J(^{13}\text{C}-^{119}\text{Sn})= 70.9$  Hz, **3**) 181.5; 36.7, 32, 30.5, 29.95, 29.9, 29.8, 29.7 29.6, 29.5, 26.2, 22.8, 20.3, 14.2 ppm

$^{119}\text{Sn NMR}$  ( $\text{CDCl}_3$ , 112 MHz)  $\delta$ : -336.5 ppm

**Bis(trifluoroacetate)-bis(3-aminopropyl)stannane (8)**

36 mg (0.7 mmol) of NaOMe and 101 mg (0.7 mmol) trifluoroacetic acid are dissolved in 80 ml methanol. 96 mg (0.3 mmol) dichloro-bis(3-aminopropyl)stannane dissolved in 10 ml methanol was added. Crystals were obtained out of methanol. Yield: 201 mg (67%)

**Bis(perfluorononanoate)-bis(3-aminopropyl)stannane (9)**

54mg (1 mmol) of NaOMe and 454mg (1 mmol) perfluoro nonanoic acid are dissolved in 150 ml methanol. 145 mg (0.5 mmol) dichloro-bis(3-aminopropyl)stannane dissolved in 10 ml methanol was added. Crystals were obtained out of toluene. Yield: 637 mg (56%)

**Bis(benzylcarboxyl)-bis(3-aminopropyl)stannane (10)**

48mg (1 mmol) of NaOMe and 121 mg (1 mmol) benzoic acid are dissolved in 20 ml methanol. 148 mg (0.5 mmol) dichloro-bis(3-aminopropyl)stannane dissolved in 10 ml methanol was added. Crystals were obtained out of benzene. Yield: Mp: 234-250 °C. 443 mg (95%)

**<sup>1</sup>H NMR** (CDCl<sub>3</sub>, 300 MHz) δ: 1.18 (t, 4H, <sup>3</sup>J(<sup>1</sup>H-<sup>1</sup>H)= 6.9 Hz, <sup>2</sup>J(<sup>1</sup>H-<sup>119</sup>Sn)= 98.6 Hz **1**), 2.49-2.38 (m, 4H, <sup>3</sup>J(<sup>1</sup>H-<sup>119</sup>Sn)= 171.2 Hz, **2**), 2.88 (t, 4H, **3**), 3.35 (bs, 4H, **4**), 7.98 (d, 4H, **7 & 8**), 7.38 (t, 4H, **9 & 10**), 7.47 (d, 2H, **11**) ppm.

**<sup>13</sup>C NMR** (CDCl<sub>3</sub>, 75.5 MHz) δ: 20.2 (2C **1**), 25.1 (2C, <sup>2</sup>J(<sup>13</sup>C-<sup>119</sup>Sn)= 52.3 Hz, **2**), 40.9 (2C, <sup>3</sup>J(<sup>13</sup>C-<sup>119</sup>Sn)= 74.2Hz **3**), 174.8 (2C, **5**), 132.5 (2C, **6**), 130.6 (4C, **7 & 11**), 129 (4C, **8 & 10**), 136.3 (2C, **9**) ppm

**<sup>119</sup>Sn NMR** (CDCl<sub>3</sub>, 112 MHz) δ: -328.2 ppm

**Bis-(4-pyribisnecarboxyl)-bis(3-aminopropyl)stannane (11)**

33 mg (0.6 mmol) of NaOMe and 82 mg (0.6 mmol) isonicotinic acid are dissolved in 15 ml methanol. 97 mg (0.3 mmol) dichloro-bis(3-aminopropyl)stannane solved in 10 ml methanol was added. Crystals were obtained out of THF. Mp: 243-244 °C. Yield: 272 mg (88%)

$^1\text{H NMR}$  ( $\text{CDCl}_3$ , 300 MHz)  $\delta$ : 1.17 (t, 4H,  $^3J(^1\text{H}-^1\text{H})= 6.1$  Hz,  $^2J(^1\text{H}-^{119}\text{Sn})= 93.6$  Hz **1**), 2.49-2.38 (m, 4H,  $^3J(^1\text{H}-^{119}\text{Sn})= 175.1$  Hz, **2**), 2.97 (s, 4H, **3**), 3.39 (bs, 4H, **4**), 7.75 (d, 4H, **7 & 8**), 8.68 (d, 4H, **9 & 10**), ppm.

$^{13}\text{C NMR}$  ( $\text{CDCl}_3$ , 75.5 MHz)  $\delta$ : 20.3 **1**), 24.1 (2C,  $^2J(^{13}\text{C}-^{119}\text{Sn})= 53.1$  Hz, **2**), 40.2 (2C,  $^3J(^{13}\text{C}-^{119}\text{Sn})= 71.3$  Hz **3**), 171.5 (2C, **5**), 142.5 (2C, **6**), 123.3 (4C, **7 & 11**), 150.2 (4C, **8 & 10**), ppm.

$^{119}\text{Sn NMR}$  ( $\text{CDCl}_3$ , 112 MHz)  $\delta$ : -334 ppm

**Bis(para-fluorbenzylcarboxyl)-bis(3-aminopropyl)stannane (12)**

51mg (1 mmol) of NaOMe and 140 mg (1 mmol) *para*-fluorobenzoic acid are dissolved in 25 ml methanol. 144 mg (0.5 mmol) dichloro-bis(3-aminopropyl)stannane solved in 10 ml methanol was added. Crystals were obtained out of DCM. Mp: 84-85 °C. Yield: 417 mg (83%)

$^1\text{H NMR}$  ( $\text{CDCl}_3$ , 300 MHz)  $\delta$ : 1.17 (t, 4H,  $^3J(^1\text{H}-^1\text{H})= 6.7$  Hz,  $^2J(^1\text{H}-^{119}\text{Sn})= 93.6$  Hz **1**), 2.49-2.38 (m, 4H,  $^3J(^1\text{H}-^{119}\text{Sn})= 176$  Hz, **2**), 2.97 (s, 4H, **3**), 3.39 (bs, 4H, **4**), 7.07 (t, 4H, **7 & 8**), 8.01 (t, 4H, **9 & 10**), ppm.

$^{13}\text{C NMR}$  ( $\text{CDCl}_3$ , 75.5 MHz)  $\delta$ : 20.2 (2C **1**), 25.1 (2C,  $^2J(^{13}\text{C}-^{119}\text{Sn})= 52.3$  Hz, **2**), 40.9 (2C,  $^3J(^{13}\text{C}-^{119}\text{Sn})= 74.2$ Hz **3**), 174.8 (2C, **5**), 132.5 (2C, **6**), 130.6 (4C, **7 & 11**), 129 (4C, **8 & 10**), 136.3 (2C, **9**) ppm.

$^{119}\text{Sn NMR}$  ( $\text{CDCl}_3$ , 112 MHz)  $\delta$ : -341.4 ppm

**Bis(cyclopropylcarboxyl)-bis(3-aminopropyl)stannane (13)**

37 mg (0.7 mmol) of NaOMe and 58 mg (0.7 mmol) cyclopropanecarboxylic acid are dissolved in 15 ml methanol. 101 mg (0.3 mmol) dichloro-bis(3-aminopropyl)stannane solved in 15 ml methanol was added. Crystals were obtained out of THF. Mp: 165-167°C. Yield: 205 mg (78%).

**<sup>1</sup>H NMR** (CDCl<sub>3</sub>, 300 MHz) δ: 0.98 (t, 4H, <sup>3</sup>J(<sup>1</sup>H-<sup>1</sup>H)= 7.1 Hz, <sup>2</sup>J(<sup>1</sup>H-<sup>119</sup>Sn)= 96.2 Hz **1**), 1.9-1.77 (m, 4H, <sup>3</sup>J(<sup>1</sup>H-<sup>119</sup>Sn)= 175.2 Hz, **2**), 2.84 (t, 4H, <sup>3</sup>J(<sup>1</sup>H-<sup>1</sup>H)= 5.5 Hz, **3**), 3.08 (bs, 4H, **4**), 1.35-1.47 (m, 2H, **6**), 0.6-0.85 (2d, 8H, **7 & 8**)

**<sup>13</sup>C NMR** (CDCl<sub>3</sub>, 75.5 MHz) δ: 20.1 (2C, **1**), 24.05 (2C, <sup>2</sup>J(<sup>13</sup>C-<sup>119</sup>Sn)= 54.3 Hz, **2**), 40.2 (2C, <sup>3</sup>J(<sup>13</sup>C-<sup>119</sup>Sn)=73.4 Hz **3**), 176.7 (2C, **5**), 14.6 (2C, **6**), 7.6 (4C, **7 & 8**) ppm.

**<sup>119</sup>Sn NMR** (CDCl<sub>3</sub>, 112 MHz) δ: -326 ppm

**Bis(cyclobutylcarboxyl)-bis(3-aminopropyl)stannane (14)**

40 mg (0.7 mmol) of NaOMe and 69 mg (0.7 mmol) cyclobutanecarboxylic acid are dissolved in 15 ml methanol. 102 mg (0.3 mmol) dichloro-bis(3-aminopropyl)stannane solved in 10 ml methanol was added. Crystals were obtained out of THF. Mp: 173-175 °C. Yield: 252 mg (89%)

**<sup>1</sup>H NMR** (CDCl<sub>3</sub>, 300 MHz) δ: : 0.96 (t, 4H, <sup>3</sup>J(<sup>1</sup>H-<sup>1</sup>H)= 6.83 Hz, <sup>2</sup>J(<sup>1</sup>H-<sup>119</sup>Sn)= 94.1 Hz **1**), 1.95-1.73 (m, 4H, <sup>3</sup>J(<sup>1</sup>H-<sup>119</sup>Sn)= 176 Hz, **2**), 2.82 (t, 4H, <sup>3</sup>J(<sup>1</sup>H-<sup>1</sup>H)= 5.5 Hz, **3**), 3.27 (bs, 4H, **4**), 2.95(p, 2H, **6**), 2.04-2.16(m, 8H, **7 & 8**), 1.46-1.63 (, 4H, **9**) ppm.

**<sup>13</sup>C NMR** (CDCl<sub>3</sub>, 75.5 MHz) δ: 19.8 (2C, **1**), 24.1 (2C, <sup>2</sup>J(<sup>13</sup>C-<sup>119</sup>Sn)= 53.3 Hz, **2**), 40.1 (2C, <sup>3</sup>J(<sup>13</sup>C-<sup>119</sup>Sn)=70.1 Hz **3**), 182.9 (2C, **5**), 40.4 (2C, **6**), 26.2 (4C, **7 & 8**), 18.3 (2C, **9**), ppm.

**<sup>119</sup>Sn NMR** (CDCl<sub>3</sub>, 112 MHz) δ: -310 ppm

**Bis(cyclopentylcarboxyl)-bis(3-aminopropyl)stannane (15)**

36 mg (0.7 mmol) of NaOMe and 76 mg (0.7 mmol) cyclopentanecarboxylic acid are dissolved in 15 ml methanol. 98 mg (0.3 mmol) dichloro-bis(3-aminopropyl)stannane solved in 10 ml methanol was added. Crystals were obtained out of benzene. Mp: 182 °C. Yield: 235 mg (77%)

<sup>1</sup>H NMR (CDCl<sub>3</sub>, 300 MHz) δ: 1.84 (t, 4H, <sup>3</sup>J(<sup>1</sup>H-<sup>1</sup>H)= 6.7 Hz, <sup>2</sup>J(<sup>1</sup>H-<sup>119</sup>Sn)= 94.2 Hz, **1**), 2.44-2.37 (m, 4H, <sup>3</sup>J(<sup>1</sup>H-<sup>119</sup>Sn)= 171.7.2 Hz **2**), 3.35 (t, 4H, **3**), 3.13 (bs, 4H, **4**), 2.63 (m, 2H, **6**), 1.57-1.44 (m, 8H, **7 & 8**), 1.72-1.63 (m, 8H, **9 & 10**)

<sup>13</sup>C NMR (CDCl<sub>3</sub>, 75.5 MHz) δ: 21 (2C, **1**), 23.9 (2C, <sup>2</sup>J(<sup>13</sup>C-<sup>119</sup>Sn)= 50.3 Hz, **2**), 40.2 (2C, <sup>3</sup>J(<sup>13</sup>C-<sup>119</sup>Sn)=72.3 **3**), 184.2 (2C, **5**), 45.1 (2C, **6**), 30.7 (2C, **7 & 8**), 25.9 (2C, **9 & 10**), ppm.

<sup>119</sup>Sn NMR (CDCl<sub>3</sub>, 112 MHz) δ: -315.9 ppm

**Bis(cyclohexylbarboxyl)-bis(3-aminopropyl)stannane (16)**

50mg (1 mmol) of NaOMe and 125 mg (1 mmol) cyclohexanecarboxylic acid are dissolved in 15ml methanol. 145 mg (0.5 mmol) dichloro-bis(3-aminopropyl)stannane solved in 10 ml methanol was added. Crystals were obtained out of THF. Mp: 187-188 °C. Yield: 410 mg (87%)

<sup>1</sup>H NMR (CDCl<sub>3</sub>, 300 MHz) δ: 1.84 (t, 4H, <sup>3</sup>J(<sup>1</sup>H-<sup>1</sup>H)= 7.1 Hz, <sup>2</sup>J(<sup>1</sup>H-<sup>119</sup>Sn)= 96.2 Hz, <sup>2</sup>J(<sup>1</sup>H-<sup>117</sup>Sn)= 91.4 Hz, **1**), 2.49-2.38 (m, 4H, <sup>3</sup>J(<sup>1</sup>H-<sup>119</sup>Sn)= 175.2 Hz, <sup>3</sup>J(<sup>1</sup>H-<sup>117</sup>Sn)= 169.1 Hz, **2**), 3.35 (t, 4H, <sup>3</sup>J(<sup>1</sup>H-<sup>1</sup>H)= 5.9 Hz, **3**), 3.13 (bs, 4H, **4**), 2.32 (p, 2H, **6**), 1.53-1.78 (m, 20H, **7 -11**)

<sup>13</sup>C NMR (CDCl<sub>3</sub>, 75.5 MHz) δ: 20.6 (2C, **1**), 24.2 (2C, <sup>2</sup>J(<sup>13</sup>C-<sup>119</sup>Sn)= 52.7 Hz, **2**), 40.2 (2C, <sup>3</sup>J(<sup>13</sup>C-<sup>119</sup>Sn)= 70.4 Hz **3**), 182.7 (2C, **5**), 44.7 (2C, **6**), 29.8 (4C, **7 & 8**), 25.9 (4C, **9 & 10**), 26.2 (2C, **11**), ppm.

<sup>119</sup>Sn NMR (CDCl<sub>3</sub>, 112 MHz) δ: -321.3 ppm

**Bis(adamantylcarboxyl)-bis(3-aminopropyl)stannane (17)**

50mg (1 mmol) of NaOMe and 152 mg (1 mmol) adamantylcarboxylic acid are dissolved in 15ml methanol. 145 mg (0.5 mmol) dichloro-bis(3-aminopropyl)stannane solved in 10 ml methanol was added. Crystals were obtained out of THF. Mp: 175 °C. Yield: 512 mg (85%)

**<sup>1</sup>H NMR** (CDCl<sub>3</sub>, 300 MHz) δ: 1.9 (t, 4H, <sup>3</sup>J(<sup>1</sup>H-<sup>1</sup>H)= 7.3 Hz, <sup>2</sup>J(<sup>1</sup>H-<sup>119</sup>Sn)= 94.2 Hz, <sup>2</sup>J(<sup>1</sup>H-<sup>117</sup>Sn)= 92.4 Hz, **1**), 2.41-2.37 (m, 4H, <sup>3</sup>J(<sup>1</sup>H-<sup>119</sup>Sn)= 174.3 Hz, <sup>3</sup>J(<sup>1</sup>H-<sup>117</sup>Sn)= 168.1 Hz, **2**), 3.32 (t, 4H, <sup>3</sup>J(<sup>1</sup>H-<sup>1</sup>H)= 5.9 Hz, **3**), 3.08 (bs, 4H, **4**), 1.72-1.89 (m, 30H, **6-15**)

**<sup>13</sup>C NMR** (CDCl<sub>3</sub>, 75.5 MHz) δ: 20 (2C, **1**), 24.5 (2C, <sup>2</sup>J(<sup>13</sup>C-<sup>119</sup>Sn)= 54 Hz, **2**), 40.1 (2C, <sup>3</sup>J(<sup>13</sup>C-<sup>119</sup>Sn)= 72 Hz **3**), 185.7 (2C, **5**), 44.7 (2C, **6**), 29.8 (4C, **7 & 8**), 26.1 (4C, **9 & 10**), 27.2 (2C, **11**), 37.5 (6C, **12 & 13 & 14**), 27.5 (2C, **15**) ppm.

**<sup>119</sup>Sn NMR** (CDCl<sub>3</sub>, 112 MHz) δ: -327.3 ppm

## 8 Appendix

### 8.1 Index of Figures

Figure 1: a) Crystal bis(propylammonia)tetrachlorostannate (2). b) Crystal bis(propylammoniatetra-bromostannate (2). All non-carbon atoms shown as 30% shaded ellipsoids. Hydrogen atoms removed for clarity. ....	26
Figure 2: Crystal structure of (3). All non-carbon atoms shown as 30% shaded ellipsoids. Hydrogen atoms removed for clarity.....	27
Figure 3: Crystal structure of diphenyldi(propyl-3-ammoniumchloride)stannane (4). All non-carbon atoms shown as 30% shaded ellipsoids. Hydrogen atoms removed for clarity.....	28
Figure 4: a) Crystal structure of acetate <sub>2</sub> SnA <sub>2</sub> . <sup>60</sup> b) Crystal structure of trifluoroacetate <sub>2</sub> SnA <sub>2</sub> (8). All non-carbon atoms shown as 30% shaded ellipsoids. Hydrogen atoms removed for clarity. ....	40
Figure 5: a) Crystal structure of benzoate <sub>2</sub> SnA <sub>2</sub> (10). b) Crystal structure of <i>p</i> -fluorobenzoate <sub>2</sub> SnA <sub>2</sub> (12). All non-carbon atoms shown as 30% shaded ellipsoids. Hydrogen atoms removed for clarity.....	40
Figure 6: a) Crystal structure of laurate <sub>2</sub> SnA <sub>2</sub> (6). b) Crystal structure of perfluorononanoate <sub>2</sub> SnA <sub>2</sub> (9) c) Crystal structure of stearate <sub>2</sub> SnA <sub>2</sub> (7). All non-carbon atoms shown as 30% shaded ellipsoids. Hydrogen atoms removed for clarity. ....	42
Figure 7: a) Crystal structure of cyclopentanecarboxylate <sub>2</sub> SnA <sub>2</sub> (15). b) Crystal structure of cyclohexanecarboxylate <sub>2</sub> SnA <sub>2</sub> (16). c) Crystal structure of adamantanecarboxylate <sub>2</sub> SnA <sub>2</sub> (17). All non-carbon atoms shown as 30% shaded ellipsoids. Hydrogen atoms removed for clarity.....	43
Figure 8: a) Crystal structure of cyclopropanecarboxylate <sub>2</sub> SnA <sub>2</sub> (13). b) Crystal structure of cyclobutanecarboxylate <sub>2</sub> SnA <sub>2</sub> (14) .c) Crystal structure of isonicotinate <sub>2</sub> SnA <sub>2</sub> (11). All non-carbon atoms shown as 30% shaded ellipsoids. Hydrogen atoms removed for clarity.....	45
Figure 9: Crystal structure of laurate <sub>2</sub> <sup>n</sup> propylSnA (18). All non-carbon atoms shown as 30% shaded ellipsoids. Hydrogen atoms removed for clarity. ....	51
Figure 10: Crystal packing diagram for adamantanecarboxylate <sub>2</sub> SnA <sub>2</sub> (17). N–H···O hydrogen bonds highlighted by dashed bonds. All non-carbon atoms shown as 30% shaded ellipsoids. Hydrogen atoms not involved in intermolecular interactions removed for clarity.....	53



- Figure 11: Crystal packing diagram for formate<sub>2</sub>SnA<sub>2</sub> (5). N–H···O hydrogen bonds highlighted by dashed bonds. All non-carbon atoms shown as 30% shaded ellipsoids. Hydrogen atoms not involved in intermolecular interactions removed for clarity. .... 54
- Figure 12: Crystal packing diagram of laurate<sub>2</sub>SnA<sub>2</sub> (6) displaying 2D sheet intercalation through the laurate moiety creating layers. N–H···O interactions highlighted by dashed bonds. All non-carbon atoms shown as 30% shaded ellipsoids. Hydrogen atoms not involved in intermolecular interactions removed for clarity. .... 55
- Figure 13: Crystal packing diagram of stearate<sub>2</sub>SnA<sub>2</sub> (7) displaying 2D sheet intercalation through the laurate moiety creating layers. N–H···O and C–H···O interactions highlighted by dashed bonds. All non-carbon atoms shown as 30% shaded ellipsoids. Hydrogen atoms not involved in intermolecular interactions removed for clarity. .... 56
- Figure 14: Crystal packing diagram for cyclobutanecarboxylate<sub>2</sub>SnA<sub>2</sub> (14). N–H···O and intramolecular C–H···O hydrogen bonds highlighted by dashed bonds. All non-carbon atoms shown as 30% shaded ellipsoids. Hydrogen atoms not involved in intermolecular interactions removed for clarity. .... 56
- Figure 15: Crystal packing diagram of perfluorononanoate<sub>2</sub>SnA<sub>2</sub> (9) displaying 2D sheet intercalation through the laurate moiety creating layers. N–H···O, C–H···F, N–H···F interactions highlighted by dashed bonds. All non-carbon atoms shown as 30% shaded ellipsoids. Hydrogen atoms not involved in intermolecular interactions removed for clarity. .... 57
- Figure 16: Crystal packing diagram for benzoate<sub>2</sub>SnA<sub>2</sub> (10). N–H···O hydrogen bonds, CH<sub>3</sub>···π and edge to face interactions highlighted by dashed bonds. All non-carbon atoms shown as 30% shaded ellipsoids. Hydrogen atoms not involved in intermolecular interactions removed for clarity. .... 58
- Figure 17: Crystal packing diagram for *p*-fluorobenzoate<sub>2</sub>SnA<sub>2</sub> (12). N–H···O and N–H···F hydrogen bonds, and π–π interactions highlighted by dashed bonds. All non-carbon atoms shown as 30% shaded ellipsoids. Hydrogen atoms not involved in intermolecular interactions removed for clarity. .... 59
- Figure 18: Crystal packing diagram for isonicotinate<sub>2</sub>SnA<sub>2</sub> (11). N–H···O and N–H···N hydrogen bonds interactions highlighted by dashed bonds. All non-carbon atoms shown as 30% shaded ellipsoids. Hydrogen atoms not involved in intermolecular interactions removed for clarity. .... 60

Figure 19: Crystal packing diagram of dichlorobis(3-aminopropyl)stannane. Sn–N, N–H···Cl and C–H···Cl interactions highlighted by dashed bonds. All non-carbon atoms shown as 30% shaded ellipsoids. Hydrogen atoms not involved in intermolecular interactions removed for clarity. .... 60

## 8.2 Index of Schemes

Scheme 1: Overview applications of organotin compounds.....	8
Scheme 2: Tetra amines as PU catalysts. ....	10
Scheme 3: Catalysts for tin replacement. ....	11
Scheme 4: Common tin catalysts (DBTDL and DBTDA). ....	12
Scheme 5: Proposed structure of DBTDL and DBTDA. ....	12
Scheme 6: Suggested Lewis acid mechanism.....	13
Scheme 7: Catalyst leach out of the polymer. ....	13
Scheme 8. Structure typ of our aminoalkyl compounds. <sup>50–52</sup> .....	14
Scheme 9: Catalyst incorporation into the polymer. ....	14
Scheme 10: Synthesis of triphenyl- $\gamma$ -N,N-diethylaminopropyltin.....	15
Scheme 11: Quartanization of triphenyl- $\gamma$ -N,N-diethylaminopropyltin.....	15
Scheme 12: Synthesis of triphenyl- $\gamma$ -N,N-dimethylaminopropyltin.....	16
Scheme 13: Derivatization of triphenyl- $\gamma$ -N,N-dimethylaminopropyltin. ....	16
Scheme 14: Hydrostannilation as synthesis strategy to generate aminopropyltin compounds. ....	17
Scheme 15: Hydrostannilation as synthesis strategy to generate aminopropyltin compounds with acidic hydrogens.....	17
Scheme 16: Synthesis of $\beta$ -aminoethyl tin species (XXVI) .....	18

---

Scheme 17: Mechanism of the Grob-fragmentation. ....	18
Scheme 18: Synthesis route to achieve aminopropyl tin compounds with acidic nitrogen hydrogens. <sup>50</sup> ..	19
Scheme 19: Derivatisation possibilities of compound XXXII .....	20
Scheme 20: Synthesis of bis(3-(dimethylamino)propyl)dichloride.....	20
Scheme 21: Alkyl/arylation of bis(3-(dimethylamino)propyl)dichloride .....	21
Scheme 22: Target precursor molecule .....	21
Scheme 23: Generating diphenylbis( <sup>t</sup> butyliminopropyl)stannane. ....	22
Scheme 24: Multistep mechanism for the cleavage of two trimethylsilyl groups.....	23
Scheme 25: Treating diphenylbis( <sup>t</sup> butyliminopropyl)stannane with HCl/H <sub>2</sub> O.....	24
Scheme 26: Treating diphenylbis( <sup>t</sup> butyliminopropyl)stannane with HCl/H <sub>2</sub> O.....	24
Scheme 27: Synthesis of the bromo derivate (2). ....	25
Scheme 28: Refluxing Ph <sub>2</sub> SnA <sub>2</sub> with HBr/H <sub>2</sub> O. ....	27
Scheme 29: Converting the ammonium chloride into the amine with MeOH/KOH.....	27
Scheme 30: Converting the imine to the corresponding ammonium chloride with HCl/Et <sub>2</sub> O. ....	28
Scheme 31: Thermal rearrangement of (4) to dichlorobis(3-aminopropyl)stannane. ....	29
Scheme 32: Overview of all used carboxylic acid and the synthesis route to carboxylates.....	30
Scheme 33: Synthesis of dicarboxylates by salt elimination.....	31
Scheme 34: Possible structural motifs for organotin(IV) esters of carboxylic acids. ....	34
Scheme 35: Coordination modes 6, 6.5, 7. ....	36
Scheme 36: Overview of all used carboxylic acid.....	36

---

Scheme 37: Near octahedral geometry coordinating in a <i>trans</i> configuration with a monodentate bonding mode Monodentate Diaminopropyltin Dicarboxylates. ....	38
Scheme 38: Structure of ferrocenoate <sub>2</sub> SnA* <sub>2</sub> (A* = -Ph(CH <sub>2</sub> NMe <sub>2</sub> ) <sup>83,84</sup> .....	39
Scheme 39: pseudo octahedral geometry coordinating in a <i>trans</i> configuration with both mono- and bidentate bonding mode in mixed dentate Diaminopropyltin Dicarboxylates .....	46
Scheme 40: a) Mixed Mono- and Pseudo Bidentate Diaminopropyltin Dicarboxylate – Coordination Number 6.5 pseudo octahedral geometry coordinating in a <i>trans</i> configuration with both mono- and bidentate bonding mode in mixed dentate Diaminopropyltin Dicarboxylates. b) Crystal structure of formate <sub>2</sub> SnA <sub>2</sub> (5). All non-carbon atoms shown as 30% shaded ellipsoids. Hydrogen atoms removed for clarity. ....	49
Scheme 41: Incorporation of a diamino catalyst into the polymer. ....	62
Scheme 42: Model reaction used for catalytic activity tests .....	62
Scheme 43: Schematic numbering of synthesized compounds.....	65

### 8.3 Index of Tables

Table 3: <sup>119</sup>Sn-NMR shift of dicarboxy tin compounds

Table 4: <sup>13</sup>C-NMR shift of 3-aminopropyl substituents of all dicarboxy tin compounds.

Table 3: Selected bond lengths and angles for Monodentate Diaminopropyltin Dicarboxylates.

Table 4: Selected bond lengths and angles for mixed Mono and- bi dentate Diaminopropyltin Dicarboxylates.

## 9 References

- (1) Bonire, J. J.; Ayoko, G. A.; Olurinola, P. F.; Ehinmidu, J. O.; Jalil, N. S.; Omachi, A. A. Synthesis and Antifungal Activity of Some Organotin(IV) Carboxylates. *Metal-based drugs* **1998**, *5*, 233–236.
- (2) Gupta, M. K.; Singh, H. L.; Varshney, S.; Varshney, A. K. Synthetic and spectroscopic characterization of organotin(IV) complexes of biologically active Schiff bases derived from sulpha drugs. *Bioinorganic chemistry and applications* **2003**, 309–320.
- (3) Nath, M.; Pokharia, S.; Yadav, R. Organotin(IV) complexes of amino acids and peptides. *Coordination Chemistry Reviews* **2001**, *215*, 99–149.
- (4) Nath, M.; Yadav, R.; Gielen, M.; Dalil, H.; Vos, D. de; Eng, G. Synthesis, characteristic spectral studies and in vitro antimicrobial and antitumour activities of organotin(IV) complexes of Schiff bases derived from amino-acids. *Appl. Organomet. Chem.* **1997**, *11*, 727–736.
- (5) Singh, H. L.; Varshney, A. K. Synthetic, structural, and biochemical studies of organotin(IV) with Schiff bases having nitrogen and sulphur donor ligands. *Bioinorganic chemistry and applications* **2006**, 23245.
- (6) Ahmad, N. W.; Mohd, S.-A.; Balabaskaran, S.; Das, V. G. K. Insecticidal effects of organotin(IV) compounds on *Plutella xylostella* (Linnaeus) larvae I: Topical application toxicity and antifeedant effect. *Appl. Organomet. Chem.* **1993**, *7*, 583–591.
- (7) Crowe, A. J. Organotin compounds in agriculture since 1980. Part 2. Acaricidal, antifeedant, chemosterilant and insecticidal properties. *Appl. Organomet. Chem.* **1987**, *1*, 331–346.
- (8) Crowe, A. J. Organotin compounds in agriculture since 1980. Part I. Fungicidal, bactericidal and herbicidal properties. *Appl. Organomet. Chem.* **1987**, *1*, 143–155.
- (9) Saxena, A. K. Organotin compounds: Toxicology and biomedical applications. *Appl. Organomet. Chem.* **1987**, *1*, 39–56.
- (10) Kimmel, E. C.; Casida, J. E.; Fish, R. H. Bioorganotin chemistry. Microsomal monooxygenase and mammalian metabolism of cyclohexyltin compounds including the miticide cyhexatin. *Journal of agricultural and food chemistry* **1980**, *28*, 117–122.

- (11) Ma, Y.-N.; Gui, W.-J.; Zhu, G.-N. The analysis of azocyclotin and cyhexatin residues in fruits using ultrahigh-performance liquid chromatography-tandem mass spectrometry. *Anal. Methods* **2015**, *7*, 2108–2113.
- (12) Matsui, H.; Wada, O.; Manabe, S.; Ono, T.; Nakajima, K.; Fujikura, T. Effects of tricyclohexyltin hydroxide on carbohydrate and lipid metabolisms. *Sangyo igaku. Japanese journal of industrial health* **1983**, *25*, 10–14.
- (13) R C Hunter. Organotin Compounds and Their Use for Insect and Mite Control. *Environ Health Perspect.*; 47–50.
- (14) Evans, C. J.; Karpel, S. *Organotin Compounds in Modern Technology*; Elsevier: Amsterdam, 1985.
- (15) Omae, I. *Applications of Organometallic Compounds*; Wiley: Chichester, 1998.
- (16) Bennett, R. F. Industrial manufacture and applications of tributyltin compounds. In *Tributyltin: Case Study of an Environmental Contaminant.*; Mora, S. J. de, Ed.; Cambridge University Press: Cambridge, 1996; pp 21–61.
- (17) Crowe, A. J.; Hill, R.; Smith, P. J.; Cox, T. R. G. Laboratory evaluation of tributyltin compounds as wood preservatives. *Internat. J. Wood preservation* **1979**, *1*, 119–124.
- (18) Mascaretti, O. A.; Furlán, R. L. E. Esterification, transesterification and deesterification mediated by organotin oxides and derivatives. *Aldrichimica Acta* **1997**, *30*, 55–68.
- (19) Mercier, F. A. G.; Biesemans, M.; Altmann, R.; Willem, R.; Pintelon, R.; Schoukens, J.; Delmond, B.; Dumartin, G. Synthesis, Characterization, and Catalytic Properties of Diphenyl- and Dichlorobutyltin Functionalities Grafted to Insoluble Polystyrene Beads by a  $-(CH_2)_n-$  ( $n = 4, 6$ ) Spacer. *Organometallics* **2001**, *20*, 958–962.
- (20) Otera, J. Transesterification. *Chem. Rev.* **1996**, *96*, 1449–1470.
- (21) Otera, J.; Danoh, N.; Nozaki, H. Novel template effects of distannoxane catalysts in highly efficient transesterification and esterification. *The Journal of organic chemistry* **1991**, *56*, 5307–5311.
- (22) Xiang, J.; Orita, A.; Otera, J. Fluoroalkyldistannoxane Catalysts for Transesterification in Fluorous Biphasic Technology. *Advanced Synthesis & Catalysis* **2002**, *344*, 84.

- (23) Xiang, J.; Toyoshima, S.; Orita, A.; Otera, J. A Practical and Green Chemical Process: Fluoroalkyldistannoxane-Catalyzed Biphasic Transesterification. *Angewandte Chemie (International ed. in English)* **2001**, *40*, 3670.
- (24) Randall, L.; Weber, J. H. Adsorptive behavior of butyltin compounds under simulated estuarine conditions. *The Science of the total environment* **1986**, *57*, 191–203.
- (25) Mushtaq, M.; Mukhtar, H.; Datta, K. K.; Tandon, S. G.; Seth, P. K. Toxicological studies of a leachable stabilizer di-n-butyltin dilaurate(DBTL): Effects on hepatic drug metabolizing enzyme activities. *Drug and chemical toxicology* **1981**, *4*, 75–88.
- (26) Gade, A. L.; Heiaas, H.; Lillicrap, A.; Hylland, K. Ecotoxicity of paint mixtures: Comparison between measured and calculated toxicity. *The Science of the total environment* **2012**, *435-436*, 526–540.
- (27) Subramoniam, A.; Khandelwal, S.; Dwivedi, P. D.; Khanna, S.; Shanker, R. Dibutyltin dilaurate induced thymic atrophy and modulation of phosphoinositide pathway of cell signalling in thymocytes of rats. *Immunopharmacology and immunotoxicology* **1994**, *16*, 645–677.
- (28) Khaliq, M. A.; Husain, R.; Seth, P. K.; Srivastava, S. P. Effect of dibutyltin dilaurate on regional brain polyamines in rats. *Toxicology Letters* **1991**, *55*, 179–183.
- (29) Hamasaki, T.; Masumoto, H.; Sato, T.; Nagase, H.; Kito, H.; Yoshioka, Y. Estimation of the hemolytic effects of various organotin compounds by structure-activity relationships. *Appl. Organomet. Chem.* **1995**, *9*, 95–104.
- (30) Alam, M. S.; Husain, R.; Seth, P. K.; Srivastava, S. P. Age and sex related behavioral changes induced by dibutyltin-dilaurate in rats. *Bull. Environ. Contam. Toxicol.* **1993**, *50*, DOI: 10.1007/BF00191735.
- (31) Schwetlick, K.; Noack, R. Kinetics and catalysis of consecutive isocyanate reactions. Formation of carbamates, allophanates and isocyanurates. *J. Chem. Soc., Perkin Trans. 2* **1995**, 395.
- (32) Silva, A. L.; Bordado, J. C. Recent Developments in Polyurethane Catalysis: Catalytic Mechanisms Review. *Catalysis Reviews* **2004**, *46*, 31–51.

- (33) Luo, S.-G.; Tan, H.-M.; Zhang, J.-G.; Wu, Y.-J.; Pei, F.-K.; Meng, X.-H. Catalytic mechanisms of triphenyl bismuth, dibutyltin dilaurate, and their combination in polyurethane-forming reaction. *J. Appl. Polym. Sci.* **1997**, *65*, 1217–1225.
- (34) Ligabue, R. A.; Monteiro, A. L.; Souza, R. F. de; Souza, M. O. de. Catalytic properties of Fe(acac)<sub>3</sub> and Cu(acac)<sub>2</sub> in the formation of urethane from a diisocyanate derivative and EtOH. *Journal of Molecular Catalysis A: Chemical* **1998**, *130*, 101–105.
- (35) Ligabue, R. A.; Monteiro, A. L.; Souza, R. F. de; Souza, M. O. de. Influence of the alcohol nature on the catalytic properties of Fe(acac)<sub>3</sub> and Cu(acac)<sub>2</sub> in the formation of urethane from a diisocyanate. *Journal of Molecular Catalysis A: Chemical* **2000**, *157*, 73–78.
- (36) Spino, C.; Joly, M.-A.; Godbout, C.; Arbour, M. Ti-catalyzed reactions of hindered isocyanates with alcohols. *The Journal of organic chemistry* **2005**, *70*, 6118–6121.
- (37) Blank, W. J.; He, Z. A.; Hessel, E. T. Catalysis of the isocyanate-hydroxyl reaction by non-tin catalysts. *Progress in Organic Coatings* **1999**, *35*, 19–29.
- (38) *Tin Chemistry*; Davies, A. G.; Gielen, M.; Pannell, K. H.; Tiekink, E. R. T., Eds.; John Wiley & Sons, Ltd: Chichester, UK, 2008.
- (39) Weng Ng, S.; Das, V.; Yip, W.-H.; Wang, R.-J.; Mak, T. C. Di-n-butyltin(IV) di-o-bromobenzoate, a weakly-bridged dimer. *Journal of Organometallic Chemistry* **1990**, *393*, 201–204.
- (40) Vatsa, C.; Jain, V. K.; Kesavadas, T.; Tiekink, E. R. Structural chemistry of organotin carboxylates. *Journal of Organometallic Chemistry* **1991**, *410*, 135–142.
- (41) Tiekink, E. R. Structural chemistry of organotin carboxylates. *Journal of Organometallic Chemistry* **1991**, *408*, 323–327.
- (42) Jaumier, P.; Jousseume, B.; Tiekink, E. R. T.; Biesemans, M.; Willem, R. Solid-State Coordination Behavior of Trichloro(4-acetoxybutyl)tin. *Organometallics* **1997**, *16*, 5124–5126.
- (43) Biesemans, M.; Willem, R.; Damoun, S.; Geerlings, P.; Lahcini, M.; Jaumier, P.; Jousseume, B. Coordination Behavior of ω-(Trichlorostannyl)alkyl Acetates, CH<sub>3</sub>COO(CH<sub>2</sub>)<sub>n</sub>SnCl<sub>3</sub> (n = 3–5): A Solution and Solid-State Multinuclear NMR and AM1 Quantum-Chemical Study. *Organometallics* **1996**, *15*, 2237–2245.



- 
- (44) Houghton, R. P.; Mulvaney, A. W. Mechanism of tin(IV)-catalysed urethane formation. *Journal of Organometallic Chemistry* **1996**, *518*, 21–27.
- (45) Young, R. H.; Wehrly, K.; Martin, R. L. Solvent effects in dye-sensitized photooxidation reactions. *Journal of the American Chemical Society* **1971**, *93*, 5774–5779.
- (46) Han, Q.; Urban, M. W. Kinetics and mechanisms of catalyzed and noncatalyzed reactions of OH and NCO in acrylic polyol-1,6-hexamethylene diisocyanate (HDI) polyurethanes. VI. *J. Appl. Polym. Sci.* **2002**, *86*, 2322–2329.
- (47) van der Weij, F. W. Kinetics and mechanism of urethane formation catalyzed by organotin compounds. II. The reaction of phenyl isocyanate with methanol in DMF and cyclohexane under the action of dibutyltin diacetate. *J. Polym. Sci. Polym. Chem. Ed.* **1981**, *19*, 3063–3068.
- (48) Reegen, S. L.; Frisch, K. C. Isocyanate–catalyst and hydroxyl–catalyst complex formation. *J. Polym. Sci. A-1 Polym. Chem.* **1970**, *8*, 2883–2891.
- (49) EU-Richtlinie 76/769/EG idgF.
- (50) Pichler, J.; Torvisco, A.; Bottke, P.; Wilkening, M.; Uhlig, F. Novel amino propyl substituted organo tin compounds. *Can. J. Chem.* **2014**, *92*, 565–573.
- (51) Pichler Johann. Dissertation- Zur Synthese und Charakterisierung von Aminopropylzinnverbindungen - Umweltfreundliche Katalysatoren für die technische Polyurethansynthese, 2014.
- (52) Pichler Johann. Diplomarbeit-Precursor für "wasserlösliche" Organozinnverbindungen, 2009.
- (53) Gilman, H.; Wu, T. C. Some Organotin Compounds Containing Water-solubilizing Groups. *Journal of the American Chemical Society* **1955**, *77*, 3228–3230.
- (54) ROSSEELS, G.; MATTEAZZI, J.; WOUTERS, G.; BRUCKNER, P.; PROST, M. 3-Aminopropylmagnesium Chloride in Aromatic Solvents. *Synthesis* **1970**, *1970*, 302–303.
- (55) Lequan, M.; Meganem, F.; Besace, Y. Synthèse et propriétés de quelques amines stanniques chirales; essais de dédoublement. *Journal of Organometallic Chemistry* **1976**, *113*, C13-C16.

- (56) Zickgraf, A.; Beuter, M.; Kolb, U.; Dräger, M.; Tozer, R.; Dakternieks, D.; Jurkschat, K. Nucleophilic attack within Ge, Sn and Pb complexes containing Me<sub>2</sub>N(CH<sub>2</sub>)<sub>3</sub>—as a potential intramolecular donor ligand. *Inorganica Chimica Acta* **1998**, *275-276*, 203–214.
- (57) Han, X.; Hartmann, G. A.; Brazzale, A.; Gaston, R. D. A water soluble, recyclable organostannatrane. *Tetrahedron Letters* **2001**, *42*, 5837–5839.
- (58) Weichmann, H.; Tzschach, A. Funktionell substituierte zinnorganische Verbindungen. III. (2-Aminoethyl)-triorganostannane. *Z. Anorg. Allg. Chem.* **1979**, *458*, 291–300.
- (59) Grob, C. A.; Schiess, P. W. Die heterolytische Fragmentierung als Reaktionstypus in der organischen Chemie. *Angew. Chem.* **1967**, *79*, 1–14.
- (60) Pichler, J.; Torvisco, A.; Bottke, P.; Wilkening, M.; Uhlig, F. Novel amino propyl substituted organo tin compounds. *Canadian Journal of Chemistry* **2014**, *92*, 565–573.
- (61) Jurkschat, K.; Tzschach, A.; Weichmann, H.; Rajczyk, P.; Mostafa, M. A.; Korecz, L.; Burger, K. Mössbauer spectroscopic investigations of intra- and intermolecularly coordinated organotin compounds. *Inorganica Chimica Acta* **1991**, *179*, 83–88.
- (62) Gielen, M. Tin-Based Antitumour Drugs. In *Main Group Elements and their Compounds*; Das, V. G. K., Ed.; Springer Berlin Heidelberg: Berlin, Heidelberg, 1996; pp 446–452.
- (63) Gielen, M. Review: Organotin compounds and their therapeutic potential: a report from the Organometallic Chemistry Department of the Free University of Brussels. *Appl. Organometal. Chem.* **2002**, *16*, 481–494.
- (64) Gielen, M. An overview of forty years organotin chemistry developed at the Free Universities of Brussels ULB and VUB. *J. Braz. Chem. Soc.* **2003**, *14*, DOI: 10.1590/S0103-50532003000600003.
- (65) Fischer, R.; Schollmeier, T.; Schürmann, M.; Uhlig, F. Syntheses of novel silylsubstituted distannanes. *Applied Organometallic Chemistry* **2005**, *19*, 523–529.
- (66) Fischer, R.; Baumgartner, J.; Marschner, C.; Uhlig, F. Tris(trimethylsilyl)stannyl alkali derivatives: Syntheses and NMR spectroscopic properties. *Inorganica Chimica Acta* **2005**, *358*, 3174–3182.
- (67) Hlina, J.; Mechtler, C.; Wagner, H.; Baumgartner, J.; Marschner, C. Multiple Silyl Exchange Reactions: A Way to Spirooligosilanes. *Organometallics* **2009**, *28*, 4065–4071.

(68) Marschner, C. A New and Easy Route to Polysilanylpotassium Compounds. *European Journal of Inorganic Chemistry* **1998**, 1998, 221–226.

(69) Hazra, S.; Chakraborty, P.; Mohanta, S. Heterometallic Copper(II)? Tin(II/IV) Salts, Cocrystals, and Salt Cocrystals: Selectivity and Structural Diversity Depending on Ligand Substitution and the Metal Oxidation State. *Crystal Growth & Design* **2016**, 16, 3777–3790.

(70) Agrawal, R.; Goyal, V.; Gupta, R.; Pallepogu, R.; Kotikalapudi, R.; Jones, P. G.; Bansal, R. K. Organotin(IV) complexes with imidazo[1,2-a]pyridines. *Polyhedron* **2014**, 70, 138–143.

(71) Agrawal, R.; Goyal, V.; Gupta, R.; Bhatnagar, P.; Bhargavi, G.; Bansal, R. K. Synthesis, characterization, and insecticidal activity of new tin (IV) complexes. *Phosphorus, Sulfur, and Silicon and the Related Elements* **2016**, 191, 1030–1035.

(72) Agrawal, R.; Goyal, V.; Gupta, R.; Pallepogu, R.; Kotikalapudi, R.; Jones, P. G.; Bansal, R. K. *CCDC 954809: Experimental Crystal Structure Determination*, 2014.

(73) Tudela, D.; Diaz, M.; Alvaro, D. A.; Ignacio, J.; Seijo, L.; Belsky, V. K. *CCDC 161241: Experimental Crystal Structure Determination*, 2001.

(74) Anslyn, E. V.; Dougherty, D. A. *Modern physical organic chemistry*; Univ. Science Books: Sausalito, Calif., 2006.

(75) Dakternieks, D.; Duthie, A.; Smyth, D. R.; Stapleton, C. P. D.; Tiekink, E. R. T. Steric Control over Molecular Structure and Supramolecular Association Exerted by Tin- and Ligand-Bound Groups in Diorganotin Carboxylates. *Organometallics* **2003**, 22, 4599–4603.

(76) Sandhu, G. K.; Sharma, N.; Tiekink, E. R. T. Structural chemistry of organotin carboxylates. *Journal of Organometallic Chemistry* **1991**, 403, 119–131.

(77) Win, Y. F.; Teoh, S.-G.; Ibrahim, P.; Ng, S.-L.; Fun, H.-K. Dibutylbis[3-(dimethylamino)benzoato]tin(IV). *Acta Crystallographica Section E* **2007**, 63, m667-m669.

(78) Win, Y. F.; Teoh, S.-G.; Ibrahim, P.; Ng, S.-L.; Fun, H.-K. Dibutylbis(3,5-dinitrobenzoato- $[\kappa]O$ )tin(IV) toluene solvate. *Acta Crystallographica Section E* **2007**, 63, m875-m877.

(79) Imtiaz ud, D.; Mazhar, M.; Dastgir, S.; Mahon, M. F.; Molloy, K. C. Crystallographic report: Bis[3-(tri-p-tolyl)germyl-3-(o-tolyl)-propionato]dibutyltin(IV). *Applied Organometallic Chemistry* **2003**, *17*, 801–802.

(80) Deák, A.; Tárkányi, G. Chiral self-assembly of methyltin(IV)-naproxenates: Combining dative Sn–O bonds, secondary Sn–O interactions and C–H–O hydrogen bonding to make an inter-helical meander-shaped network and a cross-linked Z-shaped ribbon. *Journal of Organometallic Chemistry* **2006**, *691*, 1693–1702.

(81) Baul, T. S. B.; Rynjah, W.; Willem, R.; Biesemans, M.; Verbruggen, I.; Holèapek, M.; Vos, D. de; Linden, A. Dibutyltin(IV) complexes of the 5-[(E)-2-(Aryl)-1-diazenyl]-2-hydroxybenzoic acid ligand: an investigation of structures by X-ray diffraction, solution and solid state tin NMR, electrospray ionisation MS and assessment of in vitro cytotoxicity. *Journal of Organometallic Chemistry* **2004**, *689*, 4691–4701.

(82) Alcock, N. W.; Culver, J.; Roe, S. M. Secondary bonding. Part 15. Influence of lone pairs on coordination: comparison of diphenyl-tin(IV) and -tellurium(IV) carboxylates and dithiocarbamates. *Journal of the Chemical Society, Dalton Transactions* **1992**, 1477–1484.

(83) Švec, P.; Černošková, E.; Padělková, Z.; Růžička, A.; Holeček, J. Tri- and diorganostannates containing 2-(N,N-dimethylaminomethyl)phenyl ligand. *Journal of Organometallic Chemistry* **2010**, *695*, 2475–2485.

(84) Švec, P.; Padělková, Z.; Růžička, A.; Weidlich, T.; Dušek, L.; Plasseraud, L. C,N-chelated organotin(IV) trifluoroacetates. Instability of the mono- and diorganotin(IV) derivatives. *Journal of Organometallic Chemistry* **2011**, *696*, 676–686.

(85) Goss, K.-U. The pKa Values of PFOA and Other Highly Fluorinated Carboxylic Acids. *Environ. Sci. Technol.* **2008**, *42*, 456–458.

(86) Rayne, S.; Forest, K. Theoretical studies on the pKa values of perfluoroalkyl carboxylic acids. *Journal of Molecular Structure: THEOCHEM* **2010**, *949*, 60–69.

(87) [daecr1.harvard.edu/pKa/pKa.html](http://daecr1.harvard.edu/pKa/pKa.html).

(88) Advanced Chemistry Development (ACD/Labs) Software V11.02 ed.; ACD/Labs, 1994-2017.

- (89) Arnett, E. M.; Maroldo, S. G.; Schilling, S. L.; Harrelson, J. A. Ion pairing and reactivity of enolate anions. 5. Thermodynamics of ionization of .beta.-di- and tricarbonyl compounds in dimethyl sulfoxide solution and ion pairing of their alkali salts. *Journal of the American Chemical Society* **1984**, *106*, 6759–6767.
- (90) Bordwell, F. G.; Algrim, D. Nitrogen acids. 1. Carboxamides and sulfonamides. *The Journal of organic chemistry* **1976**, *41*, 2507–2508.
- (91) International Union of, P.; Applied, C.; Commission on Equilibrium, D.; Serjeant, E. P.; Dempsey, B.; Commission on Electrochemical, D. *Ionisation constants of organic acids in aqueous solution*; Pergamon Press: Oxford, New York, 1979.
- (92) Basu Baul, T. S.; Dhar, S.; Rivarola, E.; Smith, F. E.; Butcher, R.; Song, X.; McCain, M.; Eng, G. Synthesis and characterization of some dibutylbis{5-[(E)-2-(aryl)-1-diazenyl]-2-hydroxybenzoato}tin(IV) compounds. Toxicity studies of di- and tri-organotin complexes on the second instar of *Aedes aegypti* mosquito larvae. *Applied Organometallic Chemistry* **2003**, *17*, 261–267.
- (93) Basu Baul, T. S.; Masharing, C.; Basu, S.; Pettinari, C.; Rivarola, E.; Chantrapromma, S.; Fun, H.-K. Synthesis and characterization of some diorganotin(IV) complexes of Schiff bases derived from a non-protein amino acid. Crystal structures of {HO<sub>2</sub>CC<sub>6</sub>H<sub>4</sub>[N=C(H)]C(CH<sub>3</sub>)CH(CH<sub>3</sub>)-3-OH]-p} and its di-n-butyltin(IV) complex (nBu<sub>2</sub>Sn{O<sub>2</sub>CC<sub>6</sub>H<sub>4</sub>[N=C(H)]C(CH<sub>3</sub>)CH(CH<sub>3</sub>)-3-OH]-p)<sub>2</sub>. *Applied Organometallic Chemistry* **2008**, *22*, 114–121.
- (94) Basu Baul, T. S.; Rynjah, W.; Rivarola, E.; Pettinari, C.; Holčapek, M.; Jirásko, R.; Englert, U.; Linden, A. Di-n-octyltin(IV) complexes with 5-[(E)-2-(aryl)-1-diazenyl]-2-hydroxybenzoic acid: Syntheses and assessment of solid state structures by <sup>119</sup>Sn Mössbauer and X-ray diffraction and further insight into the solution structures using electrospray ionization MS, <sup>119</sup>Sn NMR and variable temperature NMR spectroscopy. *Journal of Organometallic Chemistry* **2007**, *692*, 3625–3635.
- (95) Basu Baul, T. S.; Rynjah, W.; Rivarola, E.; Pettinari, C.; Linden, A. Synthesis and characterization of the first diorganotin(IV) complexes containing mixed arylazobenzoic acids and having skew trapezoidal bipyramidal geometry. *Journal of Organometallic Chemistry* **2005**, *690*, 1413–1421.
- (96) Desiraju, G. R. The C-H...O hydrogen bond in crystals: What is it? *Acc. Chem. Res.* **2002**, *24*, 290–296.

- (97) Desiraju, G. R. The C-h...o hydrogen bond: Structural implications and supramolecular design. *Acc. Chem. Res.* **1996**, *29*, 441–449.
- (98) Steiner, T. C[sbnd]H[sbnd]O Hydrogen Bonding in Crystals. *Crystallography Reviews* **1996**, *6*, 1–51.
- (99) Perlstein, J. The Weak Hydrogen Bond In Structural Chemistry and Biology (International Union of Crystallography, Monographs on Crystallography, 9) By Gautam R. Desiraju (University of Hyderabad) and Thomas Steiner (Freie Universität Berlin). Oxford University Press: Oxford and New York. 1999. xiv + 507 pp. \$150. ISBN 0-19-850252-4. *Journal of the American Chemical Society* **2001**, *123*, 191–192.
- (100) Desiraju, G. R. Hydrogen bonds and other intermolecular interactions in organometallic crystals †. *J. Chem. Soc., Dalton Trans.* **2000**, 3745–3751.
- (101) Steiner, T. C–H...O hydrogen bonding in crystals. *Crystallography Reviews* **2003**, *9*, 177–228.
- (102) Huber, R. G.; Margreiter, M. A.; Fuchs, J. E.; Grafenstein, S. von; Tautermann, C. S.; Liedl, K. R.; Fox, T. Heteroaromatic pi-stacking energy landscapes. *Journal of chemical information and modeling* **2014**, *54*, 1371–1379.
- (103) Hunter, C. A.; Sanders, J. K. M. The nature of .pi.-.pi. interactions. *Journal of the American Chemical Society* **1990**, *112*, 5525–5534.
- (104) Meyer, E. A.; Castellano, R. K.; Diederich, F. Interactions with aromatic rings in chemical and biological recognition. *Angewandte Chemie (International ed. in English)* **2003**, *42*, 1210–1250.
- (105) Alvarez, S. A cartography of the van der Waals territories. *Dalton transactions (Cambridge, England : 2003)* **2013**, *42*, 8617–8636.
- (106) Wobbe, M. C. C.; Zwijnenburg, M. A. Chemical trends in the optical properties of rocksalt nanoparticles. *Physical chemistry chemical physics : PCCP* **2015**, *17*, 28892–28900.
- (107) Willett, R. D.; Twamley, B.; Montfrooij, W.; Granroth, G. E.; Nagler, S. E.; Hall, D. W.; Park, J.-H.; Watson, B. C.; Meisel, M. W.; Talham, D. R. Dimethylammonium trichlorocuprate(II): Structural transition, low-temperature crystal structure, and unusual two-magnetic chain structure dictated by nonbonding chloride-chloride contacts. *Inorganic chemistry* **2006**, *45*, 7689–7697.

- 
- (108) Bruker. *APEX2 and SAINT*; Bruker AXS Inc.: Madison, Wisconsin, USA, 2012.
- (109) Blessing, R. H. An empirical correction for absorption anisotropy. *Acta Crystallographica Section A* **1995**, *51*, 33–38.
- (110) Sheldrick, G. M. A short history of SHELX. *Acta Crystallographica Section A* **2008**, *64*, 112–122.
- (111) Sheldrick, G. M. Phase annealing in SHELX-90: direct methods for larger structures. *Acta Crystallographica Section A* **1990**, *46*, 467–473.
- (112) Sheldrick, G. M. Crystal structure refinement with SHELXL. *Acta Crystallogr., Sect. C: Struct. Chem.* **2015**, *71*, 3–8.
- (113) Sheldrick, G. M. SHELXT - Integrated space-group and crystal-structure determination. *Acta Crystallogr., Sect. A: Found. Adv.* **2015**, *71*, 3–8.
- (114) Spek, A. L. Single-crystal structure validation with the program PLATON. *Journal of Applied Crystallography* **2003**, *36*, 7–13.
- (115) Spek, A. L. Structure validation in chemical crystallography. *Acta Crystallographica, Section D: Biological Crystallography* **2009**, *65*, 148–155.
- (116) Müller, P.; Herbst-Irmer, R.; Spek, A. L.; Schneider, T. R.; Sawaya, M. R. *Crystal Structure Refinement: A Crystallographer's Guide to SHELXL*; International Union of Crystallography Texts on Crystallography (Book 8); Oxford University Press, 2006.
- (117) Janiak, C. A critical account on  $\pi$ - $\pi$  stacking in metal complexes with aromatic nitrogen-containing ligands. *J. Chem. Soc., Dalton Trans.* **2000**, 3885–3896.
- (118) Hunter, C. A.; Sanders, J. K. M. The nature of  $\pi$ - $\pi$  interactions. *Journal of the American Chemical Society* **1990**, *112*, 5525–5534.
- (119) Meyer, E. A.; Castellano, R. K.; Diederich, F. Interactions with Aromatic Rings in Chemical and Biological Recognition. *Angewandte Chemie, International Edition in English* **2003**, *42*, 1210–1250.
- (120) Nayak, S. K.; Sathishkumar, R.; Row, T. N. G. Directing role of functional groups in selective generation of C-H $\cdots$  $\pi$  interactions: In situ cryo-crystallographic studies on benzyl derivatives. *CrystEngComm* **2010**, *12*, 3112–3118.

---

(121) Alvarez, S. A cartography of the van der Waals territories. *Dalton Transactions* **2013**, *42*, 8617–8636.

(122) Nelyubina, Y. V.; Antipin, M. Y.; Lyssenko, K. A. Are Halide…Halide Contacts a Feature of Rock-Salts Only? *The Journal of Physical Chemistry A* **2007**, *111*, 1091–1095.

(123) Allen, F. The Cambridge Structural Database: a quarter of a million crystal structures and rising. *Acta Crystallographica, Section B: Structural Science* **2002**, *58*, 380–388.

(124) Macrae, C. F.; Edgington, P. R.; McCabe, P.; Pidcock, E.; Shields, G. P.; Taylor, R.; Towler, M.; van de Streek, J. Mercury: visualization and analysis of crystal structures. *Journal of Applied Crystallography* **2006**, *39*, 453–457.

(125) Putz, H.; Brandenburg, K. *Diamond - Crystal and Molecular Structure Visualization*; Crystal Impact: Bonn, Germany.



---

## 9.1 Abbreviations

---

### Chemicals

---

A	3-Aminopropyl
acac	Acetylacetone
Ar	Aryl group
Bu	Butyl
<i>DABCO</i>	1,4-Diazabicyclo[2.2.2]octane
DBTDA	Dibutyltin diacetate
DBTDL	Dibutyltin dilaurate
Bu	Butyl
Et	Ethyl
Et <sub>2</sub> O	Diethyl ether
iPr	Isopropyl
KOtBu	Potassium tert-butoxide
LAH	Lithium aluminium hydride
LDA	Lithium diisopropylamide
M	Metal
Me	Methyl
MeOH	Methanol
NaOMe	Sodium methanolate
Ph	Phenyl
PTFE	Polytetrafluoroethylene
PVC	Polyvinyl chloride
PU	Polyurethane
THF	Tetrahydrofuran
TMS	Trimethylsilyl
TMS-Cl	Trimethylsilyl chloride
TMS-O <sup>t</sup> Bu	Trimethylsilyl tert-butylether

---

**Analytical terms**


---

bs	Broad singlet
d	Doublet
Hz	Hertz
J	Coupling constant
m	Multiplet
MHz	Megahertz
Hz	Hertz
Mp	Melting point
NMR	Nuclear magnetic resonance
ppm	Parts per million
TGA/DSC-MS	Thermogravimetry differential scanning calorimetry mass spectrometry
s	Singulet
t	Triplet
$\delta$	Delta

---

**Others**


---

%	Percent
°	Degree
°C	Degree centigrade
Å	Angström
Cat.	Catalyst
conc	Concentrated
<i>d</i>	Deuterated
eq	Equivalent
g	Gram
h	hour
K	Kelvin
kcal	Kilogram calorie
L	Liter
LD <sub>50</sub>	Median lethal dose

---

M	Molar
mg	Milligram
min	Minute
mL	Milliliter
mmol	Millimol
nm	Nanometer
pa	Pascal
pK <sub>a</sub>	Acid dissociation constant at logarithmic scale
rt	Room temperature
μ	Micro
Δ	Delta

## 9.2 Crystallographic Data

Compound	$\text{Cl}_4\text{SnA}^+_2$ (1)
Formula	$\text{C}_6\text{H}_{18}\text{Cl}_4\text{N}_2\text{Sn}$
Fw ( $\text{g mol}^{-1}$ )	378.71
$a$ (Å)	6.9591(9)
$b$ (Å)	11.6899(16)
$c$ (Å)	8.2685(11)
$\alpha$ (°)	90
$\beta$ (°)	108.102(5)
$\gamma$ (°)	90
$V$ (Å <sup>3</sup> )	639.36(15)
$Z$	2
Crystal size (mm)	0.15 × 0.12 × 0.10
Crystal habit	Block, colourless
Crystal system	Monoclinic
Space group	$P2_1/c$
$d_{\text{calc}}$ ( $\text{mg/m}^3$ )	1.967
$\mu$ ( $\text{mm}^{-1}$ )	2.80
$T$ (K)	100(2)
$2\theta$ range (°)	3.1–33.2
$F(000)$	372
$R_{\text{int}}$	0.064
independent reflns	2421
No. of params	62
R1, wR2 (all data)	R1 = 0.0208 wR2 = 0.0523
R1, wR2 ( $>2\sigma$ )	R1 = 0.0199 wR2 = 0.0518

Average bond lengths and angles		
Sn–C (Å) (avg.)	Sn–X (Å) (avg.)	C–Sn–C (°) (avg.)
2.1449(13)	2.6246(4) 2.6403(4)	180.0

Compound	$\text{Br}_4\text{SnA}^+_2$ (2)
Formula	$\text{C}_6\text{H}_{18}\text{Br}_4\text{N}_2\text{Sn}$
Fw ( $\text{g mol}^{-1}$ )	556.55
$a$ (Å)	7.1711(6)
$b$ (Å)	12.2012(11)
$c$ (Å)	8.4423(8)
$\alpha$ (°)	90
$\beta$ (°)	107.677(2)
$\gamma$ (°)	90
$V$ (Å <sup>3</sup> )	703.79(11)
$Z$	2
Crystal size (mm)	0.14 × 0.12 × 0.09
Crystal habit	Block, colourless
Crystal system	Monoclinic
Space group	$P2_1/c$
$d_{\text{calc}}$ ( $\text{mg/m}^3$ )	2.626
$\mu$ ( $\text{mm}^{-1}$ )	13.14
$T$ (K)	100(2)
$2\theta$ range (°)	3.0–33.0
$F(000)$	516
$R_{\text{int}}$	0.097
independent reflns	1230
No. of params	62
R1, wR2 (all data)	R1 = 0.0377 wR2 = 0.0839
R1, wR2 ( $>2\sigma$ )	R1 = 0.0318 wR2 = 0.0806

Average bond lengths and angles		
Sn–C (Å) (avg.)	Sn–X (Å) (avg.)	C–Sn–C (°) (avg.)
2.142(5)	2.7802(6) 2.7967(6)	180.0

Compound	[Br <sub>6</sub> Sn] A <sup>+Br</sup> <sub>2</sub> (3)
Formula	Br <sub>6</sub> Sn·2(C <sub>3</sub> H <sub>9</sub> BrN)
Fw (g mol <sup>-1</sup> )	876.19
<i>a</i> (Å)	10.875(2)
<i>b</i> (Å)	7.536(2)
<i>c</i> (Å)	13.149(3)
$\alpha$ (°)	90
$\beta$ (°)	110.31(3)
$\gamma$ (°)	90
<i>V</i> (Å <sup>3</sup> )	1010.7(4)
<i>Z</i>	2
Crystal size (mm)	0.12 × 0.10 × 0.09
Crystal habit	Block, colourless
Crystal system	Monoclinic
Space group	<i>P</i> 2 <sub>1</sub> / <i>c</i>
<i>d</i> <sub>calc</sub> (mg/m <sup>3</sup> )	2.879
$\mu$ (mm <sup>-1</sup> )	17.06
<i>T</i> (K)	100(2)
2 $\theta$ range (°)	3.2–33.1
<i>F</i> (000)	796
<i>R</i> <sub>int</sub>	0.070
independent reflns	1774
No. of params	91
R1, wR2 (all data)	R1 = 0.0206 wR2 = 0.0459
R1, wR2 (>2 $\sigma$ )	R1 = 0.0189 wR2 = 0.0452

Average bond lengths and angles		
Sn–C (Å) (avg.)	Sn–X (Å) (avg.)	C–Sn–C (°) (avg.)
—	2.5991(8) 2.6058(8) 2.6139(10)	—

Compound	[phenyl <sub>2</sub> SnA <sup>+</sup> <sub>2</sub> ][Cl <sup>-</sup> ] <sub>2</sub> (4)
Formula	C <sub>18</sub> H <sub>28</sub> Cl <sub>2</sub> N <sub>2</sub> Sn
Fw (g mol <sup>-1</sup> )	462.01
<i>a</i> (Å)	8.8702(19)
<i>b</i> (Å)	8.932(2)
<i>c</i> (Å)	13.717(3)
$\alpha$ (°)	103.384(8)
$\beta$ (°)	99.032(7)
$\gamma$ (°)	94.005(9)
<i>V</i> (Å <sup>3</sup> )	1037.8(4)
<i>Z</i>	2
Crystal size (mm)	0.10 × 0.05 × 0.05
Crystal habit	Block, colourless
Crystal system	Triclinic
Space group	<i>P</i> -1
<i>d</i> <sub>calc</sub> (mg/m <sup>3</sup> )	1.478
$\mu$ (mm <sup>-1</sup> )	1.49
<i>T</i> (K)	100(2)
2 $\theta$ range (°)	2.5–33.2
<i>F</i> (000)	468
<i>R</i> <sub>int</sub>	0.301
independent reflns	3642
No. of params	210
R1, wR2 (all data)	R1 = 0.2099 wR2 = 0.2786
R1, wR2 (>2 $\sigma$ )	R1 = 0.1439 wR2 = 0.2491

Average bond lengths and angles						
Sn–C	Sn–N	Sn–O	Sn–O	C–Sn–C	N–Sn–N	O–Sn–O
(Å) (avg.)	(Å) (avg.)	(Å) (avg.)	(Å) (avg.)	(°) (avg.)	(°) (avg.)	(°) (avg.)
2.1383(14)	2.3123(14)	2.3543(11)	<u>2.712(11)</u>	175.15(6)	160.53(5)	153.02(4)
2.1361(14)	2.3071(13)	2.2499(12)	3.46			155.10(4)

Compound	<b>formate<sub>2</sub>SnA<sub>2</sub> (5)</b>
Formula	C <sub>8</sub> H <sub>18</sub> N <sub>2</sub> O <sub>4</sub> Sn
Fw (g mol <sup>-1</sup> )	324.93
<i>a</i> (Å)	7.8984(2)
<i>b</i> (Å)	9.9681(3)
<i>c</i> (Å)	15.0083(5)
$\alpha$ (°)	90
$\beta$ (°)	94.789(1)
$\gamma$ (°)	90
<i>V</i> (Å <sup>3</sup> )	1177.51(6)
<i>Z</i>	4
Crystal size (mm)	0.21 × 0.18 × 0.13
Crystal habit	Block, colourless
Crystal system	Monoclinic
Space group	<i>P</i> 2 <sub>1</sub> / <i>n</i>
<i>d</i> <sub>calc</sub> (mg/m <sup>3</sup> )	1.833
$\mu$ (mm <sup>-1</sup> )	2.17
<i>T</i> (K)	100(2)
2 $\theta$ range (°)	2.7–29.0
<i>F</i> (000)	648
<i>R</i> <sub>int</sub>	0.037
independent reflns	3130
No. of params	152
R1, wR2 (all data)	R1 = 0.0185 wR2 = 0.0378
R1, wR2 (>2 $\sigma$ )	R1 = 0.0170 wR2 = 0.0372
Additional Data	
Coordination Number	6.5
Carboxylic acid pKa	3.77

Average bond lengths and angles						
Sn–C	Sn–N	Sn–O	Sn–O	C–Sn–C	N–Sn–N	O–Sn–O
(Å) (avg.)	(Å) (avg.)	(Å) (avg.)	(Å) (avg.)	(°) (avg.)	(°) (avg.)	(°) (avg.)
2.1383(14)	2.3123(14)	2.3543(11)	<u>2.712(11)</u>	175.15(6)	160.53(5)	153.02(4)
2.1361(14)	2.3071(13)	2.2499(12)	3.46			155.10(4)



Compound	acetate <sub>2</sub> SnA <sub>2</sub>
Formula	C <sub>10</sub> H <sub>22</sub> N <sub>2</sub> O <sub>4</sub> Sn
Fw (g mol <sup>-1</sup> )	352.98
<i>a</i> (Å)	5.8185(3)
<i>b</i> (Å)	7.6883(4)
<i>c</i> (Å)	7.7581(4)
$\alpha$ (°)	75.807(2)
$\beta$ (°)	83.124(2)
$\gamma$ (°)	89.113(2)
<i>V</i> (Å <sup>3</sup> )	334.01(3)
<i>Z</i>	1
Crystal size (mm)	0.10 × 0.08 × 0.02
Crystal habit	Plate, colourless
Crystal system	Triclinic
Space group	<i>P</i> -1
<i>d</i> <sub>calc</sub> (mg/m <sup>3</sup> )	1.755
$\mu$ (mm <sup>-1</sup> )	1.92
<i>T</i> (K)	100(2)
2 $\theta$ range (°)	3.4–27.4
<i>F</i> (000)	178
<i>R</i> <sub>int</sub>	0.018
independent reflns	1495
No. of params	88
R1, wR2 (all data)	R1 = 0.0190 wR2 = 0.0472
R1, wR2 (>2 $\sigma$ )	R1 = 0.0190 wR2 = 0.0472
Additional Data	
Coordination Number	6
Carboxylic acid pKa	4.76

Average bond lengths and angles						
Sn–C	Sn–N	Sn–O	Sn–O	C–Sn–C	N–Sn–N	O–Sn–O
(Å) (avg.)	(Å) (avg.)	(Å) (avg.)	(Å) (avg.)	(°) (avg.)	(°) (avg.)	(°) (avg.)
2.152(2)	2.2928(19)	2.2422(16)	3.29	180.00(5)	180.0	180.0

Compound	<b>laurate<sub>2</sub>SnA<sub>2</sub> (6)</b>
Formula	C <sub>30</sub> H <sub>62</sub> N <sub>2</sub> O <sub>4</sub> Sn
Fw (g mol <sup>-1</sup> )	633.50
<i>a</i> (Å)	18.616(5)
<i>b</i> (Å)	8.974(2)
<i>c</i> (Å)	10.391(3)
$\alpha$ (°)	90
$\beta$ (°)	99.002(10)
$\gamma$ (°)	90
<i>V</i> (Å <sup>3</sup> )	1714.6(8)
<i>Z</i>	2
Crystal size (mm)	0.10 × 0.09 × 0.07
Crystal habit	Block, colourless
Crystal system	Monoclinic
Space group	<i>P</i> <sub>2</sub> <sub>1</sub> / <i>c</i>
<i>d</i> <sub>calc</sub> (mg/m <sup>3</sup> )	1.227
$\mu$ (mm <sup>-1</sup> )	0.78
<i>T</i> (K)	100(2)
2 $\theta$ range (°)	2.5–25.5
<i>F</i> (000)	676
<i>R</i> <sub>int</sub>	0.077
independent reflns	3022
No. of params	271
R1, wR2 (all data)	R1 = 0.0353 wR2 = 0.0226
R1, wR2 (>2 $\sigma$ )	R1 = 0.0629 wR2 = 0.0553
Additional Data	
Coordination Number	6
Carboxylic acid pKa	5.3

Average bond lengths and angles						
Sn–C	Sn–N	Sn–O	Sn–O	C–Sn–C	N–Sn–N	O–Sn–O
(Å) (avg.)	(Å) (avg.)	(Å) (avg.)	(Å) (avg.)	(°) (avg.)	(°) (avg.)	(°) (avg.)
2.147(3)	2.2923(17)	2.2069(16)	3.35	180.0	180.0	180.00(4)

Compound	stearate <sub>2</sub> SnA <sub>2</sub> (7)
Formula	C <sub>42</sub> H <sub>86</sub> N <sub>2</sub> O <sub>4</sub> Sn
Fw (g mol <sup>-1</sup> )	801.81
<i>a</i> (Å)	5.5237(9)
<i>b</i> (Å)	8.0469(14)
<i>c</i> (Å)	25.989(4)
$\alpha$ (°)	83.921(7)
$\beta$ (°)	84.597(7)
$\gamma$ (°)	88.744(7)
<i>V</i> (Å <sup>3</sup> )	1143.5(3)
<i>Z</i>	1
Crystal size (mm)	0.10 × 0.09 × 0.08
Crystal habit	Block, colourless
Crystal system	Triclinic
Space group	<i>P</i> -1
<i>d</i> <sub>calc</sub> (mg/m <sup>3</sup> )	1.164
$\mu$ (mm <sup>-1</sup> )	0.60
<i>T</i> (K)	296(2)
2 $\theta$ range (°)	2.4–20.5°
<i>F</i> (000)	434
<i>R</i> <sub>int</sub>	0.122
independent reflns	4027
No. of params	225
R1, wR2 (all data)	R1 = 0.0755 wR2 = 0.1683
R1, wR2 (>2 $\sigma$ )	R1 = 0.0644 wR2 = 0.1599
Additional Data	
Coordination Number	6
Carboxylic acid pKa	4.78

Average bond lengths and angles						
Sn–C	Sn–N	Sn–O	Sn–O	C–Sn–C	N–Sn–N	O–Sn–O
(Å) (avg.)	(Å) (avg.)	(Å) (avg.)	(Å) (avg.)	(°) (avg.)	(°) (avg.)	(°) (avg.)
2.135(7)	2.300(5)	2.226(4)	3.34	180.0	180.0	180.0

Compound	trifluoroacetate <sub>2</sub> SnA <sub>2</sub> (8)
Formula	C <sub>10</sub> H <sub>16</sub> F <sub>6</sub> N <sub>2</sub> O <sub>4</sub> Sn
Fw (g mol <sup>-1</sup> )	460.94
<i>a</i> (Å)	10.8213(12)
<i>b</i> (Å)	9.2201(10)
<i>c</i> (Å)	16.1348(18)
$\alpha$ (°)	90
$\beta$ (°)	102.711(3)
$\gamma$ (°)	90
<i>V</i> (Å <sup>3</sup> )	1570.4(3)
<i>Z</i>	4
Crystal size (mm)	0.20 × 0.15 × 0.09
Crystal habit	Block, colourless
Crystal system	Monoclinic
Space group	<i>P</i> 2 <sub>1</sub> / <i>n</i>
<i>d</i> <sub>calc</sub> (mg/m <sup>3</sup> )	1.950
$\mu$ (mm <sup>-1</sup> )	1.71
<i>T</i> (K)	100(2)
2 $\theta$ range (°)	2.6–33.2
<i>F</i> (000)	904
<i>R</i> <sub>int</sub>	0.051
independent reflns	5992
No. of params	224
R1, wR2 (all data)	R1 = 0.0185 wR2 = 0.0378
R1, wR2 (>2 $\sigma$ )	R1 = 0.0170 wR2 = 0.0372
Additional Data	
Coordination Number	6
Carboxylic acid pKa	-0.25

Average bond lengths and angles						
Sn–C	Sn–N	Sn–O	Sn–O	C–Sn–C	N–Sn–N	O–Sn–O
(Å) (avg.)	(Å) (avg.)	(Å) (avg.)	(Å) (avg.)	(°) (avg.)	(°) (avg.)	(°) (avg.)
2.1325(15)	2.3091(13)	2.2549(13)	3.42	179.58(7)	178.34(5)	178.88(4)
2.1376(16)	2.2976(13)	2.2380(13)	3.47			

Compound	<b>perfluorononanoate<sub>2</sub>SnA<sub>2</sub> (9)</b>
Formula	C <sub>48</sub> H <sub>32</sub> F <sub>68</sub> N <sub>4</sub> O <sub>8</sub> Sn <sub>2</sub>
Fw (g mol <sup>-1</sup> )	2322.15
<i>a</i> (Å)	9.678(3)
<i>b</i> (Å)	10.989(3)
<i>c</i> (Å)	16.733(5)
$\alpha$ (°)	84.889(10)
$\beta$ (°)	88.997(11)
$\gamma$ (°)	89.837(11)
<i>V</i> (Å <sup>3</sup> )	1772.1(8)
<i>Z</i>	1
Crystal size (mm)	0.09 × 0.06 × 0.06
Crystal habit	Block, colourless
Crystal system	Triclinic
Space group	<i>P</i> -1
<i>d</i> <sub>calc</sub> (mg/m <sup>3</sup> )	2.176
$\mu$ (mm <sup>-1</sup> )	0.94
<i>T</i> (K)	100(2)
2 $\theta$ range (°)	2.4–32.9
<i>F</i> (000)	1124
<i>R</i> <sub>int</sub>	0.255
independent reflns	13626
No. of params	589
R1, wR2 (all data)	R1 = 0.3924 wR2 = 0.6101
R1, wR2 (>2 $\sigma$ )	R1 = 0.3341 wR2 = 0.5903
Additional Data	
Coordination Number	6
Carboxylic acid pKa	0

Average bond lengths and angles						
Sn–C	Sn–N	Sn–O	Sn–O	C–Sn–C	N–Sn–N	O–Sn–O
(Å) (avg.)	(Å) (avg.)	(Å) (avg.)	(Å) (avg.)	(°) (avg.)	(°) (avg.)	(°) (avg.)
2.144 (14)	2.318 (12)	2.248 (10)	3.56	180.0 (8)	180.0	180.0

Compound	<b>benzoate<sub>2</sub>SnA<sub>2</sub> (10)</b>
Formula	C <sub>20</sub> H <sub>26</sub> N <sub>2</sub> O <sub>4</sub> Sn
Fw (g mol <sup>-1</sup> )	477.12
<i>a</i> (Å)	12.3466(10)
<i>b</i> (Å)	7.7158(6)
<i>c</i> (Å)	11.3452(9)
$\alpha$ (°)	90
$\beta$ (°)	110.744(2)
$\gamma$ (°)	90
<i>V</i> (Å <sup>3</sup> )	1010.72(14)
<i>Z</i>	2
Crystal size (mm)	0.12 × 0.11 × 0.09
Crystal habit	Block, colourless
Crystal system	Monoclinic
Space group	<i>P</i> 2 <sub>1</sub> / <i>c</i>
<i>d</i> <sub>calc</sub> (mg/m <sup>3</sup> )	1.568
$\mu$ (mm <sup>-1</sup> )	1.29
<i>T</i> (K)	100(2)
2 $\theta$ range (°)	3.2–33.1
<i>F</i> (000)	484
<i>R</i> <sub>int</sub>	0.081
independent reflns	1782
No. of params	132
R1, wR2 (all data)	R1 = 0.0259 wR2 = 0.0606
R1, wR2 (>2 $\sigma$ )	R1 = 0.0222 wR2 = 0.0568
Additional Data	
Coordination Number	6
Carboxylic acid pKa	4.2

Average bond lengths and angles						
Sn–C	Sn–N	Sn–O	Sn–O	C–Sn–C	N–Sn–N	O–Sn–O
(Å) (avg.)	(Å) (avg.)	(Å) (avg.)	(Å) (avg.)	(°) (avg.)	(°) (avg.)	(°) (avg.)
2.139(2)	2.3118(18)	2.2148(15)	3.39	180.0	180.0	180.0

Compound	isonicotinate <sub>2</sub> SnA <sub>2</sub> (11)
Formula	C <sub>18</sub> H <sub>24</sub> N <sub>4</sub> O <sub>4</sub> Sn
Fw (g mol <sup>-1</sup> )	479.10
<i>a</i> (Å)	6.4461(5)
<i>b</i> (Å)	20.6594(16)
<i>c</i> (Å)	8.0643(6)
$\alpha$ (°)	90
$\beta$ (°)	986.88(13)
$\gamma$ (°)	90
<i>V</i> (Å <sup>3</sup> )	986.88(13)
<i>Z</i>	2
Crystal size (mm)	0.14 × 0.12 × 0.09
Crystal habit	Block, colourless
Crystal system	Monoclinic
Space group	<i>P</i> 2 <sub>1</sub>
<i>d</i> <sub>calc</sub> (mg/m <sup>3</sup> )	1.612
$\mu$ (mm <sup>-1</sup> )	1.33
<i>T</i> (K)	100(2)
2 $\theta$ range (°)	2.8–26.4
<i>F</i> (000)	484
<i>R</i> <sub>int</sub>	0.303
independent reflns	7566
No. of params	244
R1, wR2 (all data)	R1 = 0.1279 wR2 = 0.1312
R1, wR2 (>2 $\sigma$ )	R1 = 0.0660 wR2 = 0.1179
Additional Data	
Coordination Number	7
Carboxylic acid pKa	4.58

Average bond lengths and angles						
Sn–C	Sn–N	Sn–O	Sn–O	C–Sn–C	N–Sn–N	O–Sn–O
(Å) (avg.)	(Å) (avg.)	(Å) (avg.)	(Å) (avg.)	(°) (avg.)	(°) (avg.)	(°) (avg.)
2.126(8)	2.308(8)	2.477(6)	2.433(6)	176.9(4)	158.7(3)	144.4(2)
2.154(8)	2.333(7)	2.248(6)				161.3(2)

Compound	<i>p</i> -fluorobenzoate <sub>2</sub> SnA <sub>2</sub> (12)
Formula	C <sub>20</sub> H <sub>24</sub> F <sub>2</sub> N <sub>2</sub> O <sub>4</sub> Sn
Fw (g mol <sup>-1</sup> )	513.10
<i>a</i> (Å)	6.4102(3)
<i>b</i> (Å)	7.7883(3)
<i>c</i> (Å)	10.6891(4)
$\alpha$ (°)	101.258(2)
$\beta$ (°)	97.155(2)
$\gamma$ (°)	100.442(2)
<i>V</i> (Å <sup>3</sup> )	507.59(4)
<i>Z</i>	1
Crystal size (mm)	0.20 × 0.15 × 0.09
Crystal habit	Block, colourless
Crystal system	Triclinic
Space group	<i>P</i> -1
<i>d</i> <sub>calc</sub> (mg/m <sup>3</sup> )	1.679
$\mu$ (mm <sup>-1</sup> )	1.31
<i>T</i> (K)	100(2)
2 $\theta$ range (°)	2.7–33.0
<i>F</i> (000)	258
<i>R</i> <sub>int</sub>	0.043
independent reflns	1773
No. of params	141
R1, wR2 (all data)	R1 = 0.0178 wR2 = 0.0383
R1, wR2 (>2 $\sigma$ )	R1 = 0.0177 wR2 = 0.0382
Additional Data	
Coordination Number	6
Carboxylic acid pKa	4.14

Average bond lengths and angles						
Sn–C	Sn–N	Sn–O	Sn–O	C–Sn–C	N–Sn–N	O–Sn–O
(Å) (avg.)	(Å) (avg.)	(Å) (avg.)	(Å) (avg.)	(°) (avg.)	(°) (avg.)	(°) (avg.)
2.1331(17)	2.3042(16)	2.2280(12)	3.29	180.0	180.0	180.00(6)



Compound	<b>cyclopropanecarboxylate<sub>2</sub>SnA<sub>2</sub> (13)</b>
Formula	C <sub>14</sub> H <sub>26</sub> N <sub>2</sub> O <sub>4</sub> Sn
Fw (g mol <sup>-1</sup> )	405.06
<i>a</i> (Å)	18.6320(9)
<i>b</i> (Å)	11.0060(5)
<i>c</i> (Å)	17.4994(9)
$\alpha$ (°)	90
$\beta$ (°)	112.857(2)
$\gamma$ (°)	90
<i>V</i> (Å <sup>3</sup> )	3306.7(3)
<i>Z</i>	8
Crystal size (mm)	0.11 × 0.09 × 0.08
Crystal habit	Block, colourless
Crystal system	Monoclinic
Space group	<i>P</i> 2 <sub>1</sub> / <i>c</i>
<i>d</i> <sub>calc</sub> (mg/m <sup>3</sup> )	1.627
$\mu$ (mm <sup>-1</sup> )	1.56
<i>T</i> (K)	100(2)
2 $\theta$ range (°)	2.3–33.2
<i>F</i> (000)	1648
<i>R</i> <sub>int</sub>	0.089
independent reflns	12615
No. of params	379
R1, wR2 (all data)	R1 = 0.1116 wR2 = 0.2468
R1, wR2 (>2 $\sigma$ )	R1 = 0.0913 wR2 = 0.2244
Additional Data	
Coordination Number	7
Carboxylic acid pKa	4.78

Average bond lengths and angles						
Sn–C	Sn–N	Sn–O	Sn–O	C–Sn–C	N–Sn–N	O–Sn–O
(Å) (avg.)	(Å) (avg.)	(Å) (avg.)	(Å) (avg.)	(°) (avg.)	(°) (avg.)	(°) (avg.)
2.145(5)	2.313(5)	2.441(4)	2.218(4)	177.1(2)	160.81(17)	149.15(15)
2.147(6)	2.348(5)	2.450(4)				

Compound	<b>cyclobutanecarboxylate<sub>2</sub>SnA<sub>2</sub> (14)</b>
Formula	C <sub>16</sub> H <sub>30</sub> N <sub>2</sub> O <sub>4</sub> Sn
Fw (g mol <sup>-1</sup> )	433.11
<i>a</i> (Å)	9.3845(4)
<i>b</i> (Å)	11.1940(4)
<i>c</i> (Å)	17.8704(7)
$\alpha$ (°)	90
$\beta$ (°)	91.416(1)
$\gamma$ (°)	90
<i>V</i> (Å <sup>3</sup> )	1876.71(13)
<i>Z</i>	4
Crystal size (mm)	0.09 × 0.09 × 0.07
Crystal habit	Block, colourless
Crystal system	Monoclinic
Space group	<i>P</i> 2 <sub>1</sub> / <i>n</i>
<i>d</i> <sub>calc</sub> (mg/m <sup>3</sup> )	1.533
$\mu$ (mm <sup>-1</sup> )	1.38
<i>T</i> (K)	100(2)
2 $\theta$ range (°)	2.4–33.2
<i>F</i> (000)	888
<i>R</i> <sub>int</sub>	0.053
independent reflns	7154
No. of params	232
R1, wR2 (all data)	R1 = 0.0333 wR2 = 0.0716
R1, wR2 (>2 $\sigma$ )	R1 = 0.0300 wR2 = 0.0704
Additional Data	
Coordination Number	7
Carboxylic acid pKa	4.8

Average bond lengths and angles						
Sn–C	Sn–N	Sn–O	Sn–O	C–Sn–C	N–Sn–N	O–Sn–O
(Å) (avg.)	(Å) (avg.)	(Å) (avg.)	(Å) (avg.)	(°) (avg.)	(°) (avg.)	(°) (avg.)
2.131(2)	2.3318(17)	2.4838(15)	2.4255(14)	175.45(8)	158.28(6)	149.89(5)
2.132(2)	2.3477(17)	2.2247(14)				156.78(5)

Compound	<b>cyclopentanecarboxylate<sub>2</sub>SnA<sub>2</sub> (15)</b>
Formula	C <sub>18</sub> H <sub>34</sub> N <sub>2</sub> O <sub>4</sub> Sn
Fw (g mol <sup>-1</sup> )	461.16
<i>a</i> (Å)	9.7663(4)
<i>b</i> (Å)	9.4277(4)
<i>c</i> (Å)	11.2803(5)
$\alpha$ (°)	90
$\beta$ (°)	110.946(1)
$\gamma$ (°)	90
<i>V</i> (Å <sup>3</sup> )	969.98(7)
<i>Z</i>	2
Crystal size (mm)	0.08 × 0.02 × 0.02
Crystal habit	Plate, colourless
Crystal system	Monoclinic
Space group	<i>P</i> 2 <sub>1</sub> / <i>c</i>
<i>d</i> <sub>calc</sub> (mg/m <sup>3</sup> )	1.579
$\mu$ (mm <sup>-1</sup> )	1.34
<i>T</i> (K)	100(2)
2 $\theta$ range (°)	2.9–33.3
<i>F</i> (000)	476
<i>R</i> <sub>int</sub>	0.076
independent reflns	1706
No. of params	115
R1, wR2 (all data)	R1 = 0.0414 wR2 = 0.0756
R1, wR2 (>2 $\sigma$ )	R1 = 0.0321 wR2 = 0.0714
Additional Data	
Coordination Number	6
Carboxylic acid pKa	4.8

Average bond lengths and angles						
Sn–C	Sn–N	Sn–O	Sn–O	C–Sn–C	N–Sn–N	O–Sn–O
(Å) (avg.)	(Å) (avg.)	(Å) (avg.)	(Å) (avg.)	(°) (avg.)	(°) (avg.)	(°) (avg.)
2.141(4)	2.288(3)	2.194(3)	3.48	180.0	180.0	180.0

Compound	<b>cyclohexanecarboxylate<sub>2</sub>SnA<sub>2</sub> (16)</b>
Formula	C <sub>20</sub> H <sub>38</sub> N <sub>2</sub> O <sub>4</sub> Sn
Fw (g mol <sup>-1</sup> )	489.21
<i>a</i> (Å)	17.5303(8)
<i>b</i> (Å)	6.3940(4)
<i>c</i> (Å)	20.4804(9)
$\alpha$ (°)	90
$\beta$ (°)	107.697(2)
$\gamma$ (°)	90
<i>V</i> (Å <sup>3</sup> )	2187.0(2)
<i>Z</i>	4
Crystal size (mm)	0.15 × 0.12 × 0.10
Crystal habit	Block, colourless
Crystal system	Monoclinic
Space group	<i>C2/c</i>
<i>d</i> <sub>calc</sub> (mg/m <sup>3</sup> )	1.486
$\mu$ (mm <sup>-1</sup> )	1.20
<i>T</i> (K)	100(2)
2 $\theta$ range (°)	2.7–33.2
<i>F</i> (000)	1016
<i>R</i> <sub>int</sub>	0.335
independent reflns	4164
No. of params	132
R1, wR2 (all data)	R1 = 0.1767 wR2 = 0.1843
R1, wR2 (>2 $\sigma$ )	R1 = 0.0713 wR2 = 0.1450
Additional Data	
Coordination Number	6
Carboxylic acid pKa	4.91

Average bond lengths and angles						
Sn–C	Sn–N	Sn–O	Sn–O	C–Sn–C	N–Sn–N	O–Sn–O
(Å) (avg.)	(Å) (avg.)	(Å) (avg.)	(Å) (avg.)	(°) (avg.)	(°) (avg.)	(°) (avg.)
2.142(5)	2.279(5)	2.201(4)	3.33	180.0	180.00(15)	180.0(3)

Compound	<b>adamantanecarboxylate<sub>2</sub>SnA<sub>2</sub> (17)</b>
Formula	C <sub>28</sub> H <sub>46</sub> N <sub>2</sub> O <sub>4</sub> Sn
Fw (g mol <sup>-1</sup> )	593.36
<i>a</i> (Å)	6.3951(5)
<i>b</i> (Å)	10.8595(9)
<i>c</i> (Å)	11.3399(9)
$\alpha$ (°)	117.072(4)
$\beta$ (°)	95.219(4)
$\gamma$ (°)	98.560(4)
<i>V</i> (Å <sup>3</sup> )	682.07(10)
<i>Z</i>	1
Crystal size (mm)	0.39 × 0.13 × 0.12
Crystal habit	Block, colourless
Crystal system	Triclinic
Space group	<i>P</i> -1
<i>d</i> <sub>calc</sub> (mg/m <sup>3</sup> )	1.445
$\mu$ (mm <sup>-1</sup> )	0.97
<i>T</i> (K)	100(2)
2 $\theta$ range (°)	3.3–27.7
<i>F</i> (000)	310
<i>R</i> <sub>int</sub>	0.080
independent reflns	3269
No. of params	169
R1, wR2 (all data)	R1 = 0.0402 wR2 = 0.0746
R1, wR2 (>2 $\sigma$ )	R1 = 0.0356 wR2 = 0.0732
Additional Data	
Coordination Number	6
Carboxylic acid pKa	4.86

Average bond lengths and angles						
Sn–C	Sn–N	Sn–O	Sn–O	C–Sn–C	N–Sn–N	O–Sn–O
(Å) (avg.)	(Å) (avg.)	(Å) (avg.)	(Å) (avg.)	(°) (avg.)	(°) (avg.)	(°) (avg.)
2.150(3)	2.296(3)	2.182(2)	3.38	180.0	180.0	180.0

Compound	<b>laurate<sub>2</sub>'propylSnA (18)</b>
Formula	C <sub>30</sub> H <sub>61</sub> NO <sub>4</sub> Sn
Fw (g mol <sup>-1</sup> )	618.48
<i>a</i> (Å)	5.7911(5)
<i>b</i> (Å)	9.4400(8)
<i>c</i> (Å)	32.378(3)
$\alpha$ (°)	82.674(4)
$\beta$ (°)	89.992(4)
$\gamma$ (°)	72.175(3)
<i>V</i> (Å <sup>3</sup> )	1669.9(3)
<i>Z</i>	2
Crystal size (mm)	0.11 × 0.09 × 0.07
Crystal habit	Block, colourless
Crystal system	Triclinic
Space group	<i>P</i> -1
<i>d</i> <sub>calc</sub> (mg/m <sup>3</sup> )	1.230
$\mu$ (mm <sup>-1</sup> )	0.80
<i>T</i> (K)	100(2)
2 $\theta$ range (°)	2.3–23.6
<i>F</i> (000)	660
<i>R</i> <sub>int</sub>	0.210
independent reflns	5854
No. of params	422
R1, wR2 (all data)	R1 = 0.1646 wR2 = 0.1917
R1, wR2 (>2 $\sigma$ )	R1 = 0.0713 wR2 = 0.1544
Additional Data	
Coordination Number	7
Carboxylic acid pKa	5.3

Average bond lengths and angles						
Sn–C	Sn–N	Sn–O	Sn–O	C–Sn–C	N–Sn–N	O–Sn–O
(Å) (avg.)	(Å) (avg.)	(Å) (avg.)	(Å) (avg.)	(°) (avg.)	(°) (avg.)	(°) (avg.)
2.124(13)	2.322(12)	2.226(5)	2.275(5)	168.8(8)		83.02(17)
2.183(16)		2.364(7)	2.403(8)			

---

# CURRICULUM VITAE

## PERSONAL DATA

---

Name: **Philipp Müller**, BSc.

Adress: Schörgelgasse 11  
8010 Graz  
Austria

Telephone: +43677 61810990

Email: philipp.mueller@student.tugraz.at

Nationality: Austria

Date of Birth: 12.08.1992

Place of Birth: Munich, Germany

## EDUCATION

---

10/2015 – 08/2017 **Master Study in Chemistry**, Karl-Franzens-Universität Graz and Graz University of Technology  
**Master Thesis**, Graz University of Technology, Institute for Inorganic Chemistry, Prof. Frank Uhlig, Titel: “ *Novel diaminopropyltin dicarboxylates as catalysts for polyurethane synthesis*”.

10/2011 – 08/2015 **Bachelor Study in Chemistry**, Karl-Franzens-University Graz and Graz University of Technology  
**Bachelor Thesis**, Karl-Franzens-University, Institute for Inorganic Chemistry, Prof. Nadja Mösch, Titel “Aktivierung von molekularem Sauerstoff mit Molybdän(IV) Komplexen”.

09/2007 – 07/2011 **Oskar-Maria-Graf Gymnasium**, Neufahrn b. Freising

09/2004 – 07/2007 **Nymphenburger Privatschulen**, München

09/1999 – 07/2004 **Volksschule am Fürholzer Weg**, Neufahrn b. Freising

---

## OUTGOINGS

---

07/2015 **Summer Program** at Syracuse University, Syracuse, United States of America

Mn<sup>2+</sup> doped ZnCdSe\ZnS Quantum Dots for Luminescent Solar Concentrators

## WORK EXPERIENCE

---

10/2016 – 12/2016 **Student Supervisor**, Graz University of Technology, Inorganic chemistry laboratory

10/2015 – 01/2016 **Teacher** "Exercises for General Chemistry" Graz University of Technology

19/2015 – 12/2015 **Student Supervisor**, Graz University of Technology, General chemistry laboratory

07/2013 – 08/2013 **Project worker**, Graz University of Technology, Institute for Inorganic Chemistry, Prof. Frank Uhlig

05/2014 – 07/2016 **Student Supervisor**, Organic Chemistry Laboratory, Karl-Franzens-Universität Graz, Institute for Organic Chemistr

12/2009 – 12/2013 **Stocking helper**, Automaten Seitz

08/2009 – 09/2009 **ABC-Analysis**, Panther Film GmbH München

08/2008 – 09/2008 **Office and Logistic Assistent**, Automaten Seitz

## MEMBERSHIP

---

12/2011 – 2015 **Student Community**

## PERSONAL COMPETENCES

---

**Languages** German (mother tongue), English (C2), French (B1)

**IT- Knowledge** MS-Office, SciFinder, ChemOffice, ISIS Draw, SciDex CLAKS, VNMRJ, MestReNova/ MestReC, Photoshop CS6, Lightroom, Adobe Illustrator, APEX2

**Driving License** B

**Interests and Hobbies** Travel, Cooking, Badminton, Painting, Astronomy



---

## SCIENTIFIC RECORD

### POSTER PRESENTATION AT CONFERENCES

---

- 1 Müller, P.; Torvisco Gomez, A.; Uhlig, F.: „Novel diamino tin dicarboxy compounds”, **14<sup>th</sup> International Conference on the Coordination and Organometallic Chemistry of Germanium, Tin and Lead**, 28. August 2016, Pardubice, Czech Republic
- 2 Müller, P., Blake A., Hofman, E., Zheng, W.: “**Mn<sup>2+</sup> doped ZnCdSeS\ZnS Quantum Dots for Luminescent Solar Concentrators**”, **Summer Program at Syracuse University**, 06.2016 - 08.2016, Syracuse, United States of America

### ORAL PRESENTATIONS

---

- 1 Müller, P.; Torvisco Gomez, A.; Uhlig, F.: „ Novel diamino tin dicarboxy compounds”, 17<sup>th</sup> International Seminar of PhD Students on Organometallic and Coordination Chemistry, 3. April 2017, Kraskov, Czech Republic
- 2 Müller, P., Blake A., Hofman, E., Zheng, W.: “Mn<sup>2+</sup> doped ZnCdSeS\ZnS Quantum Dots for Luminescent Solar Concentrators”, **Summer Program at Syracuse University**, 06.2016 - 08.2016, Syracuse, United States of America
- 3 Müller, P.; Torvisco Gomez, M.; Uhlig, F.: “Novel diamino tin dicarboxy compounds”, 8. Deutsch-Österreichischer Mitarbeiterworkshop Hauptgruppenelement Chemie, 12.März 2016, Kassel, Germany

### PUBLICATIONS IN PEER REVIEWED JOURNALS

---

- 1 Pichler, J.; Müller, P.; Torvisco Gomez, M.; Uhlig, F.: “Novel diamino propyl tin compounds”, *Canadian journal of chemistry*, **2017**, in press.